

Universiteit
Leiden
The Netherlands

New neuroimaging approaches in Parkinson's disease

Schipper, L.J. de

Citation
Schipper, L. J. de. (2020, February 18). *New neuroimaging approaches in Parkinson's disease*. Retrieved from https://hdl.handle.net/1887/85511

Version:	Publisher's Version
License:	Licence agreement concerning inclusion of doctoral thesis in the Institutional Repository of the University of Leiden
Downloaded from:	https://hdl.handle.net/1887/85511

Note: To cite this publication please use the final published version (if applicable).

Cover Page

Universiteit Leiden

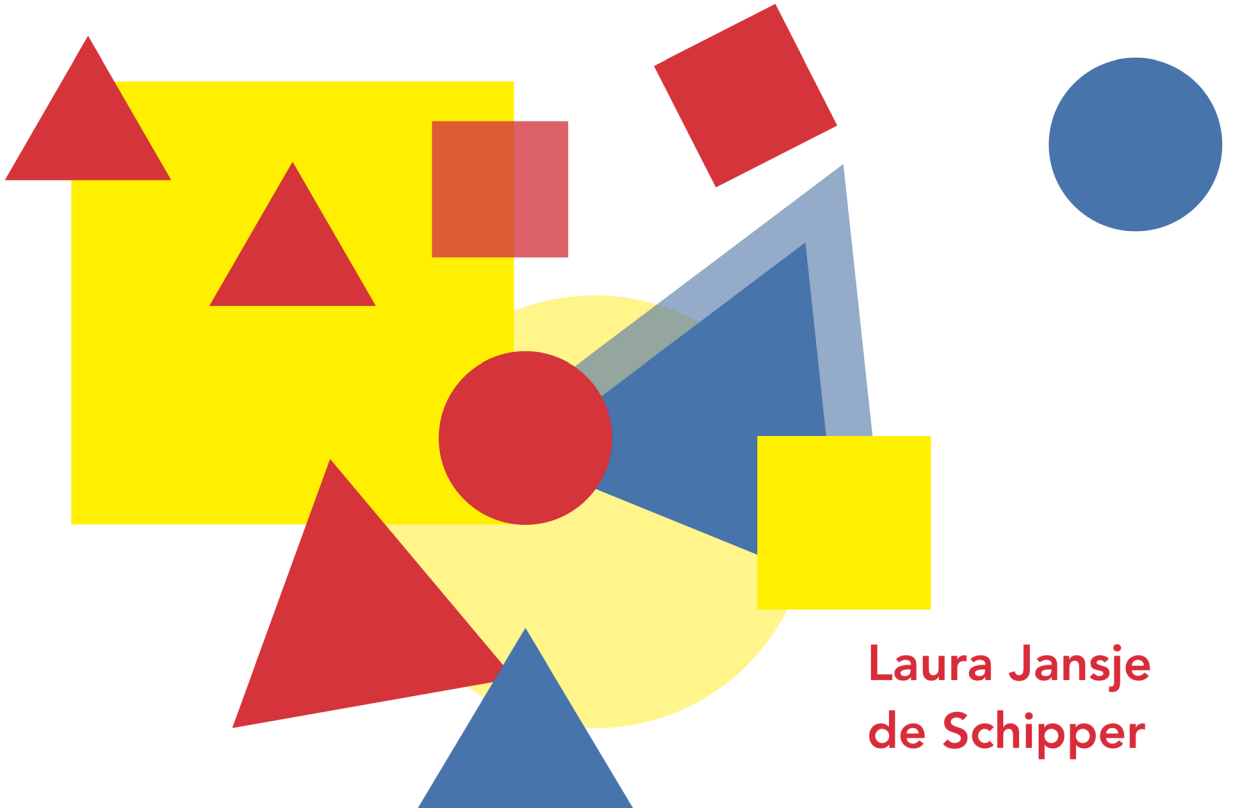


The handle http://hdl.handle.net/1887/85511 holds various files of this Leiden University dissertation.

Author: Schipper L.J. de
Title: New neuroimaging approaches in Parkinson's disease
Issue Date: 2020-02-18

New neuroimaging approaches in Parkinson's disease





Laura Jansje de Schipper

New neuroimaging approaches in Parkinson's disease

Design & layout: L.J. de Schipper
Printed by: ProefschriftMaken | Proefschriftmaken.nl

The research presented in this thesis was performed at the Department of Neurology and the Department of Radiology of the Leiden University Medical Center, Leiden, the Netherlands and was funded by 'Stichting ParkinsonFonds'.

ISBN: 978-94-6380-662-6
© L.J. de Schipper, 2020

No part of this thesis may be reproduced in any form without permission of the author or, when appropriate, of the publishers of the publications.

The printing of this thesis was financially supported by the Parkinson Vereniging, the Alkemade-Keuls foundation and UCB Pharma B.V.

New neuroimaging approaches in Parkinson's disease

Proefschrift

Ter verkrijging van de graad van Doctor
aan de Universiteit Leiden,
op gezag van de Rector Magnificus prof.mr. C.J.J.M. Stolker,
volgens besluit van het College voor promoties
te verdedigen op dinsdag 18 februari 2020
klokke 15:00 uur

door

Laura Jansje de Schipper
geboren te Knokke-Heist, België
in 1988

Promotor

Prof. dr. J.J. van Hilten

Copromotoren

Dr. J. Marinus

Dr. J. van der Grond

Promotiecommissie

Prof. dr. R.A.C. Roos

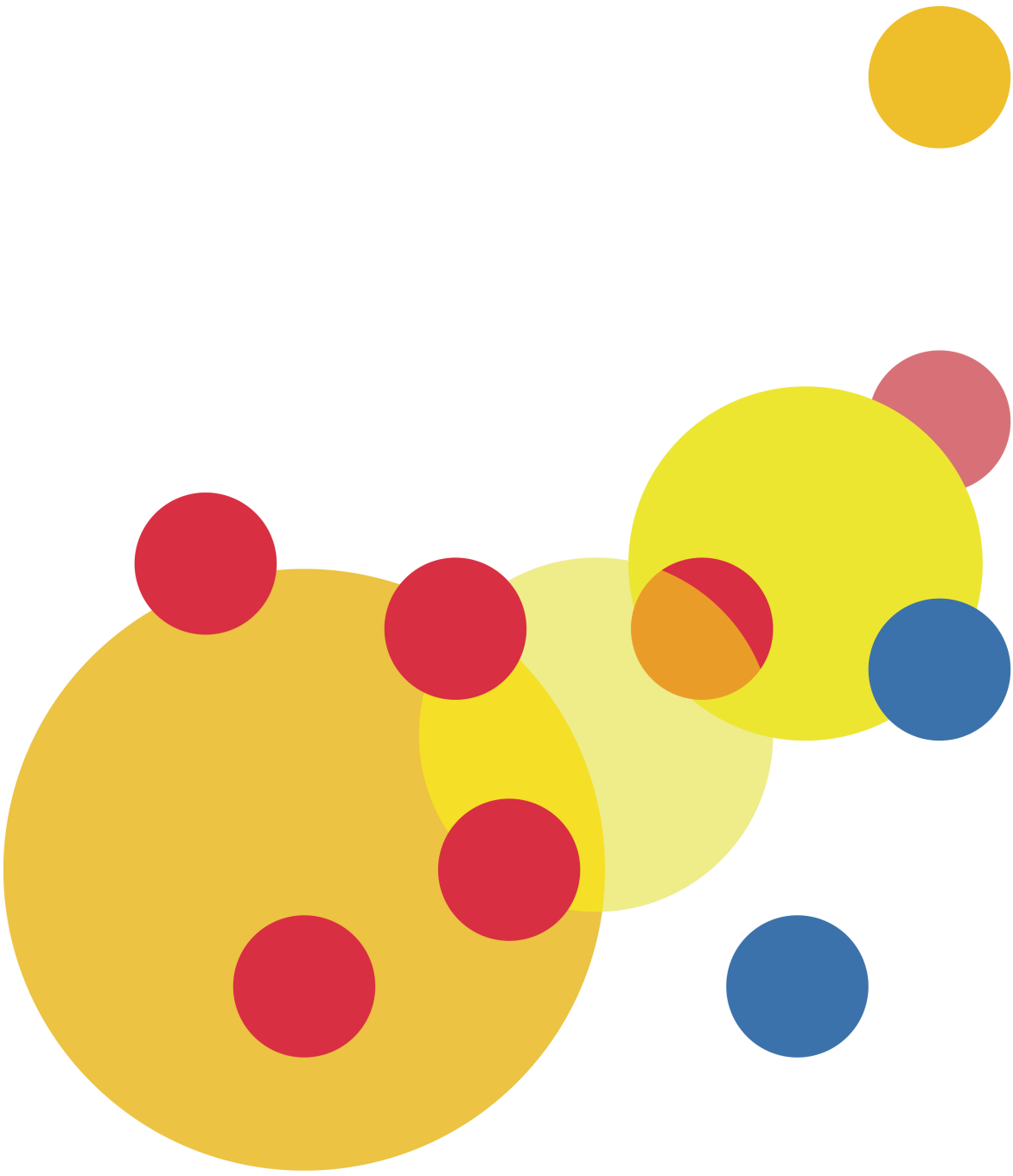
Prof. dr. O.A. van den Heuvel, Amsterdam Universitaire Medische Centra, Amsterdam, the Netherlands

Prof. dr. A. van der Lugt, Erasmus Medisch Centrum, Rotterdam, the Netherlands

Table of contents

CHAPTER 1	General introduction	7
CHAPTER 2	Loss of integrity and atrophy in cingulate structural covariance networks in Parkinson's disease	15
CHAPTER 3	Regional structural hippocampal differences between dementia with Lewy bodies and Parkinson's disease	31
CHAPTER 4	Age- and disease-related cerebral white matter changes in patients with Parkinson's disease	47
CHAPTER 5	Altered whole-brain and network-based functional connectivity in Parkinson's disease	63
CHAPTER 6	Classification of Parkinson's disease status based on resting-state functional connectivity data	81
CHAPTER 7	Summary, concluding remarks and future perspectives	95
CHAPTER 8	Nederlandse samenvatting	105
APPENDICES		115
	Abbreviations	116
	References	118
	List of publications	135
	Dankwoord	137
	Curriculum vitae	139

1 General introduction



Parkinson's disease

Parkinson's disease (PD) has typically been characterized as a progressive movement disorder, but it is nowadays recognized that non-motor domains are involved as well (Chaudhuri et al., 2006). Essential for diagnosis is parkinsonism, which is defined as bradykinesia plus resting tremor or rigidity (Postuma et al., 2015). Recent criteria for the diagnosis of PD also take non-motor symptoms into account (Postuma et al., 2015). Non-motor features, such as cognitive impairment, autonomic dysfunction, depression, nighttime sleep problems, daytime sleepiness and hyposmia, may already appear before the first clinical motor symptoms emerge (Adler and Beach, 2016; Chaudhuri et al., 2006). PD patients show considerable variability in their clinical expression and progression rate of the disease, response to treatment and extent to which different pathological pathways are involved (Foltynie et al., 2002; Linazasoro, 2007).

The cardinal motor symptoms of PD (i.e. bradykinesia, tremor, rigidity) are linked to the loss of dopaminergic neurons in the substantia nigra pars compacta (Damier et al., 1999), but neuropathological changes of PD extend far beyond the nigrostriatal system, affecting also noradrenergic, serotonergic, cholinergic and other neurotransmitter systems (Wolters, 2008). Alpha-synuclein aggregates (including Lewy bodies and Lewy neurites) are demonstrated in the central, peripheral and autonomic nervous system, and likely contribute to the various non-motor symptoms of PD (Adler and Beach, 2016). However, other protein deposits including tau and amyloid beta have been identified in PD (Kalaitzakis et al., 2008).

The identification of distinct PD subtypes may provide insights into the underlying pathophysiology, aid in the prediction of progression or offer guidance in developing more efficient personalized care approaches. Various studies have attempted to address heterogeneity in PD with classification systems, often based on clinical characteristics of patients, such as a tremor or postural-instability-and-gait disorder dominant phenotype (Mestre et al., 2018). The reproducibility of these classification systems is problematic. For instance, patients may switch from one subtype to another, due to changing clinical presentations (Mestre et al., 2018; Simuni et al., 2016). Besides classification based on a particular clinical trait, the differentiation of PD subtypes might also be based on the use of other disease features such as molecular or imaging markers (Drysdale et al., 2017). Recent research in depression, which is, like PD, not a uniform disease, identified subtypes defined by distinct patterns of connectivity on resting-state functional magnetic resonance imaging (fMRI) scans (Drysdale et al., 2017). Although these subtypes are based on distinct functional connectivity patterns, they appear associated with

certain clinical features and predict responsiveness to certain types of therapy (Drysdale et al., 2017).

Lewy Body Dementia

Patients with dementia with Lewy bodies (DLB) show important similarities with PD patients both in pathology as well as in clinical characteristics, such as the presence of Lewy bodies and symptoms of parkinsonism, but the progression rate, disease course and phenotype are different from patients with PD. Although DLB patients meeting the full criteria for PD may now be qualified as PD (DLB subtype) (Postuma et al., 2015), the progressive invalidating course of DLB and the decreased efficacy and tolerance of medication as compared to PD underscore the necessity of a clear distinction between the two in the early phase, which is at present still very difficult.

Neuroimaging

Neuroimaging offers the opportunity to study disease-related changes of the brain and the possibility to link pathology to clinical manifestations in a non-invasive manner. Many studies have evaluated conventional MRI techniques in PD, such as voxel-based morphometry, by using T1-weighted images (Pan et al., 2012). These studies have revealed reduced brain grey matter in PD patients (Pan et al., 2012); however, no PD-specific grey matter atrophy patterns have been identified so far. Several studies have studied substantia nigra volumetric differences on MRI, but with heterogeneous results as well. Some studies report no volumetric differences in the substantia nigra compared to control subjects, whereas others identified a decrease and still others even an increase in volume (Saeed et al., 2017).

High-field MRI as well as new imaging techniques became available since initial MRI studies in PD. Advanced neuroimaging techniques include diffusion-weighted imaging (DWI), magnetization transfer imaging (MTI) and fMRI. DWI can provide quantitative measures of the microstructural integrity of white matter. The concept of DWI is based on random (isotropic) movement of water molecules, without constraints. Diffusion of water molecules is usually not random, but restricted (anisotropic) by the surrounding architecture such as fiber tracts. Diffusion tensor imaging (DTI) can estimate anisotropy to provide directional information, or can measure the overall movement of molecules (mean diffusivity). MTI can be used to detect changes in brain structures that may not be visible with standard MR techniques by measuring magnetization transfer between free protons and protons bound to macromolecules. fMRI can yield important information on the brain's functional connectivity. It measures blood oxygen level

dependent (BOLD) signal fluctuation in the brain in response to a particular task or stimuli, or spontaneous BOLD fluctuations at rest, which is called resting-state fMRI (Fox and Raichle, 2007).

These advanced techniques have already shown promising results in PD. Recent studies suggest that DTI of the substantia nigra might become a valuable tool to monitor PD progression, or to distinguish PD patients from control subjects (Burciu et al., 2017; Ofori et al., 2017; Vaillancourt et al., 2009). However, it remains to be determined how these techniques can be applied to clinical practice for individual patients, as the results often represent group-wise differences between PD patients and control subjects. Further, only a limited number of studies have used these advanced MRI techniques in PD so far, and most of these studies have focused on specific patient subgroups and pre-defined regions of interest, the latter often dopamine-related structures. As we have come to appreciate that PD affects both grey matter areas and white matter tracts throughout the entire brain (Lim et al., 2009), it is important that more studies investigate the whole brain.

Brain networks

Network approaches may help to assess the widespread consequences of disease-specific changes in neurodegenerative diseases as PD. A common method to segment the brain functionality into sub-networks is independent component analysis. Resting-state networks represent spatial distinct regions with co-varying BOLD (as measured with resting-state fMRI) signals at rest. Previous fMRI studies revealed a number of networks which are consistently found across subjects, and which show remarkable correspondence to patterns of task activation (Beckmann et al., 2005; Damoiseaux et al., 2006). The default mode network, for example, is a frequently studied resting-state network in neurodegenerative diseases. Graph analytical methods can be used to investigate the global organization of the whole-brain functional connectivity network (i.e. the functional connectome). A relatively new method in the field of graph-based methods is eigenvector centrality mapping (ECM). ECM does not require a-priori knowledge, identifies prominent regions in the whole brain network hierarchy and detects localized differences between two populations (Wink et al., 2012).

In addition to functional network approaches, evidence suggests that anatomical structures that are spatially distributed but functionally linked, co-vary in grey matter density within individuals across a population (Alexander-Bloch et al., 2013; Andrews et al., 1997). The grouping of these structures, so-called structural covariance networks (SCNs), are increasingly important in uncovering in

vivo patterns of brain atrophy not readily apparent by regional structural analysis (Alexander-Bloch et al., 2013; Hafkemeijer et al., 2016, 2014). It was shown that Alzheimer's disease and frontotemporal dementia have specific SCNs of degeneration (Hafkemeijer et al., 2016) and distinct aging effects were further demonstrated on the organization of SCNs in healthy elderly (Montembeault et al., 2016; Spreng and Turner, 2013). Regarding the results in other neurodegenerative diseases, it could be valuable to study SCNs in PD.

Profiling Parkinson's disease

This cross-sectional cohort study is part of the Profiling Parkinson's disease (PROPARK) study. PROPARK research has resulted in the establishment of an extensive database of over 400 well-characterized patients which formed the basis for several projects on clinical characterization, inter-relations between clinical domains, phenotype-genotype relations and the neuroimaging study described in this thesis. Previous PROPARK research has also led to identification of a coherent grouping of some of the clinical domains in PD, largely involving symptoms that do not improve on dopaminergic medication. The severity of non-dopaminergic symptoms in Parkinson's disease (SENS-PD) scale is a composite score comprising the following six domains: postural instability and gait difficulty, psychotic symptoms, excessive daytime sleepiness, autonomic dysfunction, cognitive impairment and depressive symptoms. The grouping of these clinical domains is present early in the disease course (van der Heeden et al., 2016, 2014), worsens over time (van der Heeden et al., 2016, 2014) and may reflect advancing Lewy body pathology in the nervous system (Adler and Beach, 2016). Given the multisystem nature of PD and the increasing evidence of the importance of predominantly non-dopaminergic domains during the course of PD, the use of the SENS-PD scale could lead to a more complete and accurate evaluation of disease severity.

Aims of this thesis

The general aim of this thesis was to apply advanced neuroimaging approaches that may identify changes that are characteristic of PD, aid in the differentiation of potential PD subtypes, and contribute to the differentiation of PD and DLB. To this end, we searched for differential brain MRI features in PD patients compared to healthy control subjects, and examined the relations between these features and patient characteristics, such as age, dopaminergic medication, motor and predominantly non-dopaminergic impairments.

We started analyzing T1-weighted brain images in chapter 2 and 3. In chapter 2, we studied SCNs of grey matter in PD patients that had earlier been established in healthy elderly. We evaluated whether the integrity of SCNs is associated with clinical severity of PD, and whether SCNs showed a loss of integrity beyond the effect of aging that was shown in the normal population. In chapter 3, we assessed if studying structural characteristics of grey matter, including SCNs, may contribute in differentiating DLB and PD more clearly. We studied white matter integrity in chapter 4, using T1-weighted, fluid-attenuated inversion recovery (FLAIR), DWI and MTI brain images. We hypothesized that the decline in white matter integrity is significantly greater in PD patients than seen in healthy aging subjects and that there may be an age-by-PD interaction effect on white matter integrity. To this end, we compared macro- and microstructural integrity parameters of global white matter between PD patients and control subjects. In chapter 5 and 6, we studied resting-state fMRI data. The aim of chapter 5 was to evaluate and compare the consequences of PD on the resting-state functional connectivity on a whole-brain level of integrated networks (ECM) and on eight explicit brain networks. Finally, we aimed to use resting-state fMRI data for classification of PD on an individual patient level in chapter 6. In chapter 7 all findings are briefly summarized after which the potential future directions of MRI research in PD are discussed.

2 Loss of integrity and atrophy in cingulate structural covariance networks in Parkinson's disease

Neuroimage: Clinical. (2017) 15:587-593. doi: 10.1016/j.nicl.2017.05.012

Laura de Schipper[1]
Jeroen van der Grond[2]
Johan Marinus[1]
Johanna Henselmans[1,3]
Jacobus van Hilten[1]

[1] Leiden University Medical Center, Department of Neurology, Leiden, the Netherlands
[2] Leiden University Medical Center, Department of Radiology, Leiden, the Netherlands
[3] Antonius Hospital, Department of Neurology, Woerden, the Netherlands



ABSTRACT

Introduction: In Parkinson's disease (PD), the relation between cortical brain atrophy on MRI and clinical progression is not straightforward. Determination of changes in structural covariance networks - patterns of covariance in grey matter density - has shown to be a valuable technique to detect subtle grey matter variations. We evaluated how structural network integrity in PD is related to clinical data.

Methods: 3 Tesla MRI was performed in 159 PD patients. We used nine standardized structural covariance networks identified in 370 healthy subjects as a template in the analysis of the PD data. Clinical assessment comprised motor features (Movement Disorder Society unified Parkinson's Disease rating scale; MDS-UPDRS motor scale) and predominantly non-dopaminergic features (severity of non-dopaminergic symptoms in Parkinson's disease; SENS-PD scale: postural instability and gait difficulty, psychotic symptoms, excessive daytime sleepiness, autonomic dysfunction, cognitive impairment and depressive symptoms). Voxel-based analyses were performed within networks significantly associated with PD.

Results: The anterior and posterior cingulate network showed decreased integrity, associated with the SENS-PD score, $p = 0.001$ ($\beta = -0.265$, $\eta_p^2 = 0.070$) and $p = 0.001$ ($\beta = -0.264$, $\eta_p^2 = 0.074$), respectively. Of the components of the SENS-PD score, cognitive impairment and excessive daytime sleepiness were associated with atrophy within both networks.

Conclusion: We identified loss of integrity and atrophy in the anterior and posterior cingulate networks in PD patients. Abnormalities of both networks were associated with predominantly non-dopaminergic features, specifically cognition and excessive daytime sleepiness. Our findings suggest that (components of) the cingulate networks display a specific vulnerability to the pathobiology of PD and may operate as interfaces between networks involved in cognition and alertness.

INTRODUCTION

Parkinson's disease (PD) is characterized by a broad spectrum of motor and non-motor features. It has been proposed that widespread pathological changes (Lewy bodies and Lewy neurites) in select nuclei of the central and peripheral nervous system underlie the complex clinical presentation of PD (Jellinger, 2012). Increasing evidence points at the existence of a coherent grouping of some of the clinical domains, which largely involve symptoms that do not improve on dopaminergic medication. The grouping of these symptoms is present early in the disease course (van der Heeden et al., 2016), worsens over time (van der Heeden et al., 2016), and probably reflects advancing Lewy body pathology in the nervous system (Adler and Beach, 2016).

Previous anatomical magnetic resonance imaging (MRI) studies commonly investigated voxel-wise differences in regional grey matter volume between PD patients and control subjects. These studies revealed reduced grey matter in patients (Pan et al., 2012), which, however, is nonspecific to PD. Further, the findings are inconsistent across studies (Pan et al., 2012), which is likely explained by the clinical heterogeneity of PD and the current insensitivity of imaging techniques to detect subtle changes in brain structures. New techniques including computational network-based analyses are increasingly important in uncovering in vivo patterns of brain atrophy not readily apparent by regional structural analysis (Alexander-Bloch et al., 2013; Hafkemeijer et al., 2016). Evidence suggests that anatomical structures that are spatially distributed but functionally linked, co-vary in grey matter density (structural covariance networks; SCNs) within individuals across a population (Alexander-Bloch et al., 2013; Andrews et al., 1997).

Factors like age and disease affect SCNs (Hafkemeijer et al., 2014; Möller et al., 2015). Distinct aging effects on the organization of SCNs were demonstrated in healthy elderly (Montembeault et al., 2012; Spreng and Turner, 2013). Also, it was shown that Alzheimer's disease and frontotemporal dementia have specific SCNs of degeneration (Hafkemeijer et al., 2016). These findings support that this methodology may have the potential to identify brain regions within disease specific structural networks that confer a preferential vulnerability to the pathobiology of PD.

In this study, we studied SCN integrity in PD patients. We evaluated whether the integrity of SCNs (constructed from grey matter density in healthy elderly adults), is associated with clinical severity of PD and if the integrity is associated with predominantly dopaminergic or nondopaminergic symptoms.

MATERIALS AND METHODS

Study design and Participants

PD patients were recruited from the outpatient clinic for Movement Disorders of the Department of Neurology of the LUMC (Leiden University Medical Center) and nearby university and regional hospitals. All participants fulfilled the United Kingdom Parkinson's Disease Society Brain Bank criteria for idiopathic PD (Gibb and Lees, 1988). The present study is a cross-sectional cohort study of PD patients and is part of the Profiling Parkinson's disease (PROPARK) study. Written consent was obtained from all participants. The Medical Ethics Committee of the LUMC approved the study.

Clinical assessments

All patients underwent standardized assessments, including an evaluation of demographic and clinical characteristics. Participants were tested while on medication, except for 24 patients (22 de novo patients, defined as dopaminergic drug-naïve patients with a disease duration shorter than five years; two other dopaminergic drug-naïve patients). The Movement Disorder Society unified Parkinson's disease rating scale (MDS-UPDRS) part III (motor scale) was used to quantify the severity of motor symptoms. The severity of non-dopaminergic symptoms in Parkinson's disease (SENS-PD) scale is a composite score comprising three items with four response options (0–3) from each of the following six predominantly non-dopaminergic domains: postural instability and gait difficulty, psychotic symptoms, excessive daytime sleepiness, autonomic dysfunction, cognitive impairment and depressive symptoms (total range: 0–54) (van der Heeden et al., 2016, 2014). These six domains represent a coherent complex of symptoms that is already present in the early disease stages and increases in severity when the disease advances. The SENS-PD is a recently developed short, reliable and valid scale that includes symptoms that do not improve with dopaminergic medication and its score may therefore more accurately reflect severity and progression of the underlying disease than currently used dopamine-sensitive measures. Higher scores on both scales reflect more severe impairment. Trained research associates administered the MDS-UPDRS motor scale and the "postural instability and gait difficulty", "psychotic symptoms" and "cognitive impairment" items of the SENS-PD scale. The "excessive daytime sleepiness", "autonomic dysfunction" and "depressive symptoms" items were self-completed by patients. A levodopa dose equivalent (LDE) of daily levodopa and dopamine agonists dose was calculated for each patient. The total LDE is the sum of levodopa

dosage equivalent (LDE-Dopa) and the dopamine agonist dosage equivalent (LDE-DA) (Tomlinson et al., 2010).

MRI acquisition

Three-dimensional T1-weighted anatomical images were acquired on a 3 Tesla MRI scanner (Philips Achieva, Best, the Netherlands) using a standard 32-channel whole-head coil. Acquisition parameters were: repetition time = 9.8 ms, echo time = 4.6 ms, flip angle = 8°, field of view 220 × 174 × 156 mm, 130 slices with a slice thickness of 1.2 mm with no gap between slices, resulting in a voxel size of 1.15 mm × 1.15 mm × 1.20 mm.

Data analysis

Before analysis, all MRI scans were visually checked to ensure that no major artifacts or abnormalities were present in the data. All analyses were done using the software provided by FMRIB's software library (FSL, version 5.0.8, Oxford, United Kingdom) (Smith et al., 2004).

Pre-processing

The three-dimensional T1 images were pre-processed using the pre-processing steps used for voxel-based morphometric analysis (Douaud et al., 2007; Good et al., 2001; Smith et al., 2004). Each step was visually checked. The T1-weighted images were brain-extracted and tissue-type segmentation was performed, resulting in probability maps of a given tissue type (i.e. grey matter, white matter or cerebrospinal fluid). The grey matter images were non-linearly registered to the 2 mm Montreal Neurological Institute (MNI) 152 standard space (Montreal Neurological Institute, Montreal QC, Canada) (Andersson et al., 2007; Jenkinson et al., 2002a). The resulting images were averaged to create a study-specific grey matter template. All native grey matter images were subsequently nonlinearly re-registered to the study-specific grey matter template and "modulated" to correct for local expansions or contractions due to the non-linear component of the spatial transformation. The images were smoothed with an isotropic Gaussian kernel with a sigma of 3 mm. The modulated grey matter images in MNI space were concatenated into a four-dimensional data set, which was used for the network and voxel-based morphometry (VBM) analyses.

Structural covariance networks

We used nine bilateral standardized SCNs, identified in 370 healthy elderly with an age range of 45–85 years, which is the same as the age range in our PD population. For detailed information on the networks see Hafkemeijer et al. (2014). The networks were derived using an independent component analysis, a statistical technique that defines spatial component maps of maximal statistical independence. It is commonly used to study functional network integrity, but it can also be used to study if brain structures of a population co-vary in grey matter volume (Hafkemeijer et al., 2014; Segall et al., 2012). The four-dimensional data set of grey matter images derived from our PD population was used in a spatial regression against the nine SCN probability maps (a general linear model approach integrated in FSL) (Filippini et al., 2009). This way individual SCN integrity scores were calculated. The integrity score is the beta coefficient of the regression analysis. It can be a negative or a positive score, reflecting the strength of the individual expression in each network, with high scores indicating strong individual expression of the network. To allow comparisons of the SCNs of the template and of patients with PD, identification of the nine SCNs in patients with PD was conducted using the same approach as Hafkemeijer et al. (2014). An independent component analysis was applied on the four-dimensional data set of modulated grey matter images of all PD patients, using multivariate exploratory linear optimized decomposition into independent components (Beckmann et al., 2005). The independent component analysis was restricted to nine components, the same amount as in the study of Hafkemeijer et al. (2014). Significance of individual voxels within a spatial map was derived using a mixture model, with a standard threshold level of 0.5 (Smith et al., 2004), which indicates an equal loss is placed on false positives and false negatives.

Voxel-based morphometry

To investigate group differences in grey matter volume, a voxel-wise general linear model in FSL was used. Grey matter region-of-interest masks were obtained by identifying anatomical structures that were present in the SCNs (Hafkemeijer et al., 2014). A design matrix was constructed for estimating the relationship between grey matter volume (in each region-of-interest) and clinical measures. Gender, age and disease duration were used as covariates to correct for confounding effects. The voxel-wise general linear model was applied on the previously derived four-dimensional data set. Randomise, FSL's tool for nonparametric permutation inference on neuroimaging data, was used with 5000 permutations to perform non-

parametric statistics (Winkler et al., 2014). We used the threshold-free cluster enhancement (TFCE) technique to correct for multiple comparisons (Smith and Nichols, 2009). Brain structures were identified using the Harvard-Oxford atlas integrated in FSL.

Statistical analysis

Differences in age and gender between patients and control subjects in which the template was defined, were analyzed with an independent sample t-test (age) and a chi-square test (gender). The relationship between SCN integrity and clinical measures was investigated using general linear modeling within the PD group, adjusted for gender, age and disease duration. Associations were studied between SCN integrity scores (dependent variable) and the MDS-UPDRS motor score, and between SCN integrity scores and the SENS-PD score. Bonferroni correction was applied to account for multiple comparisons (p-value: 0.05/18 = 0.003). If the integrity score of a network showed a statistically significant association with the MDS-UPDRS motor score or the SENS-PD score, we examined associations between the SCN integrity score and the domains scores of the concerning clinical scale. A Bonferroni correction was applied across the different networks (p-value = 0.05/number of items of the concerning clinical score, i.e. six domains of the SENS-PD and four of the MDS-UPDRS motor score). To investigate whether dosage of dopaminergic medication could affect structural networks, we examined associations between the SCN integrity scores and LDE scores within the PD group who used dopaminergic medication. To study group differences between de novo patients and patients who used dopaminergic medication, we performed additional general linear modeling analyses in which network integrities were treated as dependent variables and the group (de novo patients or patients who used dopaminergic medication) as an independent, fixed, variable, while adjusting for age and gender. SPSS version 23.0 was used for all analyses (IBM SPSS Statistics for Mac, Version 23.0. Armonk, NY: IBM Corp.).

RESULTS

Demographic characteristics

159 patients were included in the analysis. Demographic and clinical data of all participants are shown in table 1.

Table 1. Main characteristics of participants

	Patients	Control subjects	
N	**159**	**370**	***P*-value**
Men/women	101/58 (63.5)	178/ 192 (48.1)	0.001
Age, year	64.9 (7.1)	65.7 (6.7)	0.234
Disease duration, year	9.1 (4.8)		
MDS-UPDRS motor score (0-132)	34.3 (15.7)		
SENS-PD, n=153 (0-54)	13.0 (6.1)		
MMSE, n=156 (0-30)	28.4 (1.8)		
Total LDE, mg/day, n=129	1010.2 (561.2)		
Dopaminergic drug-naïve patients, n=2	-		
De novo patients[a], n=22	-		
LDE-Dopa, mg/day, n=154	735.1 (507.5)		
LDE-DA dose, mg/day, n=153	198.0 (216.7)		

Values are means (standard deviation) for continuous variables, numbers for gender (% men). For all measurement instruments, the score range is presented in parentheses. SD: standard deviation; MDS-UPDRS: Movement Disorder Society unified Parkinson's disease rating scale; SENS-PD: severity of non-dopaminergic symptoms in Parkinson's disease; MMSE: mini-mental state examination; LDE: Levodopa dosage equivalent; DA: dopamine agonists.

[a] De novo patients were defined as dopaminergic drug-naïve patients with a disease duration shorter than five years.

Structural covariance network integrity

Of the nine SCNs, the integrity of the posterior and anterior cingulate network (SCN c and d) both showed a negative association with the SENS-PD score ($p = 0.001$ and $p = 0.001$, respectively; table 2). The integrity of the anterior cingulate network showed a negative association with the MDS-UPDRS motor score ($p = 0.032$). After correction for multiple comparisons, the associations between the posterior and anterior cingulate network and the SENS-PD score remained significant (table 2).

As the associations between the posterior and anterior cingulate network and the total SENS-PD score were significant, the associations between SCN integrity of the cingulate networks and the domain scores of the SENS-PD scale (postural instability and gait difficulty, cognitive impairment, depressive symptoms, psychotic symptoms, excessive daytime sleepiness and autonomic symptoms) were subsequently tested. The SCN integrity scores of the posterior and anterior cingulate network were negatively associated with cognitive impairment (posterior cingulate network: $\beta = -0.309$, $p < 0.001$, $\eta_p^2 = 0.097$; anterior cingulate network: $\beta = -0.162$, $p = 0.049$, $\eta_p^2 = 0.026$) and excessive daytime sleepiness (posterior

cingulate network: $\beta = -0.172$, $p = 0.021$, $\eta_p^2 = 0.034$; anterior cingulate network: $\beta = -0.213$, $p = 0.005$, $\eta_p^2 = 0.051$). After correction for multiple comparisons, the association between the posterior cingulate network and cognitive impairment remained significant. The association between the anterior cingulate network and EDS remained significant as well. No significant associations were found between the SCN integrity and the domain scores of postural instability and gait difficulty, depressive symptoms, psychotic symptoms and autonomic symptoms. The associations between SCN integrity and the different domain scores of the MDS-UPDRS motor scale (i.e., tremor, rigidity, bradykinesia and postural instability and gait difficulty) were not tested because no significant associations were found between SCN integrity scores and the total MDS-UPDRS motor score after correction for multiple comparisons. We found that LDE score was not associated with SCN integrity scores. For none of the nine SCNs, a significant group difference in SCN integrity score was shown between de novo patients and patients who used dopaminergic medication.

Table 2. Associations between the SCN integrity scores and the composite clinical measures (MDS-UPDRS motor scale; SENS-PD scale)

		MDS-UPDRS motor score		**SENS-PD score**	
	Predominant brain region in SCN	**Beta**	***P*-value (η_p^2)**	**Beta**	***P*-value (η_p^2)**
SCN a	Thalamus	-.052	0.511 (.003)	.040	0.617 (.002)
SCN b	Lateral occipital cortex	-.075	0.348 (.006)	-.052	0.520 (.003)
SCN c	Posterior cingulate cortex	-.155	0.052 (.024)	-.264	0.001 (.074)*
SCN d	Anterior cingulate cortex	-.172	0.032 (.030)	-.265	0.001 (.070)*
SCN e	Temporal pole	-.071	0.418 (.004)	-.025	0.785 (.001)
SCN f	Putamen	.012	0.879 (.000)	.024	0.769 (.001)
SCN g	Cerebellum	.094	0.260 (.008)	.087	0.311 (.007)
SCN h	Cerebellum	.119	0.156 (.013)	.014	0.868 (.000)
SCN i	Cerebellum	.012	0.891 (.000)	.037	0.677 (.001)

SCN: structural covariance network; MDS-UPDRS: Movement Disorder Society unified Parkinson's disease rating scale; SENS-PD: severity of non-dopaminergic symptoms in Parkinson's disease. Beta: standardized β; η_p^2: partial eta squared.

* *P*-value remained significant after correction for multiple comparisons. All analyses were adjusted for age, gender and disease duration.

Voxel-based analyses

Loss of integrity in a SCN is due to grey matter changes in one or more component(s) in the network. To detect which components were specifically

atrophied, voxel-based analysis within the posterior and anterior cingulate network was performed. We used the domain score of cognitive impairment to examine decreased grey matter in the posterior cingulate network and excessive daytime sleepiness to examine decreased grey matter in the anterior cingulate network, as is shown in figure 1. Large clusters of grey matter volume reductions in the posterior cingulate network related to cognitive impairment were localized in the posterior cingulate cortex ($p = 0.002$, peak cluster MNI coordinates: 0, −52, 24, voxel size = 509) and the central operculum cortex ($p < 0.001$, peak cluster MNI coordinates: 54, −2, 4, voxel size = 786). Smaller clusters of decreased grey matter were found in the subcallosal cortex ($p = 0.015$, peak cluster MNI coordinates: 0, 16, −12, voxel size = 103), the parietal operculum cortex ($p = 0.046$, peak cluster MNI coordinates: 38, −22, 18, voxel size = 21) and the posterior middle temporal gyrus ($p = 0.020$, peak cluster MNI coordinates: −58, −34, −10, voxel size = 28). In the anterior cingulate network, decreased grey matter related to excessive daytime sleepiness was found in the middle frontal gyrus ($p = 0.014$, peak cluster MNI coordinates: 36, 16, 48, voxel size = 191), the frontal medial cortex ($p = 0.007$, peak cluster MNI coordinates: −4, 52, −20, voxel size = 252) and the cuneus ($p = 0.013$, peak cluster MNI coordinates: 2, −86, 18, voxel size = 178).

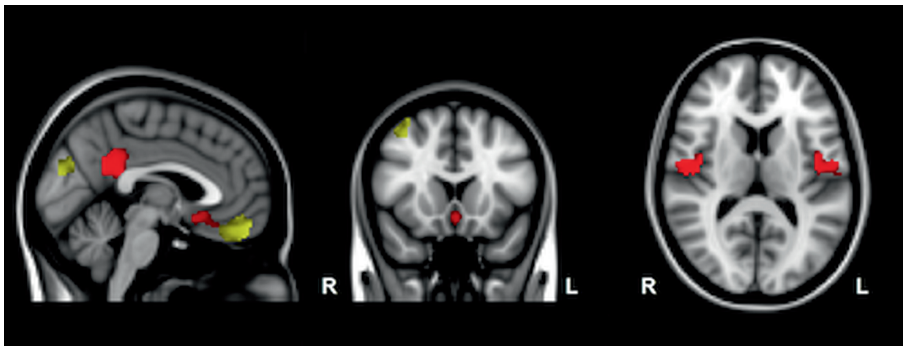


Figure 1. Regional grey matter changes in PD patients. Red: Reduced grey matter in the posterior cingulate network related to cognitive impairment. Yellow: Reduced grey matter in the anterior cingulate network related to excessive daytime sleepiness. Images are overlaid on the most informative sagittal, coronal and transversal slices of the MNI (Montreal Neurological Institute) standard anatomical image (MNI coordinates are −2, 18, 12). Results with a threshold-free cluster enhancement (TFCE)-familywise error (FWE) corrected p-value < 0.05 and a voxel size above 30 are shown.

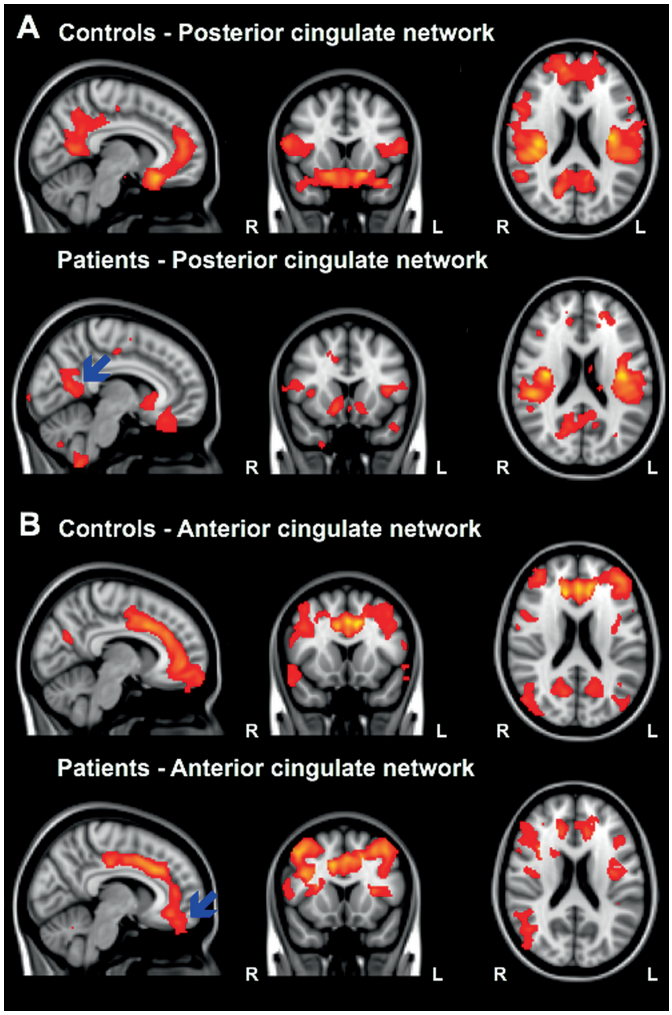


Figure 2. Cingulate networks defined in healthy control subjects and in patients. Both cingulate networks defined in healthy control subjects and in patients with Parkinson's disease, overlaid on the most informative sagittal, coronal and transversal slices of the MNI (Montreal Neurological Institute) standard anatomical image (MNI coordinates are 8, −14, 20). A: Posterior cingulate network. B: Anterior cingulate network.

Cingulate networks in patients with PD

To visualize the abnormal architecture of both cingulate SCNs, the networks were also defined in all patients with PD. As is shown in figure 2, some components of

the cingulate networks identified in healthy control subjects are missing in the networks identified in patients with PD. These missing components do not significantly co-vary in grey matter density with the network. The most prominent changes are seen in the anterior (figure 2A and B) and posterior cingulate cortex (figure 2A) and the frontal medial cortex (figure 2B).

DISCUSSION

Within individuals across a population, spatially distributed regions of the brain, which are functionally linked, may show a structural covariance of grey matter volume. Although the neurobiological underpinnings of SCNs and functional covariance network associations are unclear, it has been posited that SCNs reflects shared long-term trophic influences within functionally synchronous systems (Zielinski et al., 2010). Recently, nine SCNs were established in 370 healthy elderly (Hafkemeijer et al., 2014). In four out of nine SCNs (subcortical network, sensorimotor network, posterior cingulate network, anterior cingulate network), grey matter volume decreased with advancing age. Given the important role of age in the development and prognosis of PD, we examined the influence of PD on the topological organization of nine SCNs established in healthy elderly. Our study led to two main findings: (1) only the anterior and posterior cingulate SCN showed a loss of integrity beyond the effects of aging; (2) the reduced integrity of both cingulate SCNs was significantly associated with predominantly non-dopaminergic domains, including cognitive impairment and excessive daytime sleepiness.

To unravel if specific regions that make up the SCNs explained the clinical associations, we studied grey matter changes within both networks in relation to these two predominantly non-dopaminergic domains. The largest clusters of decreased grey matter were found in relation to cognitive impairment in two regions of the posterior cingulate network: central operculum cortex and posterior cingulate cortex. Compared to cognitive impairment, smaller clusters of decreased grey matter, albeit still significant associations, were found for excessive daytime sleepiness in three regions of the anterior cingulate network: frontal medial cortex, middle frontal gyrus and cuneus. Collectively, these findings are in line with those of others indicating a role of the cingulate cortex in mediating processes involved in cognition and vigilance in patients with PD (Leech and Sharp, 2014; Menon and Uddin, 2010; Zielinski et al., 2010).

Cognitive impairment is an important non-motor feature of PD, which reflects the variable and interacting dysfunction in a number of diffusely distributed, yet interrelated, neural networks that contribute to distinct cognitive

processes (Gratwicke et al., 2015). Compelling evidence shows that structural and functional abnormalities of the posterior cingulate cortex are found in neurological and psychiatric diseases, e.g. Alzheimer's disease, schizophrenia, autism, depression and attention deficit hyperactivity disorder (Leech and Sharp, 2014). Congruent with results of other studies in PD, our study shows that abnormalities of the posterior cingulate cortex are associated with cognitive impairment (Christopher et al., 2015; Leech and Sharp, 2014).

In PD, excessive daytime sleepiness has been found associated with various clinical factors, including cognitive impairment, postural instability and gait difficulty, hallucinations, advanced disease, and dopaminergic medication (Tholfsen et al., 2015; Zhu et al., 2016). The neurological substrates of excessive daytime sleepiness are incompletely understood, but likely involve extended subcortical-cortical networks acting to promote arousal and sleep (Brown et al., 2012). The anterior cingulate network shows spatial overlap with the functional connectivity salience network (Seeley et al., 2007). The salience network is considered to be involved in the integration of internal and external stimuli, supporting the association we found with excessive daytime sleepiness (Seeley et al., 2007). Our findings showing involvement of multiple regions of the anterior cingulate network, are congruent with those of two other studies showing cortical atrophy of occipital and frontal brain regions in PD patients with excessive daytime sleepiness as compared to PD patients without excessive daytime sleepiness (Gama et al., 2010; Kato et al., 2012).

Our patients had mild to moderate disease severity and a mean disease duration of approximately nine years. In PD, cortical alpha-synuclein aggregation occurs in advanced stages and except for the cingulate gyrus, neocortical regions have low frequencies of alpha-synuclein aggregation (Beach et al., 2009; Jellinger, 2012). However, the functional consequences of alpha-synuclein aggregation in the brain are unclear and Braak stages are not related to clinical severity of PD (Schulz-Schaeffer, 2010). Recent evidence proposes that diverse molecular and cellular pathologies involved in PD can give rise to common patterns of dysfunction at the neural systems level (Gratwicke et al., 2015).

The finding that reduced anterior and posterior cingulate network integrity is associated with two different categories of predominantly non-dopaminergic symptoms, may suggest that (components) of both SCNs act as an integrative hub. Indeed, it is suggested that both the anterior and posterior cingulate cortex may operate as important interfaces between different functional networks involved in cognition and alertness (Leech and Sharp, 2014; Menon and Uddin, 2010).

Cognition and alertness are regulated by large-scale functional networks, consisting of numerous interconnected brain areas, which act (dynamically) in concert to perform the circumscribed functions (Leech and Sharp, 2014; Seeley et al., 2007). These large-scale brain networks comprise cortical and subcortical areas and their interconnecting structural or functional connections. Some brain areas perform important integrative roles in networks (hubs) because they display an unusually high degree of intermodular connectivity which is not critical to distinctive functions of the brain (van den Heuvel et al., 2013). Findings from a human brain structural connectivity study using diffusion imaging and tractography suggest that damage to hub regions has a larger disruptive effect on network communication than damage to non-hub regions of a network (van den Heuvel et al., 2013). This finding may explain why damage of two cingulate structural networks is associated with important dysfunctions on the level of cognition and vigilance.

Strengths and limitations

The strength of this study lies in detecting grey matter changes with a novel network-based technique in a large group of clinically well characterized PD patients with simultaneous acquired MR images. Limitations of our study are related to the cross-sectional design. A longitudinal design is preferable to assess the relationship between network integrity and disease progression. Further, our population is characterized by patients with mild to moderate disease severity, limiting the generalizability of the results to the PD population at large. Nonetheless, it is notable that even in these patients SCN analysis was able to detect distinct regions of grey matter atrophy, which were related to severity of predominantly non-dopaminergic symptoms in two domains. Patients were tested while on dopaminergic medication. In addition, the depression scale (the Hospital Anxiety and Depression Scale) (Zigmond and Snaith, 1983), from which items for the depression domain of the SENS-PD were taken, inquires after symptoms in the last week and was completed in the week before the MRI was made, when patients took their regular medication. We cannot rule out that this may have resulted in a decrease of symptom scores that show some sensitivity to dopaminergic influences and possibly have attenuated the examined associations. This likely played a less prominent role with regard to the total SENS-PD scale, which includes symptoms that mainly do not improve with dopaminergic medication, although there are potentially some positive effects on depression (Chaudhuri and Schapira, 2009).

Conclusion

In conclusion, SCN analysis in mild to moderate PD revealed a loss of integrity of the anterior and posterior cingulate SCN, which in turn was explained by grey matter loss in specific brain regions within the networks. The identified structural changes were associated with cognitive impairment and excessive daytime sleepiness, suggesting that components of both cingulate SCNs may operate as important interfaces between different functional networks involved in cognition and alertness.

3 Regional structural hippocampal differences between dementia with Lewy bodies and Parkinson's disease

Journal of Parkinson's disease (2019) 9:775-783. doi: 10.3233/JPD-191600

Laura de Schipper[1]
Anne Hafkemeijer[2,3,4]
Jeroen van der Grond[2]
Johan Marinus[1]
Johanna Henselmans[5]
Jacobus van Hilten[1]

[1] Leiden University Medical Center, Department of Neurology, Leiden, the Netherlands,

[2] Leiden University Medical Center, Department of Radiology, Leiden, the Netherlands

[3] Leiden University, Department of Methodology and Statistics, Institute of Psychology, Leiden, the Netherlands

[4] Leiden University, Leiden Institute for Brain and Cognition, Leiden, the Netherlands

[5] Antonius Hospital, Department of Neurology, Woerden, the Netherlands

ABSTRACT

Introduction: Dementia with Lewy bodies (DLB) and Parkinson's disease (PD) are considered subtypes of the alpha-synucleinopathy continuum that show similar and dissimilar clinical and morphological features. To further our understanding of brain abnormalities that might differentiate both disorders more clearly, we performed quantitative magnetic resonance (MR) imaging of the subcortical and cortical grey matter.

Methods: Three-dimensional T1 weighted 3 tesla MR images of 14 DLB and 62 age- and gender-matched PD patients were examined to study cortical and subcortical grey matter structure. We used volumetric measurements to study total grey matter, and volumes of the pallidum, amygdala, putamen, caudate nucleus, thalamus and hippocampus. Whole-brain and structural network-based methods were used to identify local differences in grey matter and vertex-based shape analysis was used to assess focal hippocampal changes.

Results: Volumetric, whole-brain and network-based analyses showed reduced hippocampal ($p = 0.008$) and right parahippocampal region volumes ($p = 0.030$) in DLB compared to PD patients. Shape analysis showed atrophy in the head and body of the right ($p = 0.040$) and in the head of the left ($p = 0.030$) hippocampus of DLB patients.

Conclusion: DLB patients showed atrophy of the hippocampus and parahippocampal gyrus compared to PD patients with a differential involvement of the head and body of the hippocampus. Further studies should examine if these group-based findings can be used to differentiate both disorders on an individual level.

INTRODUCTION

Dementia with Lewy bodies (DLB) and Parkinson's disease (PD) are both conditions characterized by the presence of alpha-synuclein in Lewy bodies and Lewy neurites (Jellinger, 2009). Clinical features of patients with DLB and PD overlap, such as symptoms of parkinsonism, psychiatric/behavioral symptoms, autonomic dysfunction and cognitive impairment (McKeith et al., 2017; Postuma et al., 2015).

However, the timing of symptoms, progression rate, and severity are different, and DLB patients show a decreased efficacy and tolerance of medication. DLB is diagnosed when dementia occurs before or concurrently with parkinsonism (McKeith et al., 2017). On the contrary, dementia occurring in the presence of well-established PD, is classified as PD with dementia (PDD) (McKeith et al., 2017). It is debated whether this distinction is valid (Postuma et al., 2016, 2015), as it is increasingly recognized that cognitive impairment and dementia are common in all stages of PD, and it is the only common manifestation of both disorders that is being regarded in this manner (Chahine et al., 2016; Postuma et al., 2016).

At present, a clear distinction, if at all possible, between both disorders is also difficult, because the exact pathogenic mechanisms underlying the clinical heterogeneity are unknown. Previous structural MRI studies have shown grey matter atrophy in DLB and PD patients compared to control subjects (Mak et al., 2014; Pan et al., 2012; Sterling et al., 2016; Watson and Colloby, 2016). Notably, there is evidence that there may be structural brain differences in grey matter between DLB and PD patient as well. However, until now, most studies focused on differences between DLB patients and healthy control subjects, patients with Alzheimer's disease and patients with PDD (Mak et al., 2014). One study compared total grey matter of DLB and PD patients and showed more pronounced atrophy in DLB (Borroni et al., 2015), although DLB and PD groups were not matched for age or gender in this study, which may have influenced the results. Reduced cortical and subcortical volumes have further been found in DLB compared to PD patients, using region of interest approaches (Gazzina et al., 2016; Kenny et al., 2008; Tam et al., 2005).

In the present study, we therefore evaluated if whole-brain and network-based magnetic resonance imaging (MRI) approaches to measure total and subcortical grey matter volume(s), may contribute in differentiating both disorders more clearly. Finally, vertex-based shape analysis was used to assess focal changes of subcortical structures.

METHODS

Study design and participants

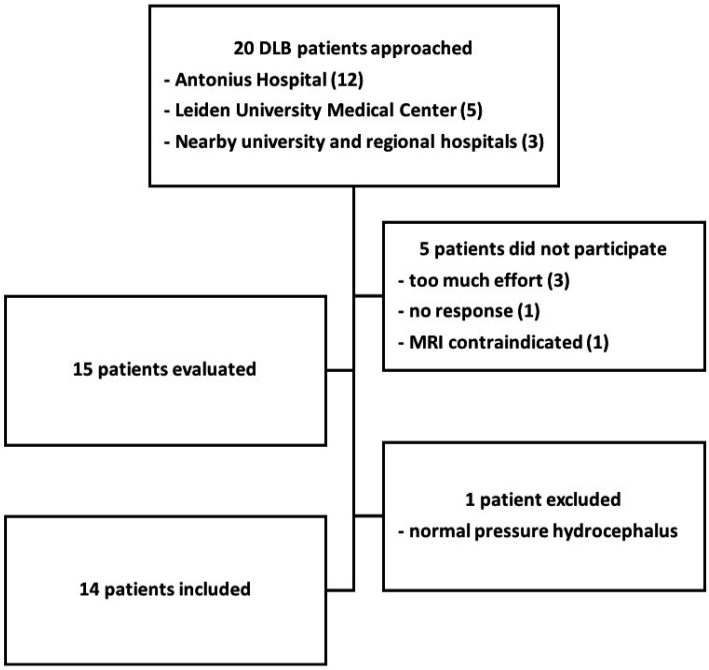


Figure 1. Flowchart of inclusion for DLB patients.

The present cross-sectional study is part of the Profiling Parkinson's disease (PROPARK) study. Patients were recruited from the outpatient clinic for Movement Disorders of the Department of Neurology of the Leiden University Medical Center (LUMC, Leiden, the Netherlands) and nearby university and regional hospitals between January 2013 and January 2016. Evaluations occurred at the LUMC. Fourteen DLB patients were included (figure 1). Sixty-two PD patients were selected from the PROPARK cohort, matched at group level for age and gender to the DLB patients. All PD patients fulfilled the United Kingdom Parkinson's Disease Society Brain Bank criteria for idiopathic Parkinson's disease (Gibb and Lees, 1988) and all DLB patients fulfilled the McKeith diagnostic criteria for probable DLB (McKeith et al., 2005). Patients were diagnosed with DLB or PD by a movement disorder specialist. Exclusion criteria were: previous or other disorders of the central nervous system, peripheral nerve disorders influencing motor and/or

autonomic functioning, and psychiatric comorbidity not related to PD. All participants or his/her closest relative provided written informed consent according to the Declaration of Helsinki. Ethical approval was given by the Medical Ethics Committee of the LUMC.

Clinical assessments

All patients underwent standardized assessments, including an evaluation of demographic and clinical characteristics. Participants were tested while on dopaminergic medication (except for nine drug-naïve PD and eight drug-naïve DLB patients). The Movement Disorder Society unified Parkinson's disease rating scale (MDS-UPDRS) motor scale (part III) was used to quantify the severity of motor signs (Goetz et al., 2008). Additionally, the severity of non-dopaminergic symptoms in Parkinson's disease (SENS-PD) scale was used (van der Heeden et al., 2016), which is a composite score comprising three items with four response options (0-3) from each of the following domains: postural instability and gait difficulty, psychotic symptoms, excessive daytime sleepiness, autonomic dysfunction, cognitive impairment and depressive symptoms (total range: 0-54). These six domains represent a coherent complex of symptoms that largely do not improve with dopaminergic medication, that is already present in the early disease stages and increases in severity when the disease advances. Higher scores on both scales reflect more severe impairment. The mini-mental state examination (MMSE) (Folstein et al., 1975) and scales for outcomes in Parkinson's disease - cognition (SCOPA-COG, cognitive functioning, range 0-43) were used to assess cognitive performance. The SCOPA-COG is a valid and reliable instrument examining the following domains: memory, attention, executive functioning and visuospatial functioning (Marinus et al., 2003); lower scores reflect more severe impairment. Hallucinations were quantified using the hallucination item of the SCOPA - psychiatric complications (PC, range 0 -3) scale (Visser et al., 2007). A levodopa dose equivalent (LDE) of daily levodopa (LDE-Dopa), dopamine agonists (LDE-DA), as well as a total LDE was calculated according to the formula developed by Tomlinson et al. (Tomlinson et al., 2010).

MRI analyses

Three-dimensional T1-weighted images were acquired on a 3 Tesla MRI scanner (Philips Achieva, Best, the Netherlands) with the following parameters: repetition time = 9.8 ms, echo time = 4.6 ms, flip angle = 8°, field of view 220 x 174 x 156 mm, 130 slices with a slice thickness of 1.2 mm with no gap between slices,

resulting in a voxel size of 1.15 mm × 1.15 mm × 1.20 mm. All MRI scans were visually checked to ensure that no major artifacts or abnormalities were present in the data. Analyses were done using the software provided by FMRIB's software library (FSL, version 5.0.8, Oxford, United Kingdom) (Smith et al., 2004). Brain structures were identified using the Harvard-Oxford atlas integrated in FSL.

Volumetric measurements

Grey matter volume was estimated with structural image evaluation, using normalization, of atrophy cross-sectional (SIENAX) (Smith et al., 2002), starting by extracting brain and skull images from the T1-weighted images. The brain image is then affine-registered to Montreal Neurological Institute (MNI) standard space, using the skull image to determine the registration scaling. This is primarily done in order to obtain the volumetric scaling factor, to be used as a normalization for head size. Next, tissue-type segmentation with partial volume estimation is carried out in order to calculate total volume of brain tissue and separate estimates of volumes of grey and white matter. FMRIB's integrated registration and segmentation tool (FIRST) (Patenaude et al., 2011) was used to determine volumes of the hippocampus, pallidum, amygdala, putamen, caudate nucleus and thalamus in cm^3. FIRST starts by registering each brain image to MNI standard space and fits models for the different structures (meshes) to the images. Boundary correction is applied for the volumetric output.

Voxel-based morphometry

VBM was used to investigate voxel-wise differences in grey matter volume between DLB and PD patients (Douaud et al., 2007; Good et al., 2001; Smith et al., 2004). Structural images were brain-extracted and grey matter-segmented before being registered to the MNI standard space using non-linear registration. The resulting images were averaged and flipped along the x-axis to create a left-right symmetric, study-specific grey matter template with the same number of DLB and PD subjects, in order to create an unbiased template. All native grey matter images were non-linearly registered to this study-specific template and modulated to correct for local expansion (or contraction) due to the non-linear component of the spatial transformation. The modulated grey matter images were then smoothed with an isotropic Gaussian kernel with a sigma of 3 mm and concatenated into a four-dimensional data set, which was also used for further network analyses. A voxel-wise general linear model was applied to the four-dimensional data set, using permutation-based non-parametric testing (Winkler et al., 2014), with 5000

permutations, correcting for multiple comparisons across space. The statistical threshold was set at $p < 0.05$, familywise error corrected, using the threshold-free cluster enhancement (TFCE) technique (Smith and Nichols, 2009). A grey matter mask was applied in the statistical analysis and age and gender were used as covariates in the model.

Structural covariance networks

Computational network-based analyses are increasingly important in uncovering patterns of brain atrophy, which are not readily apparent by regional structural analysis. It is suggested that anatomical structures that are spatially distributed but functionally linked, co-vary in grey matter density within individuals across a population. These structural covariance networks (SCNs) can be affected by factors like age and disease. We used nine bilateral standardized SCNs, for detailed information see Hafkemeijer et al. (2014). The networks were derived using an independent component analysis, a statistical technique that is also commonly used to study functional network integrity. It defines spatial component maps of maximal statistical independence. The four-dimensional data set of grey matter images derived from our participants was used in a spatial regression against the standard SCN probability maps, using a general linear model approach integrated in FSL to calculate individual SCN integrity scores. The integrity score is the beta coefficient of the regression analysis, reflecting the strength of the individual expression in each network. High scores indicate strong individual network expression.

Vertex-based shape analysis

We subsequently analyzed the hippocampal shape differences between DLB and PD patients on a per-vertex basis using hippocampal output from FIRST (Patenaude et al., 2011). Vertex locations from each subject (at a corresponding anatomical point) are projected on a surface constructed from the average shapes of all participants. The projections are scalar values that represent the signed, perpendicular distance from the average surface, where a positive value is outside the surface and a negative value is inside. The projection values were stored in a four-dimensional data set, which was used to calculate significant differences in shape between the groups. A general linear model was used with an F-test, cluster-based thresholding corrected for multiple comparisons (Patenaude et al., 2011). Age and gender were used as covariates in the statistical model.

Statistical analyses in SPSS

Demographic characteristics were compared using an independent-sample *t*-test (age) and a chi-square test (gender, number of drug-naïve patients for dopaminergic medication). Differences in normalized total grey matter volume between DLB and PD patients were analyzed with a univariate analysis of variance, adjusted for age and gender. Subcortical structure volume differences were studied using a univariate analysis of variance, adjusted for age, gender and unnormalized total brain volume. Differences in gray matter network scores were studied using a univariate analysis of variance, adjusted for age and gender. Within DLB patients, we investigated correlations between hippocampal volumes, SENS-PD and cognitive performance (SCOPA-COG and MMSE scores) and hallucinations using Spearman's rank correlation coefficient. SPSS version 23.0 was used for all statistical analyses (IBM SPSS Statistics for Mac, Version 23.0. Armonk, NY: IBM Corp.).

RESULTS

Table 1. Main characteristics of participants

	DLB patients	PD patients	
N	**14**	**62**	***P*-value**
Men/women	11/3	44/18	0.745
Age, years	73.1 (6.0)	71.9 (4.1)	0.597
Disease duration, years	5.5 (3.4)	8.7 (4.2)	0.011*
MDS-UPDRS motor score (0-132)	36.5 (19.5)	39.2 (16.7)	0.608
SENS-PD (0-54)[a]	24.5 (8.0)	16.2 (5.9)	<0.001*
MMSE[b]	20.5 (6.0)	28.3 (1.7)	<0.001*
SCOPA-COG (0-43)[c]	17.1 (5.9)	24.9 (4.1)	<0.001*
SCOPA PC hallucination item (0-3)[d]	0 (2)^	0 (0)	<0.019*
Total LDE, mg/day[e]	389.7 (283.2)	935.7 (513.6)	0.014*
Drug-naïve patients	8	9	0.001*
Grey matter volume, normalized	665.3 (32.7)	680.7 (40.7)	0.335

Values are means (standard deviation) for continuous variables, numbers for gender and median (interquartile range) for hallucinations. For all measurement instruments, the score range is presented in parentheses. MDS-UPDRS: Movement Disorder Society-unified Parkinson's disease rating scale; SENS-PD: severity of non-dopaminergic symptoms in Parkinson's disease; MMSE: minimal mental state examination; SCOPA-COG: SCOPA cognition; PC: psychiatric complications; LDE: Levodopa dosage equivalent; n/a: not applicable.

^ range: 0–3. DLB/PD: [a] N = 11/58, [b] N = 14/60, [c] N = 12/57, [d] N = 13/62 [e] N = 6/51, * $p < 0.05$.

There were no significant differences in gender, age and motor symptom severity (MDS-UPDRS III score) between the groups (table 1). The mean disease duration was 3 years shorter in DLB compared to PD patients. DLB patients had a higher predominantly non-motor symptoms burden (SENS-PD score: 8 points difference). Both groups had cognitive deficits, but DLB patients were more cognitively impaired than PD patients (SCOPA-COG: 8 points difference, range 0-43 and MMSE score: 8 points difference, range 0-30). DLB patients had more (severe) hallucinations than PD patients, as the latter had no or only mild hallucinations with complete insight. Six DLB patients used dopaminergic medication, these patients used on average 546 mg/day less dopaminergic medication than PD patients. No differences in normalized total grey matter volume were found.

Voxel-based morphometry

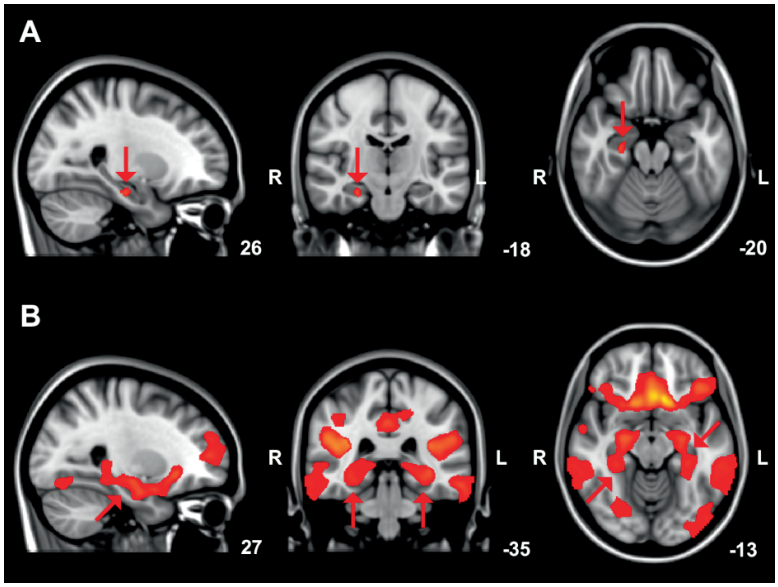


Figure 2. 2A: Brain areas showing reduced (red, red arrows) grey matter volume in DLB compared to PD patients, overlaid on the MNI standard cerebral image with accompanying coordinates. Results with a threshold-free cluster enhancement (TFCE) familywise error corrected p-value < 0.05 are shown. 2B: Grey matter structural covariance posterior cingulate cortex network (red), overlaid on the most informative slices of the MNI standard cerebral image with accompanying coordinates. Red arrows indicate the parahippocampal gyrus and hippocampus.

Whole brain voxel-wise differences in grey matter volume are shown in figure 2A. DLB patients showed reduced grey matter compared to PD patients in the right hippocampus and right parahippocampal regions (figure 2A, red areas, p = 0.030 most significant voxel).

Volumetric measurements

Mean total hippocampal volume was 0.7 cm^3 lower in DLB compared to PD patients (table 2). Volume estimates were also performed for the left and right hippocampus separately and showed lower hippocampal volumes in DLB compared to PD patients in both the right (p = 0.009, mean difference 0.4 cm^3) and left (p = 0.026, mean difference 0.3 cm^3) hemisphere. In the DLB group, associations between hippocampal volume and cognitive performance were tested and showed a correlation coefficient of 0.572 (MMSE score; p = 0.033; right hippocampus: r_s = 0.619, p = 0.018; left hippocampus: r_s = 0.384, p = 0.176) and 0.371 (SCOPA-COG score; p = 0.235; right hippocampus: r_s = 0.308, p = 0.330; left hippocampus: r_s = 0.228, p = 0.477). For hippocampal volume and predominantly non-motor symptom severity (SENS-PD score) Spearman's rho was 0.055 (p = 0.873; right hippocampus: r_s = 0.023, p = 0.947; left hippocampus: r_s = 0.077, p = 0.821). The correlation coefficient for hippocampal volume and hallucinations (hallucination item SCOPA-PC) in the DLB group was -0.477 (p = 0.100; right hippocampus: r_s = -0.547, p = 0.053; left hippocampus: r_s = -0.358, p = 0.229).

Table 2. Volumetric measurements

	DLB patients	PD patients	
N	**14**	**62**	***P*-value**
Hippocampus	6.4 (0.3)	7.1 (0.1)	0.008*
Pallidum	3.5 (0.2)	3.6 (0.1)	0.458
Amygdala	2.4 (0.1)	2.3 (0.1)	0.444
Putamen	8.5 (0.3)	8.8 (0.1)	0.291
Caudate nucleus	6.7 (0.2)	6.6 (0.1)	0.666
Thalamus	13.9 (0.3)	14.2 (0.1)	0.284

Values are estimated marginal means in cm^3 (standard error), reported as the combined volume of right and left regions, adjusted for age and gender and unnormalized total brain volume. *p < 0.05.

Vertex-based shape analysis

Based on the findings of the volumetric measurements and VBM we performed a vertex-based shape analysis to explore potential shape differences of the hippocampus between DLB and PD patients. Atrophy was found in the head and

body of the right (p = 0.040; figure 3) and in the head of the left hippocampus (p = 0.030; figure 3) of DLB compared to PD patients.

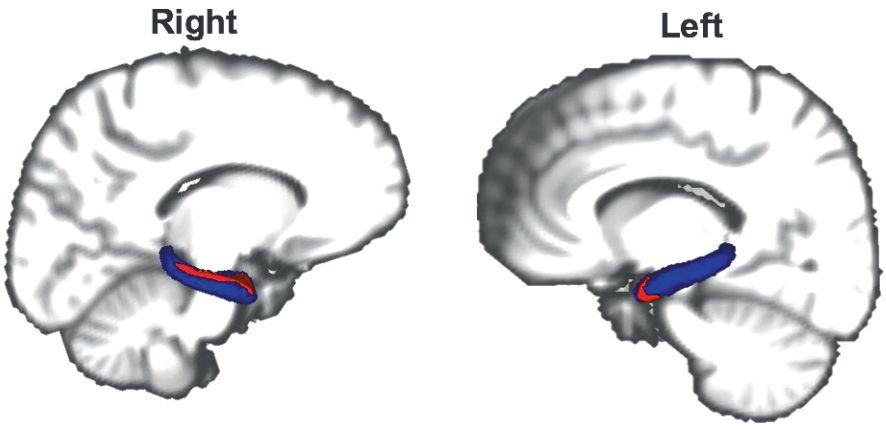


Figure 3. Atrophy (red) of the hippocampus (blue) in DLB compared to PD patients. Results with familywise error corrected p-value <0.05 are shown.

Structural covariance networks

Table 3. Structural covariance networks

		DLB patients	PD patients	
N		**14**	**62**	***P*-value**
A	Thalamus network	0.003 (0.002)	0.001 (0.001)	0.472
B	Lateral occipital cortex network	0.018 (0.002)	0.019 (0.001)	0.471
C	Posterior cingulate cortex network	0.044 (0.002)	0.050 (0.001)	0.009*
D	Anterior cingulate cortex network	0.026 (0.002)	0.028 (0.001)	0.572
E	Temporal pole network	0.005 (0.002)	0.006 (0.001)	0.391
F	Putamen network	0.019 (0.002)	0.019 (0.001)	0.825
G	Cerebellum network	0.031 (0.002)	0.030 (0.001)	0.922
H	Cerebellum network	0.016 (0.002)	0.016 (0.001)	0.959
I	Cerebellum network	0.006 (0.002)	0.008 (0.001)	0.134

Structural covariance networks are named based on the predominant brain region in the network. Values are estimated marginal means (standard error), adjusted for age and gender.
* $p < 0.05$.

Integrity scores of nine structural covariance grey matter networks are shown in table 3. In DLB patients, the integrity of the anatomical posterior cingulate cortex network (network C: comprising regions of the parahippocampal gyrus and hippocampus; figure 2B) was significantly lower than in PD patients ($p = 0.009$). No significant differences were found in the other eight structural covariance networks between DLB and PD.

DISCUSSION

The results of this study using different MRI approaches to evaluate grey matter show a consistent (para)hippocampal volume loss in DLB compared to PD patients. Vertex-based shape analysis further showed atrophy in the head and body of the right and head of the left hippocampus in DLB compared to PD patients. Except for (para)hippocampal atrophy in DLB patients, no other structural differences in grey matter between DLB and PD patients were found.

The findings in this study are in line with the results of earlier studies (Gazzina et al., 2016; Kenny et al., 2008; Tam et al., 2005), although these studies applied region of interest approaches to investigate differences between DLB and PD. Gazzina et al. and Borroni et al. further reported lower thalamus, caudate nucleus and middle occipital gyrus volume in DLB compared to PD patients (Borroni et al., 2015; Gazzina et al., 2016). In both studies, the DLB group was older (Gazzina et al: DLB 74.4 and PD 69.4 year; Borroni et al.: DLB 74.2 and PD 66.3 year), consisted of more female subjects (Gazzina et al: DLB 43.8% and PD 18.8% female; Borroni et al.: DLB 46.2% and PD 9.1% female) and had higher MDS-UPDRS motor scores than the PD group (Gazzina et al: DLB 20.1 and PD 12.7; Borroni et al.: DLB 20.1 and PD 10.7) (Borroni et al., 2015; Gazzina et al., 2016). These differences in age, gender and motor symptom severity likely contributed to the more extensive reductions in grey matter in DLB patients as compared to the findings in our study.

Our study shows regional atrophy in the head and body of the right and head of the left hippocampus in DLB compared to PD patients. To our knowledge, this is the first study in which vertex-based shape differences between DLB and PD patients are investigated. Neuropathological studies indicate a relative preservation of the CA1 and subiculum in DLB patients versus healthy control subjects, Alzheimer's disease, and PD patients (Antony J. Harding et al., 2002; Lippa et al., 1994). MRI studies investigating hippocampal subfields in Alzheimer's disease and DLB patients report a relative preservation of the CA1 in DLB patients as well (Delli Pizzi et al., 2016; Mak et al., 2016). Collectively, the findings of all

studies indicate that further exploration of regional atrophy of the hippocampus and its subfields in differentiating DLB from PD may be worthwhile.

We found that hippocampal volume correlated with cognitive performance (MMSE score) in DLB patients, although 14 is a small sample size to perform a correlation analysis. Nevertheless, the findings are in line with previous studies reporting that atrophy of the hippocampus and parahippocampal gyrus in DLB patients is correlated with cognitive decline (Tagawa et al., 2015; Yavuz et al., 2007). Brain amyloid beta deposition, including deposition in the hippocampus, is more marked in DLB (Gomperts, 2014). Although the development of cognitive impairment and dementia seems multifactorial, brain deposition of amyloid beta is proposed to contribute to cognitive impairment in DLB and PD (Gomperts, 2014). Moreover, current data suggest that concomitant amyloid beta and alpha-synuclein pathology may act synergistically to contribute to cognitive impairment (Gomperts, 2014).

Our findings in DLB patients were most pronounced in the right hemisphere, which is in accordance with earlier studies showing prominent structural and functional alterations in the right hemisphere of DLB patients (Delli Pizzi et al., 2016; Sabattoli et al., 2008). There are indications that a predominance of the right hemisphere for visuospatial processing plays a role in visual hallucinations (Delli Pizzi et al., 2016; Jonas et al., 2014; Sanchez-Castaneda et al., 2009). DLB patients in this study had more (severe) hallucinations than PD patients and although we do not have data on the different types of hallucinations, visual hallucinations generally predominate in DLB and PD (Eversfield and Orton, 2018). Visual hallucinations are a core feature of DLB (McKeith et al., 2017) and, compared to PD, their prevalence is much higher (Antony J. Harding et al., 2002). In particular the atrophy that we found of the right parahippocampal gyrus in this study could be related to visual hallucinations in DLB patients (A. J. Harding et al., 2002; Heitz et al., 2015). Heitz et al. found a correlation between perfusion of the right parahippocampal gyrus and the severity of visual hallucinations in DLB patients (Heitz et al., 2015), while Harding et al. showed that higher Lewy body densities in the parahippocampal gyrus were associated with visual hallucinations in DLB patients (A. J. Harding et al., 2002). Another study compared DLB with AD patients and also found parahippocampal atrophy in DLB patients (Delli Pizzi et al., 2016), supporting the hypothesis that the parahippocampal gyrus plays an important role in visual hallucinations in DLB patients.

We used well-established, reproducible, data-driven methods to investigate grey matter in DLB and PD. We found consistent (para)hippocampal

volume loss in DLB compared to PD patients, despite the relatively small number of DLB patients. Nevertheless, the results should be verified in a larger number of subjects. The mean disease duration of the DLB group was shorter than of the PD group in this study and our results may have been more pronounced with similar mean disease durations in both groups. Both groups had a comparable motor symptom severity, but DLB patients had higher predominantly non-dopaminergic symptoms scores and a worse cognitive performance than PD patients. Especially cognitive performance may have contributed to the hippocampal atrophy in DLB patients that we found. An additional group of PDD patients may provide additional inside into the relationship between cognition and our findings. However, it should be considered that PDD generally develops quite late in the disease course, and a large difference in disease duration between groups might lead to difficulties in attributing potential group differences to either differences in disease duration or disease type. It should further be noted that our study was set up to examine structural grey matter differences between DLB and PD patients, and the absence of a group of healthy control subjects did not allow for the detection of regions that are affected by atrophy in both PD and DLB patients. However, previous studies have shown grey matter atrophy in PD and DLB patients as compared to healthy control subjects (Mak et al., 2014; Pan et al., 2012; Sterling et al., 2016; Watson and Colloby, 2016).

To summarize, our data unequivocally show atrophy of the hippocampus and parahippocampal gyrus in DLB patients as compared with PD patients. Vertex-based shape analysis confirmed atrophy of the hippocampus in DLB, localized in the head and body. Moreover, integrity of the anatomical network that comprised (para)hippocampal regions, was significantly lower in DLB. These findings indicate that regional hippocampal differences between DLB and PD may be important in the distinction between the two disorders.

4 Age- and disease-related cerebral white matter changes in patients with Parkinson's disease

Neurobiology of Aging. (2019) 80:203-209. doi: 10.106/j.neurobiolaging.2019.05.004

Laura de Schipper[1]
Anne Hafkemeijer[2,3,4]
Mark Bouts[2-3]
Jeroen van der Grond[2]
Johan Marinus[1]
Johanna Henselmans[1,5]
Jacobus van Hilten[1]

[1] Department of Neurology, Leiden University Medical Center, Leiden, the Netherlands
[2] Department of Radiology, Leiden University Medical Center, Leiden, the Netherlands
[3] Leiden University, Department of Methodology and Statistics, Institute of Psychology, Leiden, the Netherlands.
[4] Leiden University, Leiden Institute for Brain and Cognition, Leiden, the Netherlands
[5] Department of Neurology, Antonius Hospital, Woerden, the Netherlands

ABSTRACT

Introduction: As age and Parkinson's disease (PD) both play a role in the degeneration of brain white matter, we aimed to investigate a possible interaction effect of age and disease presence on white matter integrity in patients with PD.

Methods: We studied white matter hyperintensity (WMH) volume, global fractional anisotropy, mean diffusivity and mean magnetization transfer ratio of normal appearing white matter in 163 patients with PD and 218 age and gender-matched healthy control subjects. We investigated the relationship between age and these parameters in both groups, and interaction between age and disease presence.

Results: Patients with PD had higher total, periventricular and anterior WMH volumes as compared with control subjects. Age-related WMHs were found in both groups in periventricular and posterior, but not in anterior brain regions. Visuospatial functioning was related to total and postural instability and gait difficulty were related to periventricular WMH volume in patients with PD. Global microstructural integrity of the normal appearing white matter did not differ between patients and control subjects. In both groups, the global microstructural integrity decreased with advancing age. No age-by-disease interaction effects were found.

Conclusion: Patients with PD had a higher load of WMHs with a preferential periventricular and anterior distribution as compared with healthy control subjects. The age-related decline of white matter integrity was similar for both groups. Global microstructural integrity of the normal appearing white matter was relatively normal in patients with PD, suggesting that PD-specific changes do not exceed normal age-associated change in white matter without lesions.

INTRODUCTION

The clinical spectrum of motor and non-motor symptoms in Parkinson's disease (PD) is linked to a progressive formation of alpha-synuclein aggregates, predominantly located in presynaptic terminals (Jellinger, 2012; Kramer and Schulz-Schaeffer, 2007). The primary determinant of neurodegeneration in patient with PD may be alpha-synuclein aggregate related synaptic and axonal dysfunction (Jellinger, 2012; O'Malley, 2010; Tagliaferro et al., 2015). White matter changes represent degeneration of axons and myelin damage, and white matter degeneration is increasingly recognized in patients with PD (Chiang et al., 2017; Chondrogiorgi et al., 2016; Sterling et al., 2017).

Magnetic resonance imaging (MRI) studies have found white matter changes in patients with PD (Atkinson-Clement et al., 2017; Bohnen and Albin, 2011), but such changes may occur as a consequence of aging (Galluzzi et al., 2008; Lockhart and DeCarli, 2014). With advancing age, the prevalence of white matter hyperintensities (WMHs) increases (Galluzzi et al., 2008; Grueter and Schulz, 2012), and white matter microstructural integrity surrounding these lesions (the so called normal appearing white matter; NAWM), declines (Lockhart and DeCarli, 2014; Vernooij et al., 2008). These findings thus raise the question to what extent white matter changes in PD are related to aging.

We hypothesized that the white matter integrity decline is significantly greater in patients with PD than seen in healthy aging subjects and that there may be an age-by-PD interaction effect on white matter integrity. To this end, we compared macrostructural integrity of global white matter and the microstructural integrity of the surrounding NAWM between patients with PD and control subjects. The relationship between age and white matter integrity was estimated in both groups, and the interaction between age and disease presence was examined to investigate if age-related white matter changes are different in PD compared with healthy aging. We further explored associations of clinical variables, other than age, with white matter integrity.

METHODS

Participants

We included 163 patients with PD in this cross-sectional MRI study, which is a project of the Profiling Parkinson's disease (PROPARK) research group. Patients were recruited between 2013 and 2016 from the outpatient clinic for Movement Disorders of the Department of Neurology of the LUMC (Leiden University Medical Center; Leiden, the Netherlands) and nearby university and regional hospitals. All

patients with PD fulfilled the United Kingdom Parkinson's Disease Society Brain Bank criteria for idiopathic PD (Gibb and Lees, 1988). Exclusion criteria were previous or other disorders of the central nervous system, peripheral nerve disorders influencing motor and/or autonomic functioning, and psychiatric comorbidity not related to PD. Patients were matched at group level for age and gender with 218 healthy control subjects from the Leiden Longevity study (LLS), a study set up to identify genetic and phenotypic determinants of longevity in healthy long-living families (Altmann-Schneider et al., 2013). Written consent was obtained from all participants. The Medical Ethics Committee of the LUMC approved the PROPARK study and LLS.

Clinical assessments

Standardized assessments were performed in all patients, including an evaluation of demographic and clinical characteristics. Patients were tested while on dopaminergic medication, except for 24 "de novo" patients, defined as dopaminergic drug-naïve patients with a disease duration shorter than 5 years, and 2 other drug-naïve patients with a disease duration longer than 5 years. Motor symptoms were quantified with the Movement Disorder Society unified Parkinson's disease rating scale (MDS-UPDRS) motor scale (part III) (Goetz et al., 2008). Missing values were imputed with the average score of the remaining questions, allowing a maximum of 7 missing values (Goetz et al., 2015). We calculated motor domain scores as well: Bradykinesia (items 3.4, 3.5, 3.6, 3.7, 3.14); rigidity (item 3.3); tremor: items 3.16, 3.17, 3.18); postural instability and gait difficulty (items 3.9, 3.10, 3.11, 3.12, 3.13). We used the severity of non-dopaminergic symptoms in Parkinson's disease (SENS-PD) scale, representing a coherent complex of symptoms that largely do not improve with dopaminergic medication, that is already present in the early disease stages, and increases in severity when the disease advances (van der Heeden et al., 2016). It comprises three items with four response options (0-3) from each of the following six domains: postural instability and gait difficulty, psychotic symptoms, excessive daytime sleepiness, autonomic dysfunction, cognitive impairment and depressive symptoms (total range: 0-54) (van der Heeden et al., 2016). Higher scores on both scales reflect more severe impairment. Cognitive performance was assessed with the scales for outcomes in Parkinson's disease - cognition (SCOPA-COG; cognitive functioning; range 0-43), which is a valid and reliable instrument examining the following domains: memory, attention, executive functioning and visuospatial functioning (Marinus et al., 2003); lower scores reflect more severe impairment. A levodopa dose equivalent (LDE)

was calculated according to the formula developed by Tomlinson et al. (Tomlinson et al., 2010). Patients were further asked if they had vascular risk factors: smoking, myocardial infarction, diabetes mellitus, hypertension, use of statins, transient ischemic attack and stroke, although previous stroke was an exclusion criterion for the study.

MRI acquisition and analysis

Imaging was performed on a 3 Tesla MRI scanner (Philips Achieva, Best, the Netherlands). Three-dimensional T1-weighted anatomical images were acquired with the following parameters: repetition time (TR)/echo time (TE) = 9.8/4.6 ms, flip angle = 8°, field of view (FOV) = 220 × 174 × 156 mm, voxel size = 1.15 × 1.15 × 1.20 mm. Fluid attenuated inversion recovery (FLAIR) images were acquired with TR/TE = 9249/56 ms, flip angle = 90°, FOV = 220 × 220 × 128 mm, voxel size = 1.96 × 1.96 × 2.00 mm. DTI images were acquired along 32 non-collinear directions with a b-value of 1000 s/mm^2 and one b = 0 image with TR/TE = 9249/56 ms, flip angle = 90°, 32 axial slices, voxel size = 1.96 × 2.00 × 2.00 mm, FOV = 220 × 220 × 128. MTI parameters were: TR/TE = 100/11 ms, flip angle = 9°, voxel size = 1.00 × 1.00 × 7.20 mm, FOV = 224 × 180 × 144 mm. Before analysis, all MRI scans were visually checked to ensure that no major artifacts or abnormalities were present in the data. MR images were analyzed with software provided by FSL (version 5.0.8, Oxford, United Kingdom) (Smith et al., 2004).

White matter hyperintensities

WMH volume was quantified in an automated manner, defined as hyperintense regions on FLAIR. The T1-weighted images were brain-extracted (Smith, 2002) and FLAIR and T1-weighted images were non-linearly registered to MNI standard space (Andersson et al., 2007). White matter was extracted from the FLAIR image using an MNI152 white matter mask. A threshold of 2.5 standard deviations above the mean of FLAIR intensities for white matter was set to identify which white matter voxels were hyperintense. We additionally calculated WMH volumes for periventricular and deep white matter (Fazekas et al., 1987). We created a periventricular white matter mask by subtracting an MNI ventricle mask from an MNI ventricle mask that was dilated using a 4 × 4 × 4 kernel. An anterior deep white matter mask was created using the anterior part of the previously used MNI white matter mask (most frontal part of the corpus callosum, MNI coordinate Y = 33), of which the periventricular white matter mask was subtracted. A posterior

deep white matter mask was created similarly (most posterior part of the corpus callosum, MNI coordinate Y = -44).

Diffusion tensor imaging

The preprocessing of the DTI data consisted of brain extraction (Smith, 2002), motion and eddy current correction (Andersson and Sotiropoulos, 2016). The corrected DTI was subsequently used to create individual fractional anisotropy (FA) and mean diffusivity (MD) images using a weighted least squares fitting procedure. All subjects' FA and MD data were aligned into a common space using nonlinear registration (Andersson et al., 2007). The resulting images were used for quantification of global mean FA and MD values of each subjects NAWM (i.e. white matter without lesions). T1-weighted images were brain-extracted (Smith, 2002) and segmented in order to create individual white matter masks (Zhang et al., 2001), which were linearly registered to MNI space (Jenkinson et al., 2002b). Then, WMHs of each subject were dilated using a 3 × 3 × 1 kernel and subtracted from the individual white matter mask in order to create a NAWM mask. Finally, individual mean FA and MD values were calculated using the normal appearing white matter mask.

Voxel-wise statistical analyses of the FA and MD data were carried out with tract-based spatial statistics (TBSS), using default settings (Smith et al., 2006). TBSS projects all subjects' aligned FA (or MD) data onto a mean white matter tract skeleton. The resulting four-dimensional data was used for further statistical analysis.

Magnetization transfer imaging

The MT images and the previously derived individual NAWM (WMHs subtracted from white matter) were linearly registered to T1 space (Jenkinson et al., 2002b). Global magnetization transfer ratio (MTR) values were calculated per voxel as (M0 – Ms) / M0 (Ms: saturated image; M0: unsaturated image). MTR histograms were generated using the normal appearing white matter mask in order to calculate the mean MTR from each histogram, which is the mean of the MTR value of all voxels in the histogram.

Statistical analysis

Differences between patients and control subjects in WMH volumes, global mean FA, MD and mean MTR values of NAWM (white matter integrity measurements) and age were analyzed with independent-sample T-tests, dichotomous variables

using a chi-square test or Fisher exact test. We used linear regression analyses for estimating the relationships between age and measurements of white matter integrity in patients and control subjects. Total WMH volumes were transformed using the logarithm function to meet normality assumptions. We examined the interaction between age and disease presence on white matter integrity (dependent variable) in a general linear model, with disease presence and age also included as independent variables; gender was included in the model as an independent variable as well. Within the PD group, we used a linear regression analysis to estimate the relationships between clinical variables (independent variable; disease duration, MDS-UPDRS motor, SENS-PD and SCOPA-COG score, total LDE, presence of vascular risk factors and hypertension) and WMH volumes (dependent variable; total, deep anterior and periventricular WMH volume). With regard to the sum scores of the MDS-UPDRS motor, SENS-PD and SCOPA-COG scale, we first examined associations between sum scores and WMH volume. We subsequently examined associations between the domain scores and WMH volume if there was a statistically significant association (defined as $p < 0.05$) with one of the MDS-UPDRS motor, SENS-PD, or SCOPA-COG scale sum scores. We added age to the statistical model if a relationship was statistically significant after Bonferroni correction was applied. Statistics were performed in SPSS (IBM SPSS Statistics for Mac, Version 23.0. Armonk, NY: IBM Corp.).

Voxel-wise statistical analysis of the FA and MD data was carried out using a general linear model approach as implemented in FSL, with gender used as covariate in the model as we did in the other statistical analyses. The spatial relationship between age and FA, and age and MD data was studied in the PD as well as in the control group. Permutation-based non-parametric testing was used (Winkler et al., 2014), with 5000 permutations, correcting for multiple comparisons across space. The statistical threshold was set at $p < 0.05$, familywise error (FWE) corrected, using the threshold-free cluster enhancement (TFCE) technique (Smith and Nichols, 2009).

RESULTS

Demographic characteristics

There were no statistically significant differences in age and gender between the patient and the control group (table 1). Patients with PD had higher WMH volumes ($p < 0.001$) compared with control subjects. The periventricular ($p < 0.001$) and deep anterior ($p < 0.001$) WMH volumes were larger in PD patients than in control subjects. We did not find statistically significant differences in deep posterior WMH

volumes, and also white matter microstructure parameters (i.e., FA, MD, MTR) did not significantly differ between groups.

Table 1. Main characteristics of participants

	PD patients	Control subjects	
N	**163**	**218**	***P*-value**
Men/women	59/104 (63.8)	137/81 (62.8)	0.915
Age, years	64.8 (7.2)	65.0 (6.2)	0.462
Disease duration, years	9.1 (4.9)	n/a	n/a
MDS-UPDRS motor score (0-132)	34.3 (15.6)	n/a	n/a
SENS-PD (0-54)	13.2 (6.1)	n/a	n/a
SCOPA-COG (0-43)	27.5 (11 - 41)	n/a	n/a
Total LDE, mg/day	1017.1 (558.7)	n/a	n/a
Vascular risk factors			
Hypertension	32 (20.0)	39 (25.0)	0.345
Use of statins	19 (11.7)	15 (7.8)	0.211
Diabetes mellitus	6 (3.9)	10 (5.0)	0.616
Myocardial infarction	4 (2.6)	5 (3.2)	0.748
Transient ischemic attack	2 (1.3)	2 (1.3)	1.000
Smoking	10 (6.1)	29 (13.4)	0.006*
White matter hyperintensity volume, ml	8.8 (7.2)	4.8 (5.1)	<0.001*
Periventricular white matter	3.6 (2.3)	2.2 (1.7)	<0.001*
Anterior deep white matter	0.2 (0.2)	0.03 (0.1)	<0.001*
Posterior deep white matter	1.6 (1.7)	1.7 (1.7)	0.378
Mean FA normal appearing white matter	0.30 (0.02)	0.29 (0.02)	0.090
Mean MD[a] normal appearing white matter	0.92 (0.06)	0.92 (0.05)	0.850
Mean MTR normal appearing white matter	0.33 (0.02)	0.33 (0.01)	0.858

Values are means (standard deviation) for continuous variables, except for SCOPA-COG score (range), and numbers for gender (% men) and vascular comorbidity (% yes). For all measurement instruments, the score range is presented in parentheses. MDS-UPDRS: Movement Disorder Society-unified Parkinson's disease rating scale; SENS-PD: severity of non-dopaminergic symptoms in Parkinson's disease; SCOPA-COG: scales for outcomes in Parkinson's disease - cognition; LDE: Levodopa dosage equivalent; n/a: not applicable.

[a] Absolute mean MD white matter values multiplied by 1000; * $p < 0.05$.

Age and white matter hyperintensity volume

In the PD group and the control group, total WMH volume increased with age (PD group: $\beta = .329$, $p < 0.001$; control group: $\beta = .341$, $p < 0.001$; see figure 1a). There was no statistically significant interaction of age and disease presence in their effects on WMH volume. Periventricular (PD group: $\beta = .364$, $p < 0.001$; control group: $\beta = .364$, $p < 0.001$) and deep posterior (PD group: $\beta = .242$, $p < 0.002$;

control group: β = .312, p < 0.001) WMH volumes also increased with age, but anterior WMH volume did not.

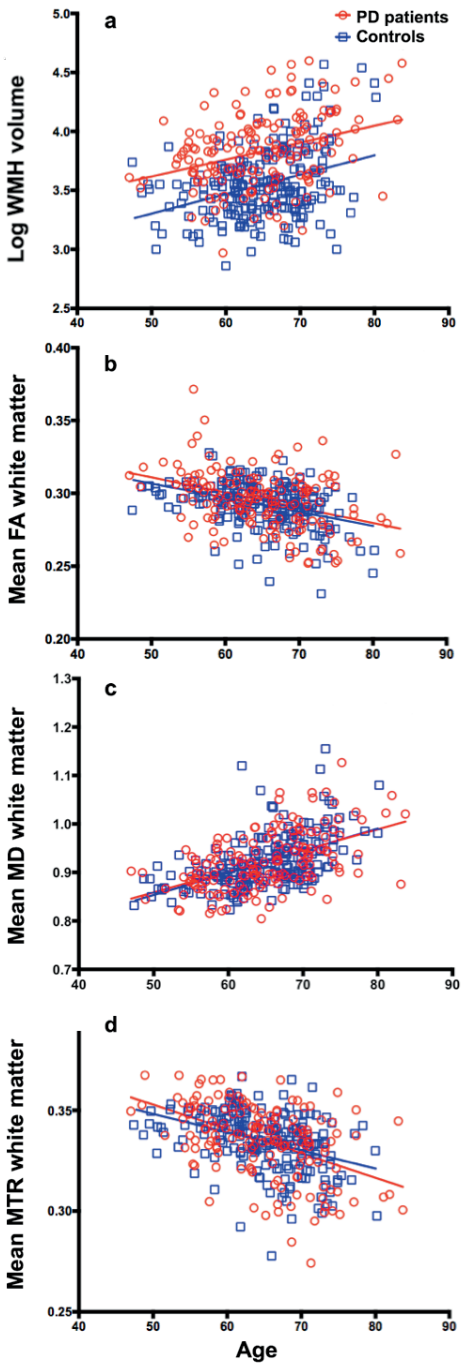


Figure 1. Scatterplot of the relation between age and log-transformed white matter hyperintensity (WMH) volume (a), normal appearing white matter fractional anisotropy (FA; b), normal appearing white matter mean diffusivity (MD) multiplied by 1000 (c) and normal appearing white matter mean magnetization transfer ratio (MTR; d). Abbreviation: PD, Parkinson's disease.

We found that in the PD group, visuospatial functioning (SCOPA-COG score) was related to total WMH volume (β = -.214, p = 0.006) and postural instability and gait difficulty (UPDRS motor score) to periventricular WMH volume (β = .257, p = 0.001). Both relationships remained significant after including age in the model: visuospatial functioning with total WMH volume: β = -.175, p = 0.020 (age with total WMH volume: β = .307, p < 0.001) and postural instability and gait difficulty with periventricular WMH volume: β = .163, p = 0.037 (age with periventricular WMH volume: β = .314, p < 0.001). No other significant relationships between clinical variables and WMH volumes emerged.

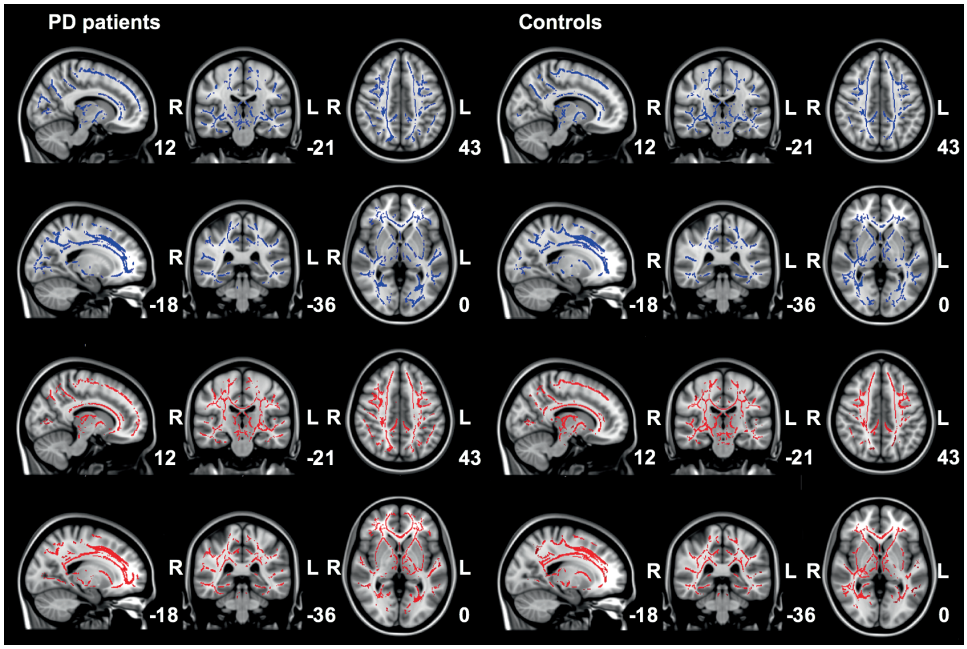


Figure 2. Areas of age-related decline in white matter fractional anisotropy (FA, blue) and age-related increase in white matter mean diffusivity (MD, red), overlaid on the MNI standard cerebral image with accompanying coordinates. Left: patients with Parkinson's disease. Right: control subjects.

Age and global white matter microstructural integrity

Age had a statistically significant association with FA (PD group: β = -.380, p < 0.001; control group: β = -.392, p < 0.001; see figure 1b), MD (PD group: β = .522, p < 0.001; control group: β = .528, p < 0.001; see figure 1c) and mean MTR (PD group: β = -.470, p < 0.001; control group: β = -.393, p < 0.001; see figure 1d) in

both groups. There was no statistically significant interaction effect of age and disease presence on FA, MD, or mean MTR.

We used TBSS to investigate the spatial voxel-wise relationship between age and FA and MD values in the PD as well as in the control group (figure 2). This shows that the spatial effect of age on FA and MD is distributed throughout the entire brain across white matter tracts in both patients with PD and control subjects.

DISCUSSION

As age and PD both play a role in the degeneration of brain white matter, we investigated the relationship between age and white matter integrity in patients with PD and control subjects. Although patients with PD had a higher load of white matter lesions, the influence of age on the decline of white matter integrity was similar to healthy control subjects. In both groups, measures of white matter integrity were associated with advancing age, which appeared homogeneously distributed across white matter tracts. No differences were found in the degree of NAWM degeneration.

The patients with PD in this study had a higher WMH load than expected for their age. The excess of WMHs was partly located in periventricular and deep frontal white matter of patients with PD. Besides age, visuospatial functioning and postural instability and gait difficulty were related to WMH volume in patients with PD. Given the similar age-related increase of WMHs in patients with PD and control subjects, our findings may suggest that the pathobiology of PD plays a role in the development of WMHs. Our findings are in line with those of other studies showing more WMHs in patients with PD (Compta et al., 2016; Dunet et al., 2019; Ham et al., 2016; Piccini et al., 1995). Nevertheless, other studies did not show differences between patients with PD and healthy control subjects (Acharya et al., 2006; Beyer et al., 2006; Dalaker et al., 2009; Sartor et al., 2017). Differences in field strength (ranging from 0.5 to 3 Tesla), methodology to asses WMHs, and selection of a specific subset of patients with PD (i.e., with/without dementia or mild cognitive impairment) in these studies likely contributed to the inconsistent findings. Importantly, previous MRI studies investigating WMHs in patients with PD used visual rating scales, such as the Fazekas grading system and the Scheltens visual rating scale, or semiautomated visual approaches that require manual contouring of the lesions. Increased field strength can possibly result in a better delineation of white matter lesions (Zwanenburg et al., 2010) and the accuracy of visual rating systems may depend on the WMH load. Some scales do not discriminate between

no abnormalities and few WMHs or moderate and severe quantities of WMHs, or suffer from ceiling effects in patients with a more extensive WMH load (Tiehuis et al., 2008; Wardlaw et al., 2004). The automated threshold method to measure WMH volume used in our study, however, provides objective and quantitative data (Tiehuis et al., 2008).

Previous studies have shown that WMHs independently contribute to postural instability and gait difficulty in patients with PD as well (for review, see (Bohnen and Albin, 2011)). There are indications that WMHs may have a substantial impact especially on axial motor disability (Lee et al., 2009; Moccia et al., 2016). There are also indications that WMHs contribute to cognitive impairment in patients with PD (Dadar et al., 2018; Veselý and Rektor, 2016). A recent study found increased MD in frontal and parietal white matter tracts in newly diagnosed, cognitively intact, patients with PD patients as compared with control subjects, which was related to cognitive performance tasks (Duncan et al., 2016). These findings suggest that white matter may already be affected in the very early stages of PD, predicting future cognitive decline (Dadar et al., 2018; Duncan et al., 2016; Veselý and Rektor, 2016). However, some studies reported that the correlations found between cognitive measures and WMHs disappeared after adjusting for strong confounders, such as age (Bohnen and Albin, 2011; Lee and Lee, 2016). Indeed, our findings show that postural instability, gait difficulty, and visuospatial functioning are related to the total and to periventricular WMH volume in patients with PD, but the relationship between visuospatial functioning and WMHs weakened after adjustment for the effect of age in our study too. In addition, the relationship between age and WMHs appeared stronger than the relationship between visuospatial functioning and WMHs. WMHs might exacerbate cognitive or motor dysfunction in patients with PD through aggravation of already impaired neuronal connectivity (Veselý and Rektor, 2016). Especially periventricular WMHs could interfere with cortico-subcortical circuits that are important for gait and balance (Blahak et al., 2009; Bohnen and Albin, 2011). It is debatable whether the associations that we found are specific for PD, as WMHs are associated with motor and cognitive symptoms in otherwise normal elderly individuals as well (Bohnen and Albin, 2011).

WMHs have been linked to vascular disease, including depositions of amyloid beta (Pantoni, 2010). A recent study found more severe WMH burden in patients with PD with dementia compared with nondemented patients with PD and control subjects, which was related to decreased amyloid beta levels in the cerebrospinal fluid in the entire PD sample. Because this finding was independent

of age, dementia, APOE-4, and vascular risk factors, the authors suggested a possible relationship between brain amyloid deposition and the occurrence of WMHs in patients with PD (Compta et al., 2016). At this stage, it remains unclear whether the relationship between amyloid beta levels in the cerebrospinal fluid and WMHs in PD also reflects vascular amyloid beta deposition. Periventricular WMHs may further result from chronic hemodynamic insufficiency (hypoperfusion), Wallerian degeneration secondary to neocortical neuron loss in neurodegenerative diseases (Bohnen and Albin, 2011; Kim et al., 2008; Leys et al., 1991), or low grade inflammation (Bohnen and Albin, 2011; Wersching et al., 2010) to which regional differences in gene expression may contribute, resulting in a spatial distribution of pathogenic pathways (Ritz et al., 2017).

The microstructural integrity of the white matter in patients with PD without WMHs was normal in terms of global FA, MD, and MTR, compared with age-matched control subjects. Previous cross-sectional studies have shown that DTI and MTR are particularly relevant for subcortical areas (Atkinson-Clement et al., 2017; Tambasco et al., 2015), and show conflicting results in cortical white matter, which might be explained by the low statistical power due to small sample sizes these studies (Atkinson-Clement et al., 2017; Hall et al., 2016; Tambasco et al., 2015). A recent meta-analysis, however, suggested that the cognitive status of patients with PD is associated with damage in the temporal and cingulate cortices (Atkinson-Clement et al., 2017). A major difference between previously conducted studies and our study is that these studies generally applied region of interest approaches (Cochrane and Ebmeier, 2013; Tessitore et al., 2016), while we used global FA and MD measures of white matter, in order to investigate the relationship between age and global white matter integrity in patients with PD. Two previous longitudinal studies used a whole brain white matter approach as well, and observed similar levels of decline in white matter integrity in patients with PD and control subjects (Melzer et al., 2015; Rossi et al., 2014). Other studies measured FA reductions and increased MD over time in regions of interest (including regions of gray matter), such as the substantia nigra and caudal and cerebellar white matter (Pozorski et al., 2018; Zhang et al., 2016). Collectively, all findings suggest that PD-specific changes do not exceed normal age-associated change in cortical white matter tracts.

The strengths of our study are the large sample patients with PD and control subjects in whom we performed structural MRI as well as DTI and MTI to investigate the relationship between age and white matter integrity. We further used automated techniques for individual quantification of WMH volume, based

on thresholding of hyperintense white matter voxels, which have the advantage of improved quantitative assessment of WMHs compared with visual grading (Bohnen and Albin, 2011). A limitation of our study is the cross-sectional design to assess the age-related decline of white matter, as cross-sectional data rely on between-person comparisons and not model intraindividual change. White matter changes, aging, and cardiovascular risk factors are closely related to each other (Debette and Markus, 2010; Erten-Lyons et al., 2013; Wardlaw et al., 2013). It could be assumed that the control subjects in this study, who were selected from the LLS, may have had a more favorable cardiovascular risk profile as compared with the patients with PD in this study. However, cardiovascular risk factors did not differ between groups, although it should be noted that the assessed cardiovascular risk factors may not have been complete (e.g., the use of statins were compared, but not the presence of hyperlipidemia). Of note is that there were more missing values in the control group than in the patient group, but we consider it unlikely that this may have led to additional bias because there is no reason to assume a relationship between missingness and the risk profile of the patient. WMH volume may be associated with a worse response to dopaminergic medication for postural stability and gait difficulty (Arena et al., 2016). We therefore added total LDE score to the model, but this did not change our results. The effects of dopaminergic medication on white matter microstructure are not really known, except for a study that showed that DTI is not affected by acute antiparkinsonian medication (Chung et al., 2017). In our study, microstructural integrity of white matter without WMHs did not differ between patients with PD and age-matched control subjects, but subtle differences between groups may become apparent through the use of a region of interest approach (Pozorski et al., 2018; Zhang et al., 2016). In addition, the rate of age-related change may vary across multiple white matter regions, although the spatial effect of age on FA and MD was uniformly distributed across white matter tracts in both groups.

Conclusion

Patients with PD had a higher load of WMHs with a preferential periventricular and anterior distribution as compared with healthy control subjects. Visuospatial functioning was related to total and postural instability and gait difficulty were related to periventricular WMH volume in patients with PD. The age-related decline of white matter integrity was similar for both groups. Global mean FA, MD, and MTR of the NAWM were relatively normal in patients with PD, suggesting that

PD-specific changes do not exceed normal age-associated change in white matter without lesions.

5 Altered whole-brain and network-based functional connectivity in Parkinson's disease

Frontiers in Neurology. (2018) 9:419. doi: 10.3389/fneur.2018.00419

Laura de Schipper[1]
Anne Hafkemeijer[2,3,4]
Jeroen van der Grond[2]
Johan Marinus[1]
Johanna Henselmans[1,5]
Jacobus van Hilten[1]

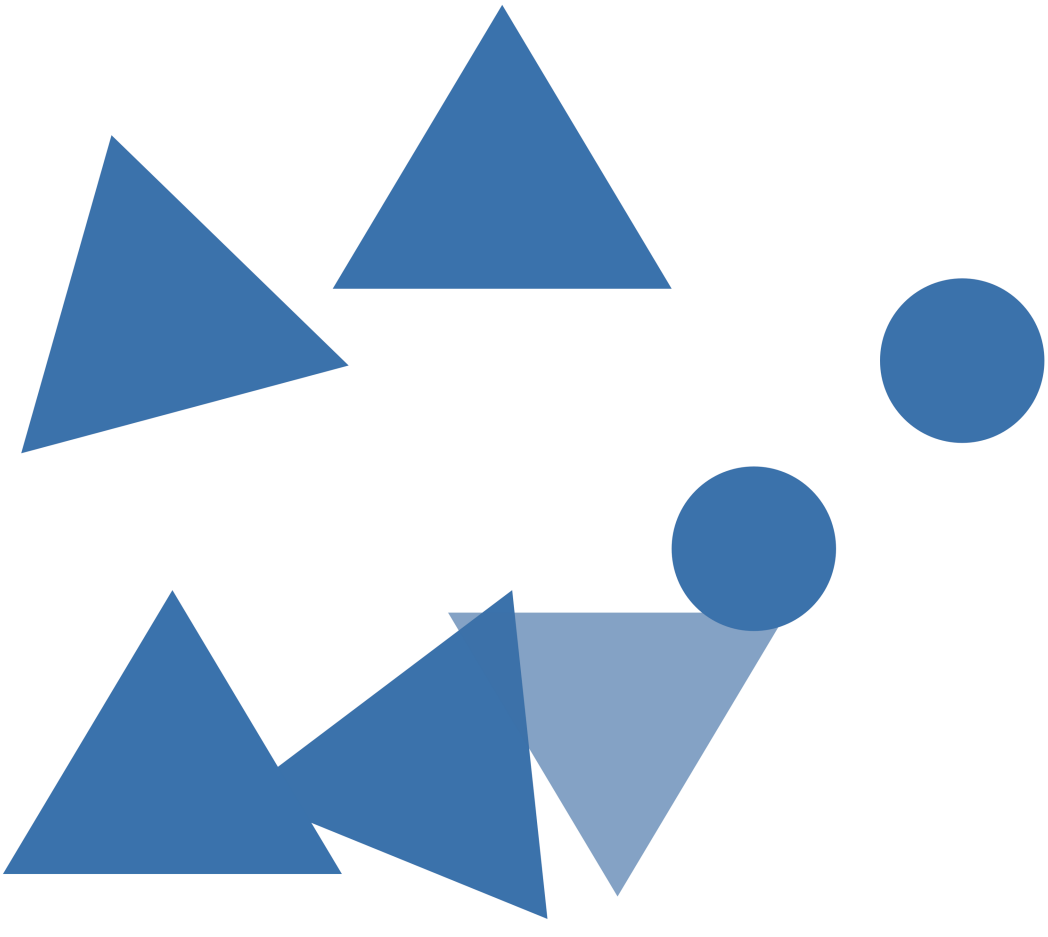
[1] Leiden University Medical Center, Department of Neurology, Leiden, the Netherlands,

[2] Leiden University Medical Center, Department of Radiology, Leiden, the Netherlands

[3] Leiden University, Department of Methodology and Statistics, Institute of Psychology, Leiden, the Netherlands

[4] Leiden University, Leiden Institute for Brain and Cognition, Leiden, the Netherlands

[5] Antonius Hospital, Department of Neurology, Woerden, the Netherlands



ABSTRACT

Introduction: Functional imaging methods, such as resting-state functional magnetic resonance imaging, reflect changes in neural connectivity and may help to assess the widespread consequences of disease-specific network changes in Parkinson's disease (PD). In this study we used a relatively new graph analysis approach in functional imaging: eigenvector centrality mapping. This model-free method, applied to all voxels in the brain, identifies prominent regions in the brain network hierarchy and detects localized differences between patient populations. In other neurological disorders, eigenvector centrality mapping has been linked to changes in functional connectivity in certain nodes of brain networks. Here we examined changes in functional brain connectivity architecture on a whole brain and network level in patients with PD.

Methods: Whole brain resting-state functional architecture was studied with a recently introduced graph analysis approach (eigenvector centrality mapping). Functional connectivity was further investigated in relation to eight known resting-state networks. Cross-sectional analyses included group comparison of functional connectivity measures of PD patients (n = 107) with control subjects (n = 58) and correlations with clinical data, including motor and cognitive impairment and a composite measure of predominantly non-dopaminergic symptoms.

Results: Eigenvector centrality mapping revealed that frontoparietal regions were more prominent in the whole-brain network function in patients compared to control subjects, while frontal and occipital brain areas were less prominent in patients. Using standard resting-state networks, we found predominantly increased functional connectivity, namely within sensorimotor system and visual networks in patients. Regional group differences in functional connectivity of both techniques between patients and control subjects partly overlapped for highly connected posterior brain regions, in particular in the posterior cingulate cortex and precuneus. Clinico-functional imaging relations were not found.

Conclusion: Changes on the level of functional brain connectivity architecture might provide a different perspective of pathological consequences of Parkinson's disease. The involvement of specific, highly connected (hub) brain regions may influence whole brain functional network architecture in PD.

INTRODUCTION

Parkinson's disease (PD) is characterized by a broad spectrum of motor and non-motor symptoms, which are linked to a progressive formation of alpha-synuclein (alpha-SynA) aggregates in presynaptic terminals, Lewy neurites and Lewy bodies in neurons of the central and peripheral nervous system (Adler and Beach, 2016; Jellinger, 2012). Alpha-SynA are not randomly distributed in the brain, but appear in select regions, which likely are affected because of shared anatomical and functional properties among neurons (McCann et al., 2016; Surmeier et al., 2017). Depositions are most distinct in the midbrain, pontine and medullary nuclei and limbic structures, but are also found in the neocortex in the more advanced stages of the disease (Jellinger, 2012; McCann et al., 2016). Compelling evidence shows that alpha-SynA-related synaptic dysfunction antedates nerve cell loss, suggesting that altered neuronal connectivity is a key feature in PD (Schulz-Schaeffer, 2015).

Functional imaging methods, such as resting-state functional magnetic resonance imaging (fMRI), reflect changes in neural connectivity and may help to assess the widespread consequences of disease-specific network changes in neurodegenerative diseases (Pievani et al., 2011). Former fMRI studies indicate decreases as well as increases in functional connectivity in PD patients (Baggio et al., 2015; Göttlich et al., 2013). Most of these studies focused on functional connectivity of (multiple) brain regions or networks of interest, thus precluding inferences on a whole-brain level of integrated networks that are spatially distributed, but functionally linked.

A relatively new graph analysis approach in functional imaging concerns eigenvector centrality mapping (ECM). ECM identifies prominent regions in the brain network hierarchy and detects localized differences between patient populations (Wink et al., 2012). Since this model-free method is applied to all voxels in the brain it does not require a priori selection of potentially involved networks and is not restricted to one area (regions of interest) of the brain. The main difference between the method used in our study and other graph analysis studies in PD is that our approach counts the neighbors of each vertex, weighted by their centralities (Wink et al., 2012). ECM has been linked to changes in functional connectivity in certain nodes of brain networks that might contribute to depression in patients with PD (Lou et al., 2015). Changes in ECM have also been linked to loss in cognition in APOE **ε**4 carriers (Luo et al., 2017), but also to neurodegenerative changes in type 1 diabetes mellitus (van Duinkerken et al., 2017), and cognitive dysfunction and physical disability in multiple sclerosis (Schoonheim et al., 2014).

The aim of this study was to evaluate and compare the consequences of PD on the resting-state functional connectivity on a whole-brain level of integrated networks and on eight explicit brain networks. We hypothesized that these combined approaches can identify regionally specific differences in functional connectivity of the brain between PD patients and control subjects.

PATIENTS AND METHODS

Study design and participants

The present cross-sectional study in PD patients is part of the Profiling Parkinson's disease (PROPARK) study. PD patients were recruited from the outpatient clinic for Movement Disorders of the Department of Neurology of the Leiden University Medical Center (LUMC; Leiden, the Netherlands) and nearby university and regional hospitals. All participants fulfilled the United Kingdom Parkinson's Disease Society Brain Bank criteria for idiopathic Parkinson's disease (Gibb and Lees, 1988). Evaluations occurred between January 2013 and 2016. Exclusion criteria were: previous or other disorders of the central nervous system, peripheral nerve disorders influencing motor and/or autonomic functioning, and psychiatric comorbidity not related to PD. Patients were matched at group level for age and gender with a group of healthy control subjects. Control subjects were recruited from the Leiden Longevity study (LLS), a study set up to identify genetic and phenotypic determinants of longevity in healthy long-living families (Altmann-Schneider et al., 2013).

Clinical assessments

All patients underwent standardized assessments, including an evaluation of demographic and clinical characteristics. Almost all patients, except for 13 individuals (12 de novo patients, defined as dopaminergic drug-naïve patients with a disease duration shorter than 5 years; one other dopaminergic drug-naïve patient), were tested while on dopaminergic medication. The Movement Disorder Society unified Parkinson's Disease Rating Scale (MDS-UPDRS) motor scale (part III) was used to quantify the severity of motor symptoms (Goetz et al., 2008). Additionally, the severity of non-dopaminergic symptoms in Parkinson's disease (SENS-PD) scale was used, which is a composite score comprising three items with four response options (0–3) from each of the following six domains: postural instability and gait difficulty, psychotic symptoms, excessive daytime sleepiness, autonomic dysfunction, cognitive impairment and depressive symptoms (total range: 0–54) (van der Heeden et al., 2016). These six domains represent a coherent

complex of symptoms that largely do not improve with dopaminergic medication, that is already present in the early disease stages, and increases in severity when the disease advances (van der Heeden et al., 2016). Higher scores on both scales reflect more severe impairment. The scales for outcomes in Parkinson's disease - cognition (SCOPA-COG; cognitive functioning; range 0–43) was used to assess cognitive performance. The SCOPA-COG is a valid and reliable instrument examining the following domains: memory, attention, executive functioning and visuospatial functioning (Marinus et al., 2003); lower scores reflect more severe impairment. A levodopa dose equivalent (LDE) of daily levodopa (LDE-Dopa), dopamine agonists (LDE-DA), as well as a total LDE was calculated according to the formula developed by Tomlinson et al. (Tomlinson et al., 2010).

MRI acquisition

Imaging was performed on a 3 Tesla MRI scanner (Philips Achieva, Best, the Netherlands). Resting-state fMRI images were acquired with the following parameters: repetition time = 2.2 s, echo time = 30 ms, flip angle = 80°, 37 slices, resulting in a voxel size of 2.75 × 2.75 × 2.72 mm, with a 10% interslice gap, 200 volumes, scan duration 7 min and 29 s. Participants were instructed to lie still with their eyes closed and not to fall asleep during the scan. For registration purposes three-dimensional T1-weighted anatomical images were acquired with the following parameters: repetition time = 9.8 ms, echo time = 4.6 ms, flip angle = 8°, FOV 220 × 174 × 156 mm, 130 slices with a slice thickness of 1.2 mm with no gap between slices, resulting in a voxel size of 1.15 × 1.15 × 1.20 mm. Additionally, a high resolution echo planar image was obtained with the following parameters: repetition time = 2.2 s, echo time = 30 ms, flip angle =80°, 84 slices, resulting in a voxel size of 1.96 × 1.96 × 2.00 mm with no gap between slices.

Data analysis

Before analysis, all MRI scans were visually checked to ensure that no major artifacts or abnormalities were present in the data. Analyses were done using the software provided using the FMRIB's software library (FSL; version 5.0.8, Oxford, United Kingdom) and Matlab software (version 6.1, The MathWorks Inc., Natick, MA, 2000)(Smith et al., 2004).

Preprocessing

The preprocessing of the resting-state fMRI data consisted of motion correction using motion correction FMRIB's linear image registration tool (MCFLIRT)

(Jenkinson et al., 2002a), brain extraction (Smith, 2002), spatial smoothing using a Gaussian kernel with a full width at half maximum of 5 mm, high-pass temporal filtering with a cutoff frequency 0.01 Hz, non-linear registration with Boundary-Based Registration to the 2 mm isotropic Montreal Neurological Institute -152 standard space image (MNI; Montreal, QC, Canada) and a 10 mm warp resolution (Greve and Fischl, 2009), via the T1-weighted images, using high-resolution echo planar images for an additional registration step between functional images and T1-weighted images (Andersson et al., 2007). ICA-based Automatic Removal Of Motion Artifacts (ICA-AROMA) was used to identify and remove residual motion-related artifacts from the resting-state data (Pruim et al., 2015a, 2015b).

Eigenvector centrality mapping

ECM was used to identify prominent nodes in the whole brain network per group. Localized differences between PD patients and control subjects were subsequently calculated. Each voxel is assigned its own value of relevance to the network (Lohmann et al., 2010). Higher EC indicates a more prominent role in the brain network hierarchy and lower EC a less prominent role. For each participant, we calculated a whole brain eigenvector centrality map in standard space, using the fast ECM algorithm (Binnewijzend et al., 2014; Wink et al., 2012). The EC maps of all participants (i.e., PD patients and control subjects) were concatenated into a single four-dimensional data set. A gray matter mask was applied to make sure that only gray matter centrality was studied. FSL-Randomise permutation-testing tool for nonparametric permutation inference was used for statistical analysis, with 5000 permutations (Winkler et al., 2014). Group differences in mean EC values were calculated using a two-sample T-test. The threshold-free cluster enhancement (TFCE) technique was used to correct for multiple comparisons across space. Statistical threshold was set at $p < 0.05$, familywise error (FWE) corrected, applying a minimum cluster size of 40 mm^3 (Smith and Nichols, 2009).

Resting-state networks

Eight standard resting-state networks were used as a template to study whole-brain functional connectivity in a standardized way: (1) medial visual network; (2) lateral visual network; (3) auditory system network; (4) sensorimotor system network; (5) default mode network; (6) executive control network; (7 and 8) dorsal visual stream networks (Beckmann et al., 2005; Hafkemeijer et al., 2015). Resting-state functional connectivity was studied using the dual regression method of FSL (Beckmann et al., 2009), according to Hafkemeijer et al. (2015). In short, this

method results in ten three-dimensional images per individual (eight resting-state networks and a white matter and cerebrospinal fluid template to further account for noise) with voxel-wise z-scores representing the functional connectivity in each of the templates (Hafkemeijer et al., 2015). Voxel-wise group differences between spatial maps of PD patients and control subjects were tested using FSL-Randomise using the same design as in the ECM analysis, TFCE-FWE corrected and a statistical threshold of $p < 0.05$ (Smith and Nichols, 2009; Winkler et al., 2014). The standard resting-state networks were used as masks in the analyses.

Statistical analysis

The following statistics were performed in SPSS (IBM SPSS Statistics for Mac, Version 23.0. Armonk, NY: IBM Corp.). Differences in demographic data between patients and control subjects were analyzed with an independent-sample T-test (age) and a chi-square test (gender). For brain areas with significant group differences in EC, mean EC values were extracted. Z-scores were extracted from brain areas with significant group differences in resting-state functional connectivity networks. Within the PD group, relationships between mean functional connectivity measures (i.e., mean EC values and z-scores; dependent variable) and the MDS-UPDRS motor score, SENS-PD score and SCOPA-COG were studied using a general linear model. Age, gender and gray matter volume, normalized for subject head size as estimated with structural image evaluation using normalization of atrophy cross-sectional (SIENAX) (Smith et al., 2004), were included as covariates in the model (Oakes et al., 2007). Relationships were subsequently studied within the group of PD patients who used dopaminergic medication, while adjusting for the total LDE. Bonferroni correction was applied to account for multiple comparisons.

RESULTS

Demographic characteristics

In total, one hundred and sixty-five subjects, of which one hundred and seven patients and fifty-eight control subjects were included in the analysis. Demographic and clinical data of all participants are shown in table 1. There were no significant differences in age ($p = 0.605$) and gender ($p = 0.206$) between the patient and the control group.

Table 1. Main characteristics of participants

	PD patients	Control subjects
N	**107**	**58**
Men/women (% men)	68/39 (63.6)	31/27 (53.4)
Age, years	64.6 (6.9)	65.2 (7.5)
Disease duration, years	9.5 (4.8)	n/a
MDS-UPDRS motor score (0-132)	33.2 (15.5)	n/a
SENS-PD, n=99 (0-54)	13.5 (6.1)	n/a
SCOPA-COG, n=100 (0-43)	27.5 (5.8)	n/a
Total LDE, mg/day, n=92	995.6 (550.4)	n/a
Drug-naïve patients, n=1	n/a	n/a
De novo patients, n=12*	n/a	n/a
LDE-Dopa, mg/day, n=92	739.8 (486.4)	n/a
LDE-DA dose, mg/day, n=92	184.6 (208.2)	n/a

Values are means (standard deviation) for continuous variables and numbers for dichotomous variables. For all measurement instruments, the score range is presented in parentheses. MDS-UPDRS: Movement Disorder Society unified Parkinson's disease rating scale; SENS-PD: severity of non-dopaminergic symptoms in Parkinson's Disease; SCOPA-COG: SCOPA cognition; LDE: Levodopa dosage equivalent; DA: dopamine agonists; n/a: not applicable.

* De novo patients: drug-naïve patients with disease duration shorter than five years.

Eigenvector centrality maps

Mean eigenvector centrality maps

The mean EC group map of control subjects and the mean EC group map of PD patients both showed highest cortical mean EC values in the precuneus, posterior cingulate gyrus and occipital lobe. In the control group, highest subcortical mean EC values were found in the thalamus, hippocampus and caudate nucleus. In the patient group, highest subcortical mean EC values in patients were found in the thalamus and hippocampus.

Patient – control subject comparisons (figure 1)

Compared to control subjects, PD patients had increases in EC in large areas of the parietal and frontal lobe (opercular cortex, superior division of the lateral occipital cortex, posterior cingulate gyrus, precuneus, superior parietal lobe, supplementary motor area (SMA), pre- and postcentral gyrus, frontal gyrus and right middle frontal gyrus), right temporal lobe, right thalamus and a small region of the right hippocampus (figure 1, red areas).

Further, compared to control subjects, patients had areas of decreased EC in the occipital lobe (cuneus, intracalcarine cortex, lingual gyrus, occipital pole),

frontal lobe (frontal gyrus, frontal medial cortex, anterior cingulate gyrus, paracingulate gyrus, and frontal pole), inferior division of the lateral occipital cortex, precuneus and right pallidum and anterior putamen (figure 1).

We found no significant relations between mean EC values of brain areas with group differences and the MDS-UPDRS motor score, SENS-PD score, or SCOPA-COG score.

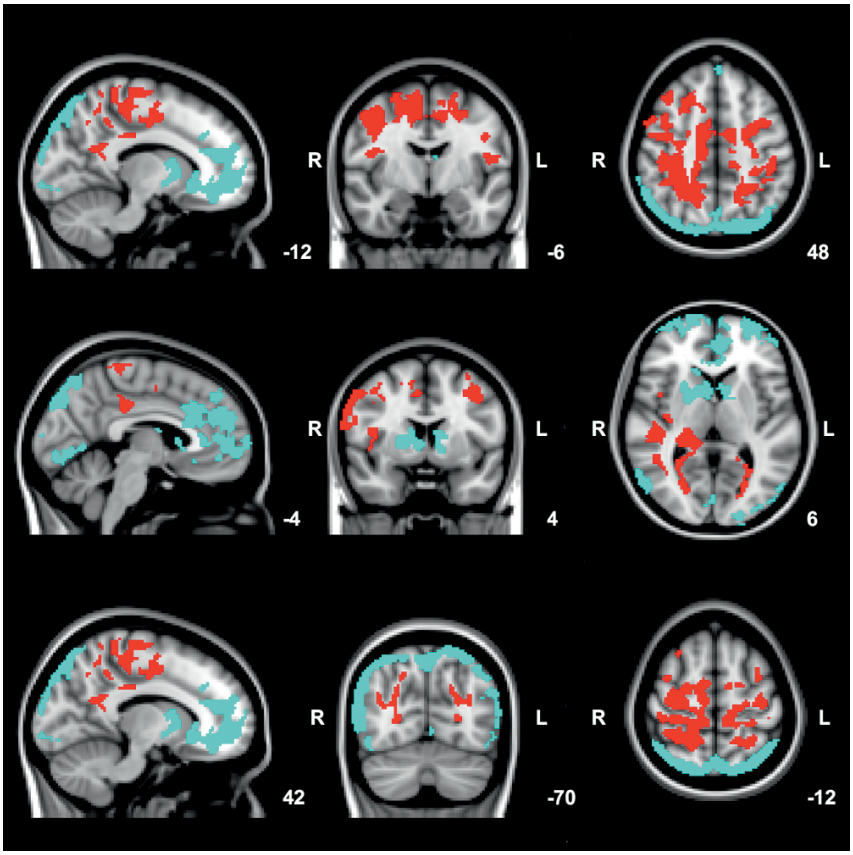


Figure 1. Significant group differences between patients and control subjects in mean EC values. Red: clusters of increased EC in patients compared to control subjects. Blue: clusters of decreased EC in patients compared to control subjects. Results are corrected for age, gender and voxel-wise grey matter volume per subject. Images are overlaid on the most informative, sagittal, coronal, and axial slices of the MNI standard anatomical image (MNI coordinates of each slice are given).

Resting-state network analyses

Voxel-wise group comparisons of the resting-state network connectivity revealed group differences in functional connectivity between PD patients and control subjects in seven out of eight resting-state networks (figure 2). Group differences were most pronounced in the medial and lateral visual network and the sensorimotor system network (figure 2, network 1, 2, and 4). Increased functional connectivity in PD patients compared to control subjects was found between the cuneus, precuneus, superior division of the lateral occipital cortex, intra- and supracalcarine cortex and lingual gyrus, and the medial visual network; between the superior parietal lobe, superior division of the lateral occipital cortex, lingual gyrus, occipital pole and the lateral visual network; and between the superior parietal lobe, SMA, pre- and postcentral gyrus, precuneus, cingulate gyrus, supramarginal gyrus and the sensorimotor system network (figure 2, network 1, 2, and 4). Smaller regions of increased connectivity were found between the precuneus, superior division of the lateral occipital cortex and the default mode network (DMN) and right frontoparietal network (figure 2, network 5 and 7); and between the superior division of the lateral occipital cortex, angular gyrus, supramarginal gyrus, subcallosal cortex, superior parietal lobe and the left frontoparietal network (figure 2, network 8).

Decreased functional connectivity in PD patients compared to control subjects was found between the insular cortex, opercular cortex, frontal orbital cortex, precentral cortex, right putamen and the auditory system network; between the superior division of the lateral occipital cortex and the right frontoparietal network; and between the frontal orbital cortex and frontal gyrus and the left frontoparietal network (figure 2, network 3, 7, and 8). No changes in functional connectivity were observed in the executive control network (figure 2, network 6).

We found no significant relations between mean z-scores of regions with group differences and clinical data after applying correction for multiple comparisons.

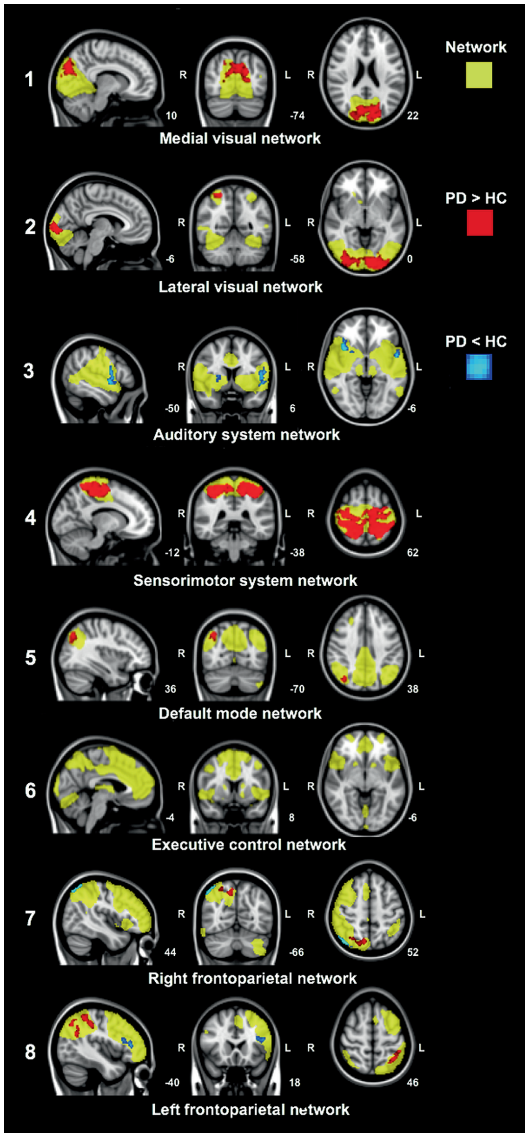


Figure 2. Significant group differences in functional connectivity between Parkinson's disease patients (PD) and control subjects (HC) in resting state networks. Analyses were adjusted for age, gender and voxel-wise grey matter volume per subject. Yellow: Spatial maps of eight standard resting state networks. Increased (red) and decreased (blue) network connectivity in patients compared to control subjects. Images are overlaid on the most informative, sagittal, coronal, and axial slices of the MNI standard anatomical image (MNI coordinates of each slice are given).

DISCUSSION

We used two complementary methods to analyze resting-state brain functional connectivity to study the cerebral functional reorganization at a network and whole brain level in patients with PD. Using a novel graph analysis approach (ECM), we found that frontoparietal regions display a stronger connectivity to the whole-brain network function in PD patients compared to control subjects, while a decreased connectivity was found for frontal and occipital areas of the brain (figures 1 and 3). In the resting-state networks of the brain, we found predominantly increased functional connectivity within the sensorimotor system and visual networks (figures 2 and 3). Comparing both approaches highlights a partial overlap of regional alterations of the whole brain functional connectivity architecture in PD (figure 3).

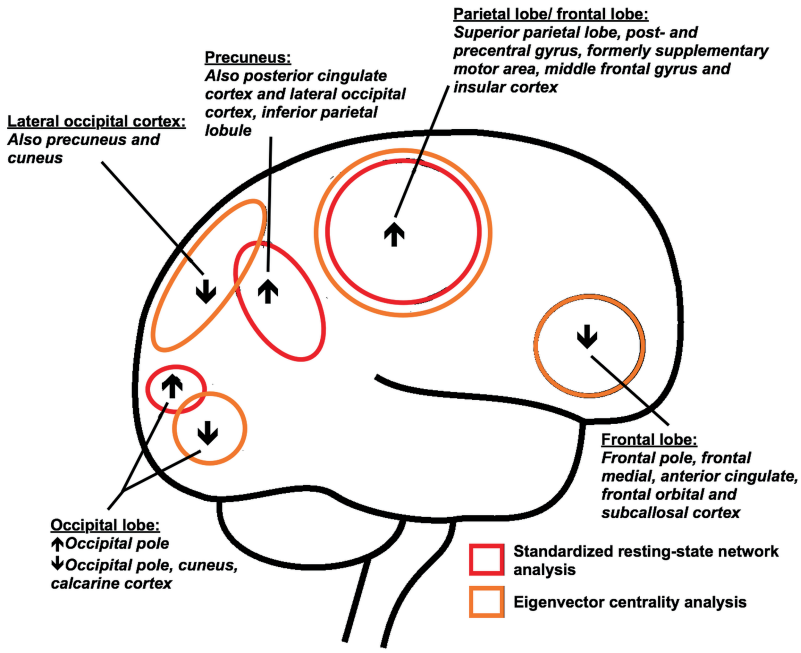


Figure 3. Main cortical differences (eigenvector centrality mapping and standard resting state network analysis results) in resting state functional connectivity between Parkinson's disease patients and control subjects are shown. Orange: whole-brain functional connectivity differences as measured with eigenvector centrality mapping; Red: functional connectivity differences in relation to eight standard resting state networks; ↑: increased functional connectivity; ↓: decreased functional connectivity.

Regions of increased functional connectivity in Parkinson's disease

Mean EC values were increased in large frontoparietal brain regions of PD patients (figures 1 and 3), indicating that these regions fulfill a more prominent role within the overall brain network of PD patients. The method used in our study counts the neighbors of each vertex, weighted by their centralities, while prior studies often used degree centrality in PD, another graph analysis technique that estimates the number of connections of a node. These studies showed higher frontoparietal connectivity in patients compared to control subjects (Göttlich et al., 2013; Zhang et al., 2015). It was further found that the efficiency among these connections was increased in PD patients (Zhang et al., 2015). The frontoparietal regions identified with ECM partly overlapped with increased regional functional connectivity identified by standard resting-state network analysis within the sensorimotor system network, including the sensorimotor, primary motor and premotor cortex, and SMA (figures 1–3). Increased resting-state functional connectivity of regions involved in motor control is a consistent finding in treated PD patients, which may suggest a role of dopaminergic medication (Göttlich et al., 2013; Onu et al., 2015; Prodoehl et al., 2014; Vo et al., 2017; Wu et al., 2009). Alternatively, the findings may reflect compensatory reorganization of basal ganglia thalamo-cortical motor loops (Eckert et al., 2006; Sabatini et al., 2000), since increased resting-state functional connectivity in frontoparietal regions has been described in PD patients in the "off-medication-state" as well (Zhang et al., 2015).

A recurrent finding in this study, identified with both approaches, was increased functional connectivity of the precuneus and posterior cingulate cortex in PD patients (figures 1–3). Both brain structures are considered as highly connected and are key nodes in the DMN (Beckmann et al., 2005; Utevsky et al., 2014; van den Heuvel and Sporns, 2011). Disruption of the DMN seems to be associated with cognitive deficits in PD patients (Baggio et al., 2015). A recent study further observed increased connectivity between the precuneus and frontoparietal regions during task conditions, suggesting that the precuneus simultaneous interacts with multiple brain networks depending on the cognitive status (Pievani et al., 2011; Utevsky et al., 2014). However, the association of functional connectivity within the DMN with cognitive performance in the present study did not survive correction for multiple comparisons.

Regions of decreased functional connectivity in Parkinson's disease

Occipital and frontal parts of the brain showed reduced EC in PD patients, indicating a diminished role of these regions within the overall brain functional

architecture network in PD. Only two other studies applied whole brain ECM in PD. The first study aimed to investigate EC in depressed PD patients and also reported small frontoparietal regions of decreased EC in the non-depressed PD group scanned in the "off-medication-state," compared to control subjects (Lou et al., 2015). The second study investigated ECM changes in PD patients following surgery, and reported that penetration of electrodes in the subthalamic nucleus was associated with increased EC in the brainstem, which was related to motor improvement (Holiga et al., 2015). However, this is the first study in which whole brain ECM results of mild to moderate PD patients are compared to healthy control subjects. Resting-state fMRI studies using other techniques than ECM in PD, report connectivity reductions of frontal and occipital regions as well (Göttlich et al., 2013; Yao et al., 2015), possibly related to cognitive dysfunction (Lewis et al., 2003; Vossel et al., 2014).

In Alzheimer's disease, ECM shows decreased EC in the occipital cortex, but increased EC in frontal brain areas (Binnewijzend et al., 2014). Decreased occipital EC was associated with a poorer cognitive performance in Alzheimer's disease patients, as well as in control subjects (Binnewijzend et al., 2014). In PD, decreased EC of the occipital cortex of patients may further be related to disruption of visual networks (Göttlich et al., 2013; Onu et al., 2015). Distinct spatial regions of the visual system that were identified with ECM, showed increased intra-network connectivity in PD patients within standard resting-state visual networks in this study (figures 2 and 3). Collectively, these findings suggest disrupted visual network organization and integration, which could be related to visual deficits or visuo-spatial attention deficits (Beckmann et al., 2005; Tessitore et al., 2012; Vossel et al., 2014).

Spatial distribution of altered functional connectivity

The regions of altered functional connectivity identified with two complementary techniques in this study are shown in figure 3. Post mortem studies show that neocortical deposition of Lewy pathology occur in the temporo-occipital, temporal and frontal gyrus and the cingulate, insular and inferior parietal cortex (Jellinger, 2012; McCann et al., 2016). We found altered functional connectivity in these structures with known Lewy pathology, but predominant regions of altered functional connectivity were located posterior in the brain, in particular the precuneus and posterior cingulate cortex. If the regionally altered functional connectivity in PD reflects the selective vulnerability of neuronal regions of the brain to alpha-SynA, cannot be assessed from this study. However, it is of interest

that it was shown that the majority of alpha-SynA are not localized in Lewy bodies, but are in the form of much smaller aggregates than Lewy bodies (Schulz-Schaeffer, 2015, 2010). These alpha-SynA were detected throughout the cortex of Lewy body disease patients and were most dense in the cingulate cortex (Schulz-Schaeffer, 2015, 2010). In PD, smaller alpha-SynA than Lewy bodies can also be observed at predilection sites (Schulz-Schaeffer, 2015, 2010).

The identified posterior brain regions further showed highest mean EC values in healthy control subjects, which is in line with findings of other studies reporting these regions as highly connected (hub) regions (Binnewijzend et al., 2014; Buckner et al., 2009; van den Heuvel and Sporns, 2011). In Alzheimer's disease patients, positon emission tomography amyloid imaging showed high levels of amyloid beta deposition in cortical hubs compared to control subjects (Buckner et al., 2009). It is proposed that cortical hub regions display a preferential vulnerability to pathology in neurodegenerative diseases, due to their intrinsic high activity level, or due to the possibility that increased neuronal activity enhances the process of misfolded protein in the brain (Buckner et al., 2005; de Haan et al., 2012; Pievani et al., 2014; Surmeier et al., 2017). Noninvasive imaging of alpha-SynA has proven more challenging than imaging amyloid-β deposition, making it difficult to study the presence and density of alpha-SynA levels in specific cortical (hub) regions and test these assumptions in PD.

Increased functional connectivity: pathogenic and compensatory mechanisms

A prominent finding in this study is the increased functional connectivity in PD patients. Increased functional connectivity is a common finding in neurodegenerative diseases (Gregory et al., 2017; Pievani et al., 2014), but the mechanism underlying increased functional connectivity is unclear. It may simply reflect the primary disease process, or appear secondary in response to altered function elsewhere in the brain (Grady, 2008). The latter is often explained as a compensation mechanism in fMRI resting-state and task-based studies that found increased connectivity associated with lower symptom scores (Gregory et al., 2017; Pievani et al., 2014). In PD, for instance, there is evidence for increased functional connectivity between the putamen and the cerebellum in mild to moderate stages of the disease, correlating with better motor performance (Simioni et al., 2016). In the presence of manifested disease, as in our patient group, increased connectivity can indicate unsuccessful or only partial compensation (Pievani et al., 2014) In this study, we found an altered balance of functional brain connectivity in symptomatic stages of PD in which alpha-SynA pathology involves neocortical areas (Jellinger,

2012; McCann et al., 2016). Longitudinal fMRI studies are needed to assess if assumingly preserved neuronal areas show increased connectivity early in the disease process, if connectivity in these regions changes as the disease progresses, and if this is related to network levels of clinical performance.

Potential limitations

Patients were scanned while taking their usual medications in this study. A potential modulatory role of dopaminergic medication cannot be ruled out. Several fMRI studies have reported a normalizing effect of dopaminergic medication on connectivity in PD, especially of sensorimotor regions, which might suggest that our findings would have been more pronounced if patients were scanned in the "off-medication-state" (Tahmasian et al., 2015). Moreover, dopaminergic medication may lead to prolonged motor responses and its chronic use may alter brain organization (Anderson and Nutt, 2011; Kaasinen et al., 2003). Hence, if scanning PD patients after a certain period of withdrawal of dopaminergic drugs solely measures the influence of the disease process, is still open for debate. Further, scanning patients in the "on-medication-state" may reduce motion-related artifacts, which are especially problematic in resting-state fMRI studies. To reduce motion related artifacts, we additionally visually inspected the data, performed standard motion correction and included white matter and cerebrospinal fluid templates in the analyses (Jenkinson et al., 2002; Pruim et al., 2015a, 2015b).

After strict correction for multiple comparisons, we found no relationship between functional connectivity and severity of motor symptoms (MDS-UPDRS motor scale), predominantly non-motor (non-dopaminergic) symptoms (SENS-PD scale) and cognition (SCOPA-COG scale) in PD. Dopaminergic medication may have attenuated the examined associations through a decrease of symptom scores that are responsive to dopaminergic stimulation and through a possible normalizing effect on functional connectivity in PD (Tahmasian et al., 2015). However, we used LED as an additional covariate in our model and this did not alter the significance of our findings. Moreover, no relations were found between functional connectivity measures and clinical measures. Previous studies in PD using structural imaging methods used to study brain atrophy or changes of white matter tracts (fractional anisotropy or mean diffusivity), however have revealed moderate clinico-imaging relationships (de Schipper et al., 2017; Pievani et al., 2011; Zhang et al., 2016). This likely suggests that changes of the functional connectivity architecture of the brain provide a different perspective of the

consequences of the pathobiology of PD, which do not necessarily have to be associated with clinical measures. This assumption is in line with studies in other neurodegenerative diseases, such as Alzheimer's disease, progressive nuclear palsy and Huntington's disease, where no clear associations have yet emerged between measures of functional connectivity and clinical measures of disease severity (Pievani et al., 2011).

Conclusion

The findings in this study on functional brain network organization in PD indicate a diminished role of frontal and occipital brain areas, while posterior parietal and frontoparietal areas display a more prominent connectivity to the whole-brain network function. We did not find significant correlations between clinical measures and functional imaging parameters, suggesting that changes on the level of functional connectivity architecture of the brain provide a different perspective of the pathological consequences of PD. Regionally altered functional connectivity was most pronounced in highly connected (hub) regions, particularly the posterior cingulate cortex and precuneus, which may account for the distributed abnormalities across the whole brain network architecture in PD.

6 Classification of Parkinson's disease status based on resting-state functional connectivity data

Sheila Rood[1,2*]
Laura de Schipper[3*]
Jeroen van der Grond[4]
Johan Marinus[3]
Johanna Henselmans[3,5]
Jacobus van Hilten[3]
Frank de Vos[1,4,6]

[1] Leiden University, Institute of Psychology, Department of Methodology and Statistics, Leiden, the Netherlands
[2] Leiden University, Faculty of Social and Behavioral Sciences, Leiden, the Netherlands
[3] Leiden University Medical Center, Department of Neurology, Leiden, the Netherlands
[4] Leiden University Medical Center, Department of Radiology, Leiden, the Netherlands
[5] Antonius Hospital, Department of Neurology, Woerden, the Netherlands
[6] Leiden University, Leiden Institute for Brain and Cognition, Leiden, the Netherlands

[*] Joint first author



ABSTRACT

Introduction: Recent research shows that resting-state fMRI data in combination with machine-learning techniques can be used to distinguish patients with neurodegenerative disease, like Alzheimer's disease, from healthy control subjects. We aimed to explore the potential of an elastic net model to recognize Parkinson's disease (PD) patients (at an individual level) using resting-state fMRI.

Methods: We used resting-state fMRI scans from 114 PD patients and 58 age- and sex-matched healthy control subjects. We calculated functional connectivity matrices and dynamics for full and partial correlations, resulting in four feature types, which have been used separately as well as combined in a cross-validated elastic net regularized logistic regression. We calculated the area under the curve to determine classification performance.

Results: The area under the curve values ranged between 0.752 and 0.858. Highest values were found for partial correlation functional connectivity dynamics. We also investigated whether particular clinical features contributed to the individual classification scores of PD patients and no associations were found.

Conclusion: These results show that resting-state functional connectivity dynamics in an elastic net regression is a promising method to differentiate between PD patients and healthy control subjects at an individual level.

INTRODUCTION

Parkinson's disease (PD) is the most common neurodegenerative disorder after Alzheimer's disease (AD), and its prevalence is growing (De Rijk et al., 2000; Dorsey et al., 2018). The clinical spectrum of PD comprises a broad range of motor and non-motor symptoms (Chaudhuri et al., 2006). Patients show conspicuous differences in the course or occurrence of symptoms, the severity of symptoms, as well as in the progression rate of the disease (Foltynie et al., 2002). The heterogeneity of PD can complicate diagnosis in clinical practice. Adding to the complexity of early diagnosis is the long pre-symptomatic phase of the disease, when neurodegeneration has commenced, but the (motor) symptoms are yet insufficient to define PD (Berg et al., 2015).

Resting-state functional magnetic resonance imaging (fMRI) of the brain might have the potential to identify early PD or persons at risk, before overt expression of the disease. Resting-state fMRI data of PD patients have shown differences between PD patients and control subjects in functional connectivity (de Schipper et al., 2018). Furthermore, a recent study showed changes in PD patients in the variations of functional connectivity over a short time (dynamics) (Kim et al., 2017). However, these results represent group-wise comparisons and are not applicable to individual patients with PD. In AD, resting-state fMRI research has shown promising results in distinguishing patients and control subjects at an individual level through classification approaches that enable the incorporation of numerous functional connectivity parameters as predictors into one model and automatically select the most relevant ones (de Vos et al., 2018; Schouten et al., 2016).

The aim of the present study is to investigate whether resting-state fMRI data can be used to classify PD patients and healthy control subjects. We calculated whole-brain functional connectivity using full and partial correlations, and calculated functional connectivity dynamics using a sliding window approach (Hutchison et al., 2013). These features were used as input for machine-learning techniques to calculate classification scores for each measure (full and partial functional connectivity matrices and dynamics) separately and all measures combined in order to determine the most accurate prediction model. We further investigated whether classification scores were correlated to clinical measures of PD.

METHODS

Study design and participants

The sample for the current study consists of 172 participants: 114 PD patients, of which 11 patients were diagnosed as PD with Lewy bodies (DLB) subtype, and 58 healthy control subjects. In line with the most recent MDS-PD criteria, we qualified patients with DLB who met the clinical criteria for PD, as PD (Gibb and Lees, 1988; Postuma et al., 2015). Patients were recruited from the outpatient clinic for Movement Disorders of the Department of Neurology of the Leiden University Medical Center (LUMC; Leiden, the Netherlands) and nearby university and regional hospitals. PD patients fulfilled the United Kingdom Parkinson's Disease Society Brain Bank criteria for idiopathic Parkinson's disease (Gibb and Lees, 1988) and DLB patients the McKeith DLB diagnostic criteria for probable DLB (McKeith et al., 2005). Exclusion criteria were previous or other disorders of the central nervous system, peripheral nerve disorders influencing motor and/or autonomic functioning, and psychiatric comorbidity not related to PD. Control subjects were selected from the Leiden Longevity Study (Altmann-Schneider et al., 2013), matched at group level for age and gender with the PD patients.

Clinical measures

The Movement Disorder Society unified Parkinson's disease rating scale (MDS-UPDRS) motor scale (part III) was used to quantify the severity of motor symptoms (Goetz et al., 2008). Fluctuating cognition and recurrent visual hallucinations are two core features of DLB, besides spontaneous features of parkinsonism (McKeith et al., 2005). We therefore included measures of cognition and hallucinations to our examinations as well. The mini-mental state examination (MMSE) was used to assess cognitive performance (Folstein et al., 1975). We quantified hallucinations using the hallucination item of the SCOPA psychiatric complications (PC, range: 0 -18) scale (Visser et al., 2007). We further used the severity of non-dopaminergic symptoms in Parkinson's disease (SENS-PD) scale to measure symptoms that largely do not improve with dopaminergic medication (Goetz et al., 2008; van der Heeden et al., 2016). The SENS-PD is a composite score comprising three items with four response options (range: 0-3) from each of the following six domains: postural instability and gait difficulty, psychotic symptoms, excessive daytime sleepiness, autonomic dysfunction, cognitive impairment and depressive symptoms (total range: 0-54) (van der Heeden et al., 2016). These six domains represent a coherent complex of symptoms that may already be present in the early disease stages, and increases in severity when the disease advances (van der

Heeden et al., 2016). Higher scores reflect more severe impairment. The formula of Tomlinson et al. was used to calculate a levodopa equivalent dose (LDE) of daily levodopa (Tomlinson et al., 2010).

fMRI acquisition

Imaging was performed on a 3 Tesla MRI scanner (Philips Achieva, Best, the Netherlands). Participants were instructed not to fall asleep during the scan and to lie with their eyes closed without moving. The following parameters were used for the resting-state fMRI scans: repetition time = 2.2 s, echo time = 30 ms, flip angle = 80°, 37 slices, resulting in a voxel size of 2.75 × 2.75 × 2.72 mm, with a 10% interslice gap, 200 volumes, scan duration 7 min and 29 s. Three-dimensional T1-weighted anatomical images were obtained with the following parameters: repetition time = 9.8 ms, echo time = 4.6 ms, flip angle = 8°, FOV 220 × 174 × 156 mm, 130 slices with a slice thickness of 1.2 mm with no gap between slices, resulting in a voxel size of 1.15 × 1.15 × 1.20 mm. A 32-channel and an 8-channel head coil was used for the PD group and the control group respectively.

Resting-state fMRI preprocessing

Resting-state fMRI data was preprocessed applying: motion correction with the motion correction FMRIB's linear image registration tool (MCFLIRT) (Jenkinson et al., 2002a), brain extraction (Smith, 2002) and spatial smoothing using a Gaussian kernel with a full width at half maximum of 5 mm. Preprocessing further consisted of high-pass temporal filtering with a cutoff frequency 0.01 Hz and finally a non-linear registration with boundary-based registration to the 2 mm isotropic Montreal Neurological Institute standard space image (MNI; Montreal, QC, Canada) and a 10 mm warp resolution (Greve and Fischl, 2009), via the T1-weighted images, using high-resolution echo planar images for an additional registration step between functional images and T1-weighted images (Andersson et al., 2007; de Schipper et al., 2018). We further used independent component analysis based automatic removal of motion artifacts (ICA-AROMA) to identify and remove residual motion-related artifacts data (Pruim et al., 2015a, 2015b). The resting-state fMRI scan was subsequently weighted by a gray matter probability map, because neuronal activity predominantly takes place in gray matter voxels. The Harvard-Oxford cortical structural atlas (as provided by FSL version 5.0) was used to separate the preprocessed scans into 48 different brain regions. Time courses for each of the 48 brain regions were calculated for each subject, which were subsequently used in the functional connectivity analyses.

Functional connectivity matrices

We used the time courses of the 48 brain regions to calculate functional connectivity matrices, using both full and sparse partial correlations. Whereas full correlations represent the total correlation between two brain regions, sparse partial correlations focus on the unique correlation between two regions (Peng et al., 2009). Sparse partial correlations were calculated using the graphical lasso algorithm implemented in R package "glasso" (Friedman et al., 2010). For each subject we calculated both full and sparse partial correlations between all pairs of brain regions, resulting in two functional connectivity matrices both consisting of $(48 \bullet (48 - 1))/2$ = 1128 correlations.

Functional connectivity dynamics

The dynamics of the above described functional connectivity matrices were calculated, using a sliding window approach (Chang and Glover, 2010; Hutchison et al., 2013; Jones et al., 2012), in which functional connectivity is calculated within a limited time window. This window was shifted over the total length of the scan and the standard deviation over all these windows was calculated. The size of the window was set at 11 scan volumes, which equals 24.7 seconds, and was slided one volume at a time. Functional connectivity dynamics was calculated for both the full and sparse partial correlation matrices, resulting in two functional connectivity dynamics matrices both consisting of $(48 \bullet (48 - 1))/2$ = 1128 correlations.

Statistical analyses

The full and partial functional connectivity and dynamical matrices were used as input for elastic net regularized logistic regression models in order to classify subjects as either control subject (0) or PD patient (1). Elastic net regularized logistic regression has been commonly used for neuroimaging classifications studies (de Vos et al., 2018; Schouten et al., 2016; Teipel et al., 2017, 2015). We performed elastic net regularized logistic regression with all feature types separately as input, as well as with all feature types combined. In elastic net regression, only the most relevant predictors will enter the regression model (Friedman et al., 2010; Zou and Hastie, 2005). Elastic net regression uses a combination of an L1-regularisation (lasso) (Tibshirani, 1996) and an L2-regularisation (ridge) (Hoerl and Kennard, 1970) and compromises between the two (Zou and Hastie, 2005). R package "glmnet" was used for the elastic net analyses (Friedman et al., 2010).

We used nested cross-validation to ensure that we were not overfitting the classification model. The inner cross validation loop was used to tune the sizes of the L1 and L2 penalties, and the ratio between those two penalties. The outer cross validation loop was used to train and evaluate the classification model. For both the inner and outer cross validation loop we used tenfold cross-validation, where the data was split repeatedly into ten percent test set and ninety percent training set, making sure each part of the data had been used as test set once. The training set in the outer cross validation loop was used for the inner cross validation loop (figure 1). The whole cross validation procedure was repeated ten times in order to reduce the variability resulting from the random partitioning of subjects into training and test folds.

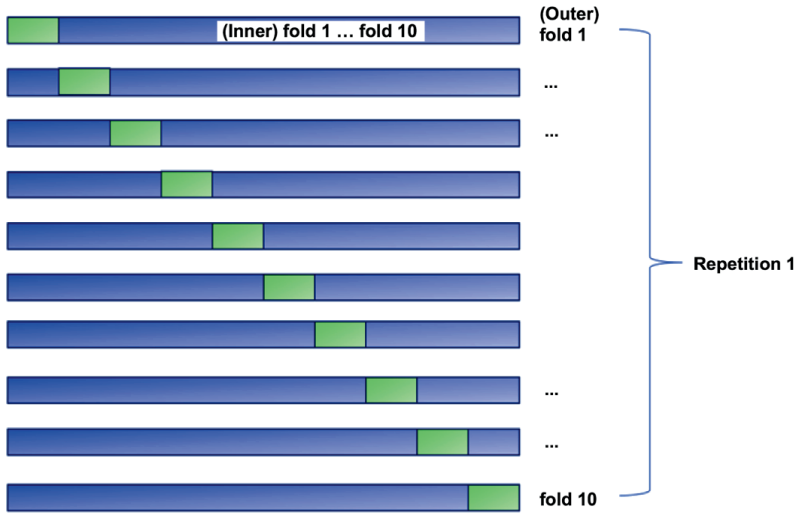


Figure 1. Cross-validation approach. Repeated, nested, tenfold cross-validation represented schematically. Green bars represent the test set, blue bars represent the training set. In reality, it was randomly chosen in which fold each of the subjects was part of the test or training set, making sure each of the subjects was only part of the test set once. For the purpose of the figure, however, the test and training set are portrayed as fixed blocks.

As the current study has an unbalanced design, we used receiver operator characteristic (ROC) curves to measure classification performance, as this method controls for unbalanced groups. The ROC curve was first computed and

subsequently the area under the curve (AUC) was calculated using the R-package "auc" (Balling & Van den Poel, 2013). Since there was no clear preference for a lower number of false positive diagnoses or a lower number of false negative diagnoses, the cut-off value to calculate the sensitivity and specificity was determined for each feature type individually, and was based on the Youden Index. This index reflects the value at which the sum of the sensitivity and the specificity is the highest (Fluss et al., 2005). The classification accuracy, sensitivity, and specificity were calculated for all features separately and combined.

Within the group of PD patients, we investigated the relationship between clinical variables (disease duration, MDS-UPDRS motor, SENS-PD and MMSE scores, hallucinations) and classification scores of the most accurate classification model using linear regression models (IBM SPSS Statistics for Mac, Version 23.0. Armonk, NY: IBM Corp.). The relationship between classification scores of the most accurate classification model and total LDE was investigated within the group of PD patients on dopaminergic medication. We also investigated group differences in classification scores of the most accurate classification model between drug-naïve patients and patients on dopaminergic medication using an independent-samples t-test. Bonferroni correction was applied in all cases.

RESULTS

Demographic data of the PD patients and healthy control subjects and clinical data of the PD patients are shown in table 1. Gender and age did not significantly differ between the patient and control group.

Classification accuracy

In table 2 the average AUC values over all cross-validation repetitions per feature type are shown. Combining all types resulted in an average classification accuracy of 0.818. Using the types of features separately resulted in a higher average classification accuracy for both partial correlation features, that is 0.832 for partial correlation functional connectivity and 0.858 for partial correlation functional connectivity dynamics, which is the highest AUC value obtained in the current study. Combining all types of features did not yield a higher AUC value than using all types of features separately. The individual predictions of the subjects are plotted in figure 2.

Table 1. Main characteristics of participants

	Patients	Control subjects
N	**114**	**58**
Men/women	74/40 (64.9)	31/27 (53.4)
Age, years	65.3 (7.0)	65.2 (7.5)
Disease duration, years	8.8 (4.7)	n/a
MDS-UPDRS motor score (0-132)	32.9 (15.3)	n/a
SENS-PD (0-54)	14.2 (6.4)	n/a
MMSE	28.0 (2.6)	n/a
SCOPA PC hallucination item (0-3)	4[a]	n/a
Total LDE, mg/day[b]	954.9 (570.9)	n/a
Drug-naïve patients	20	n/a

Values are means (standard deviation) for continuous variables and numbers for gender (% men). For all measurement instruments, the score range is presented in parentheses. MDS-UPDRS: Movement Disorder Society unified Parkinson's disease rating scale; SENS-PD: severity of non-dopaminergic symptoms in Parkinson's disease; MMSE: mini-mental state examination; LDE: Levodopa dosage equivalent; n/a: not applicable.
[a] 4 Patients had a score > 1, range: 0–3; [b] N = 94 (20 patients were drug-naïve).

Table 2. Mean AUC, sensitivity and specificity

	FFC	PFC	FFD	PFD	All
AUC	0.752	0.832	0.753	0.858	0.818
Sensitivity	0.655	0.828	0.709	0.809	0.831
Specificity	0.781	0.778	0.744	0.822	0.705

AUC: area under the curve; FFC: full correlation functional connectivity; PFC: partial correlation functional connectivity; FFD: full correlation functional connectivity dynamics; PFD: partial correlation functional connectivity dynamics; All: FFC, PFC, FFD and PFD combined.

Correlations with clinical scores

We investigated the relationship between individual elastic net partial correlation functional connectivity dynamics classification scores of the PD patients and clinical variables, but after correction for multiple comparisons, no statistically significant associations were found. The mean classification scores between drug-naïve patients (0.77) and patients on dopaminergic medication (0.83) did not significantly differ between groups ($p = 0.205$).

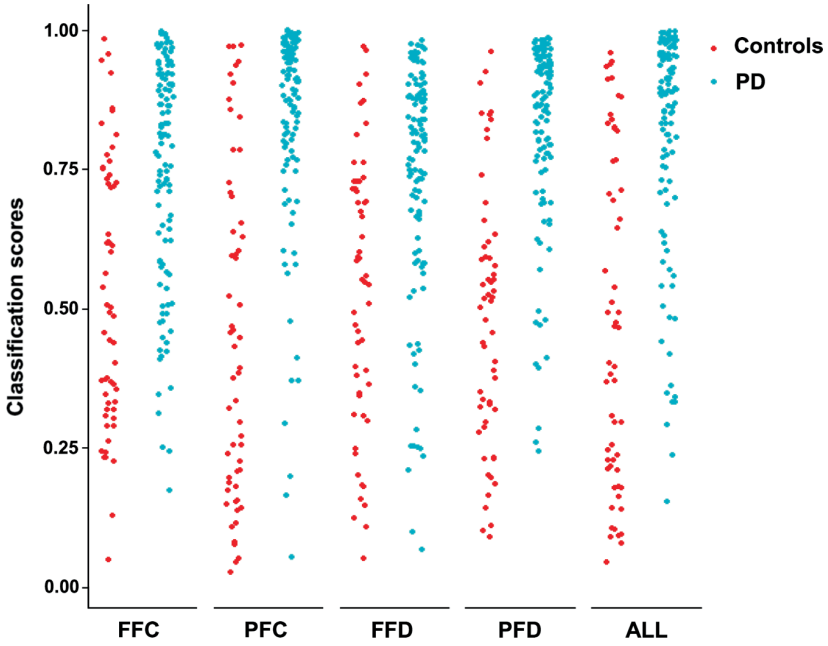


Figure 2. Classifications per feature type against diagnosis. FFC = full correlation functional connectivity, PFC = partial correlation functional connectivity, FFD = full correlation functional connectivity dynamics, PFD = partial correlation functional connectivity dynamics, ALL = FFC, PFC, FFD and PFD combined.

DISCUSSION

We studied the accuracy of different resting-state fMRI measures in combination with machine-learning techniques for the (individual) classification of PD patients. Full and partial functional connectivity matrices and dynamics were computed and used as input in an elastic net regression to discriminate PD patients from healthy control subjects. For both the functional connectivity matrices and dynamics, partial correlations resulted in higher classification accuracy than full correlations. The functional connectivity dynamics resulted in a (slightly) higher classification accuracy than the functional connectivity matrices. Combining multiple feature types did not improve the classification accuracy compared to using the features separately.

The partial functional connectivity dynamics model resulted in an AUC of 0.86. Previous MRI studies that investigated machine learning techniques in PD,

have used T1-weighted MRI data for differentiation of PD from control subjects, patients with progressive supranuclear palsy or subjects with scans without evidence of dopaminergic deficit (SWEDD) (Sakai and Yamada, 2018). Previous studies using grey and white matter volumes of regions of interest for differentiation of PD and control subjects reported an overall accuracy 0.82 (Adeli et al., 2016) and 0.71 (Liu et al., 2016). Another study used T1-weighted MRI data alone as well, but incorporated structural connectivity between brain regions, and found an overall accuracy of 0.86 (Peng et al., 2017). A proposed approach for early diagnosis of PD that combined T1-weighted MRI markers with clinical scores typical of prodromal PD even reached an AUC value of 0.97 (Amoroso et al., 2018). Overall, the findings of these studies combined with our results, suggest that a combination of structural and functional imaging combined with machine learning approaches are a promising classification method for PD diagnosis, and in time possibly early or prodromal PD. The integration of other imaging modalities, such as diffusion tensor imaging (DTI), may further improve classification performances.

The dynamic changes of functional connectivity, which is relatively new in the field of PD, resulted in the highest classification accuracy. In a recent study, functional connectivity dynamics suggested two distinct connectivity states: a more frequent, sparsely connected within-network state and a less frequent, more strongly interconnected between-network state (Kim et al., 2017). Their results show that PD patients spent less time in the sparsely connected state, while they spent more time in the more strongly interconnected state (Kim et al., 2017). This suggests that the connectivity state that is characterized by increased interactions between cerebral networks predominates in PD, at the expense of the more sparsely within-network state (Kim et al., 2017). Our findings stressing the relevance of dynamic changes in classifying patients with PD are in line with those from previous studies in AD (de Vos et al., 2018; Jones et al., 2012). Functional dynamics may reflect aspects of functional capacity of neural systems (Deco et al., 2011; Kucyi et al., 2017), and are suggested as possible biomarkers of disease (Kim et al., 2017).

For both the functional connectivity matrices and dynamics, partial correlations resulted in higher classification accuracy than full correlations. As partial correlations are controlled for the potential effect of other brain regions on that relation (Peng et al., 2009), they provide unique information of the relationship between two brain regions and functional connectivity measures based on partial correlations therefore likely provide a better estimation of functional connectivity than full correlations (Smith et al., 2011).

Although the AUC value obtained for the functional connectivity dynamics model based on partial correlations in the current study was quite high, no associations with clinical variables were found. This may be attributed to the fact that the model was trained to differentiate PD patients from healthy control subjects, using a combined set of predictors selected from correlations between multiple brain regions, and classification scores. In turn, this approach renders the occurrence of correlations between partial functional connectivity dynamics and individual symptoms or clinical domains less likely.

This is the first study using resting-state fMRI data in combination with elastic net regression analysis for (individual) classification of PD patients, resulting in moderate to good PD classification. Machine-learning methods could be of use for early diagnosis of PD, or possibly detect brain changes in persons at risk for developing PD. However, the patient group used to train and test the prediction models in this study included few de novo PD patients, had a moderate mean disease severity and a mean disease duration of approximately nine years. A population comprising a larger number of de novo patients is possibly more suitable for the purpose of early diagnosis of PD. Further, 92 patients in this study were scanned while taking their usual dopaminergic medications, while 20 patients were drug-naïve. The acute effect of dopaminergic medication may normalize functional connectivity in PD (Tahmasian et al., 2015), and its chronic use may alter brain organization (Anderson and Nutt, 2011; Kaasinen et al., 2003). Dopaminergic medication was not related to the classifications scores of our partial functional connectivity dynamics model, and mean classification scores did not differ between patients on dopaminergic medication and those who were not, but we cannot rule out a potential modulatory role of dopaminergic medication. A potential limitation of our study could be that the MRI acquisition of our two cohorts (control persons and patients with PD) were performed with a different type of head coil (8-channel versus 32-channel, respectively) (Panman et al., 2019), which might have affected our classification score, although another study comparing resting-state fMRI data using an 8- and 32-channel head coil on a 3 Tesla MRI scanner did not find significant differences between the two head coils (Paolini et al., 2015). Of note is that the scans in this study last 7 minutes and 29 seconds, and a timeframe of 24.7 seconds was taken as one window in the sliding-window approach, which is quite short to calculate functional connectivity dynamics (Hindriks et al., 2016). There exists an arbitrary trade-off between the number of measurement moments in one window and the number of different windows that can be used for calculation of functional connectivity dynamics. In the current study, using a higher number of

different windows was preferred over using more measurements in one window. However, using larger windows may yield even better classification accuracies than the ones that we found in the current study (Shirer et al., 2012).

Conclusion

We showed that it is possible to achieve moderate to good PD classification using elastic net regularized logistic regression combined with resting-state fMRI data, in particular with partial functional connectivity dynamics. This approach has potential as a suitable method for use in future PD classification studies.

7 Summary, concluding remarks and future perspectives

In this thesis, the consequences of PD were studied using advanced approaches in neuroimaging, including structural as well as functional connectivity networks, examination of the role of aging in white matter degeneration in PD, and the use of machine learning classification models. Our main findings are summarized and discussed in the next paragraphs of this chapter, followed by possible directions for future research.

Summary

Chapter 1 is the introduction to this thesis. In **chapter 2**, we investigated the integrity of nine standardized structural covariance networks (SCNs) in relation to clinical severity of PD (Hafkemeijer et al., 2014). An SCN is based on interdependent regions of grey matter density. We found that two out of nine networks showed atrophy and a loss of integrity. We identified atrophy and loss of integrity in the anterior and posterior cingulate networks in PD patients. Abnormalities of both networks were associated with predominantly non-dopaminergic features, specifically cognition and excessive daytime sleepiness. Our findings suggest that (components of) the cingulate networks display a specific vulnerability to the pathobiology of PD and may operate as interfaces between networks involved in cognition and alertness.

DLB and PD are considered subtypes of the alpha-synucleinopathy spectrum that show similar and dissimilar clinical and morphological features. In **chapter 3**, we used the same technique as in chapter 2 (SCNs) to further our understanding of brain grey matter abnormalities that might differentiate PD and DLB more clearly, combined with voxel-based morphometry, volumetric measures and vertex-based shape analysis. This study showed atrophy of the hippocampus and parahippocampal gyrus in DLB compared with PD patients, with a differential involvement of the head and body of the hippocampus. Moreover, integrity of the posterior cingulate network, which also comprises (para)hippocampal regions, was significantly lower in DLB. The findings of this study show that regional hippocampal differences between DLB and PD may be important in the distinction between the two disorders.

As we identified a loss of integrity and atrophy beyond the strong effects of aging in two SNCs (see chapter 2 for explanation), we hypothesized that there may be an interaction effect of age and disease presence on white matter integrity in PD and this was addressed in **chapter 4**. White matter is especially prone to the effects of

aging, and it is increasingly recognized that white matter is already affected in early stages of PD. We found a similar age-related decline of white matter integrity for PD patients and healthy control subjects in this study, but PD patients had more white matter hyperintensities (WMHs) than expected for their age. The excess of WMHs was partly located in periventricular and deep frontal white matter of PD patients, and was, besides age, related to visuospatial functioning and postural instability and gait difficulty. Global microstructural integrity of the normal appearing white matter did not differ between patients and healthy control subjects, suggesting that PD-specific changes do not exceed normal age-associated change in white matter without lesions.

In **chapter 5**, we studied PD-related changes of the brain with network approaches again, but with a different method. We used a novel graph analytic approach in functional imaging (eigenvector centrality mapping; ECM), to examine changes in functional brain connectivity architecture on a whole brain network level in patients with PD. We found that frontoparietal regions display a stronger connectivity to the whole-brain network function in PD patients compared with healthy control subjects, while a decreased connectivity was found for frontal and occipital areas of the brain. Additionally, we used eight standardized resting-state subnetworks of the brain, which pointed at predominantly increased functional connectivity within the sensorimotor system and visual networks. Comparing both approaches highlighted altered functional connectivity in highly connected (hub) regions, particularly in the posterior cingulate cortex and precuneus, which may account for the distributed abnormalities across the whole brain network architecture in PD patients. The regional altered functional connectivity was not related to clinical measures in this study, indicating that changes on the level of functional connectivity architecture of the brain are not necessarily associated with clinical measures.

In **chapter 6**, we explored the use of machine learning techniques in combination with resting-state fMRI data to differentiate between PD patients and healthy control subjects at an individual level. We computed functional connectivity matrices and dynamics for full and partial correlations, resulting in four feature types, which have been used separately as well as combined in a cross-validated elastic net regularized logistic regression. We calculated the area under the curve (AUC) to determine classification performance. The AUC values ranged between 0.752 and 0.858. The highest values were found for partial correlation functional

connectivity dynamics. We also investigated whether particular clinical features contributed to the individual classification scores of PD patients and no associations were found. We showed that it is possible to achieve moderate to good PD classification using elastic net regularized logistic regression combined with resting-state fMRI data, in particular with the use of functional connectivity dynamics.

Concluding remarks

Structural and functional connectivity

Chapter 2, 3 and 5 in this thesis showed that network approaches provide valuable insights in the structural and functional brain architecture of patients with PD. It is hypothesized that neurodegenerative diseases show a selective, network-driven neuronal vulnerability (Seeley et al., 2009). The findings in chapter 2 and 3 showed specific structural network degeneration in PD and DLB, namely degeneration of the anterior and posterior cingulate network. The anterior cingulate network shows spatial overlap with a network described in a previous study that identified a structural network that was also degenerated in PD (Zeighami et al., 2015). The cortical regions in this network included the anterior cingulate cortex as well (Zeighami et al., 2015). Another study used this network in their analysis of subtypes with "mild motor-predominant", "diffuse malignant" and "intermediate" PD. This study showed more pronounced atrophy in the anterior cingulate cortex in "diffuse malignant" PD patients compared with the other two subtypes (Fereshtehnejad et al., 2017). These findings indicate that the cingulate cortex is particularly vulnerable in PD, and that the changes in the networks in which the cingulate cortex is involved, relate to disease progression in PD.

Further we found regionally altered functional connectivity in the precuneus and posterior cingulate cortex, which are important regions of the posterior cingulate structural connectivity network (chapter 5). The precuneus and posterior cingulate cortex are key nodes in the default mode network, which is a functional connectivity network that is frequently described to be disrupted in PD, and is possibly associated to cognitive deficits in PD (Baggio et al., 2014). These structures are considered as central and highly connected brain regions (Hagmann et al., 2008; van den Heuvel and Hulshoff Pol, 2010), and are suggested to be part of a set of posterior medial and parietal cortical regions that form a structural core of the brain (Hagmann et al., 2008). The structural core may have a central role in integrating information across structurally segregated and functionally specialized brain

regions (Hagmann et al., 2008). Changes in the structural core may therefore have widespread changes across the brain network architecture. Combined, these findings point out an important role of these highly connected (hub) regions in structural and functional covariance in PD, and connectional variability of the precuneus and posterior cingulate cortex may relate to specific subsets or characteristics of PD patients, such as our finding in chapter 2 that loss of integrity of the posterior cingulate network related to predominantly non-dopaminergic features.

Age

Several studies suggested that age is an important modulating factor in the disease progression and phenotype expression of PD. For example, advancing age is associated with a more rapid decline in motor function and more severe cognitive impairment in patients with PD (Alves et al., 2005; Levy, 2007). The exact role of aging in PD, however, and changes that underlie the relationship between age and PD, are unclear. Numerous neuroimaging studies have shown an age-related decline in MRI parameters of brain structure and function (Ferreira and Busatto, 2013; Good et al., 2001; Hafkemeijer et al., 2012; Jernigan et al., 2001; Raz et al., 2005; Resnick et al., 2003). Our results showed grey matter atrophy in DLB and PD patients compared with age-matched healthy control subjects in regions that explicitly show age-dependent decreased grey matter volume, such as the hippocampus and cingulate cortex (Good et al., 2001; Jernigan et al., 2001; Raz et al., 2005; Resnick et al., 2003). Further, regional altered functional connectivity was mainly expressed in the precuneus and posterior cingulate cortex, which are also regions that are associated with functional disruption at high age (Ferreira and Busatto, 2013; Hafkemeijer et al., 2012). These findings suggests that the pathobiology of PD has a preferential susceptibility for regions that are already affected by the aging process, or that the age-effect is possibly influenced by disease in a region dependent manner (Claassen et al., 2016). Our results of chapter 4, combined with the results of previous studies, suggest a similar age-related decline of global white matter integrity in PD and healthy control subjects. The results of chapter 4 further showed that WMHs in PD may already be present in an early phase of the disease. This is in line with other studies suggesting that white matter may be affected in the very early stages of PD (Dadar et al., 2018; Duncan et al., 2016; Veselý and Rektor, 2016). A possible explanation could be that PD patients show a non-linear trajectory of an early accelerated age-related decline, which stabilizes with advancing age (Claassen et al., 2016).This explanation

is supported by the absence of any relation between disease duration and WMHs in chapter 4.

Dopaminergic medication

Except for a group of drug-naïve patients, the patients in the studies described in this thesis were scanned while taking their usual medications. MRI scanning of PD patients without dopaminergic treatment is problematic, as tremor may result in motion-related artifacts (Tahmasian et al., 2015) and participation may be jeopardized when patients have to travel from home during the off-state. Resting-state fMRI is particularly prone to noise due to motion, and the effects of head motion should be considered when it differs between groups (van Dijk et al., 2012). The reduction of motor symptoms through dopaminergic treatment may reduce the effects of excessive involuntary head motion, in addition to the other approaches used in this thesis for motion artifact removal (Jenkinson et al., 2002b; Pruim et al., 2015a, 2015b; Tahmasian et al., 2015). However, scanning PD patients in the "on-medication state" may also hamper the interpretation of data since functional connectivity changes secondary to dopaminergic therapy may occur in PD patients (Tahmasian et al., 2017). fMRI studies have reported a normalizing effect of dopaminergic medication on abnormal functional connectivity associated with PD, which might suggest that our findings would have been more pronounced if patients were scanned in the "off-medication-state" (Tahmasian et al., 2015). The results of other studies suggest that dopaminergic medication may also alter the functional connectivity between brain regions that are not necessarily involved in the improvement of symptoms of PD (Ng et al., 2017). However, there is evidence that these effects of dopaminergic medication are small, in particular in the well-established resting-state networks that we used in chapter 5 (Flodin et al., 2012). Moreover, scanning PD patients in the "off-medication-state" may result in group functional connectivity differences secondary to dopaminergic treatment as well, due to changed brain organization caused by the long-term use of dopaminergic medication (Kaasinen et al., 2003; Kurani et al., 2015). De novo patients are therefore the only population to study pathophysiology independent of dopaminergic therapy. In PD populations using dopaminergic treatment the dopaminergic state of PD patients should be considered when interpreting or comparing results of MRI studies.

Study population

The research presented in this thesis was performed in a cross-sectional setting in PD and DLB patients. Some studies described in this thesis required the use of a control group. These control subjects were selected from the Leiden Longevity Study (Altmann-Schneider et al., 2013), which comprises a large pool of healthy subjects from which matched controls can be selected. It should be considered that there were some slight differences in some of the variables collected and the methods of data collection between patients and control subjects. The MRI acquisition in our control group and PD group was performed with a different type of head coil (8-channel versus 32-channel, respectively), which may have influenced our findings, although we used MRI approaches relatively insensitive to a potential coil effect (Geng et al., 2012; Panman et al., 2019; Paolini et al., 2015). However, the use of different head coils may hamper the analysis of MRI data and standardization of head coils across groups of interest is recommended in future study designs (Panman et al., 2019). Patients and control subjects were matched for age and gender, two known confounders of particular importance in MRI studies (Barnes et al., 2009). A critical consideration related to the control group selected for the study presented in chapter 4 is that control subjects were not matched for cardiovascular risk profile, in addition to age and gender, although it should be noted that patients and control subjects did not differ in those cardiovascular risk factors that were assessed in both the PROPARK and Leiden Longevity study.

Future perspectives

Multimodal neuroimaging studies

We studied brain MRI in PD and DLB patients with five different MRI sequences in this thesis, which, amongst other things, highlighted a spatial overlap of altered structural and functional connectivity, in particular of the cingulate cortex. Structural and functional MRI are increasingly combined to provide more informative insights into both structural as well as functional connectivity in neurodegenerative diseases (Arbabshirani et al., 2017; Seeley et al., 2009). Combining data of different imaging modalities, such as MRI, Positron-Emission Tomography (PET), magnetoencephalography (MEG) or electroencephalography (EEG), may yield even more insights into the relationships between function and structure (Arbabshirani et al., 2017; Calhoun and Sui, 2016). In schizophrenia, several studies combined MRI data with EEG or MEG data (Calhoun and Sui, 2016). One study showed considerable spatial consistency between function (MEG) and

structure (white matter integrity), with regional reduced MEG amplitude and FA in a posterior visual network, which was related to cognitive performance (Stephen et al., 2013). There is increasing knowledge on the integrated analysis of multimodal data. The combination of deep learning and multimodal data or multimodal classification may reveal unique information that cannot be obtained when using one modality (Arbabshirani et al., 2017; Calhoun and Sui, 2016). Several combinations of PET and MRI results have been applied in PD and DLB, indicating striatal dopamine modulation of functional connectivity networks (Baik et al., 2014; Lebedev et al., 2014; Weingarten et al., 2015), and showing that combined data distinguished DLB from Alzheimer's disease better than measurements from one modality (Kantarci et al., 2012; Weingarten et al., 2015).

Artificial intelligence and big data

We used machine learning in chapter 6, which is a current application of artificial intelligence based on algorithms that can learn from data and subsequently construct a model in order to make predictions or decisions without being explicitly programmed. Machine learning approaches are increasingly applied to MRI data to study neurodegenerative diseases. A promising unsupervised machine learning method that allows for the exploration of previously unidentified disease subtypes based on neuroimaging, is cluster-wise ICA (C-ICA) (Durieux, 2015). C-ICA aims to cluster subjects in a data-driven fashion into homogeneous groups based on similarities and differences in the functional connectivity patterns that characterize them. The functional connectivity patterns that are associated with these subgroups could further provide information about neurodegenerative diseases such as PD. Components of a thus identified cluster may serve as a marker for the differentiation of subtypes with differing patterns of abnormal functional connectivity and potentially distinct clinical symptom profiles. Possible extensions of the C-ICA model include applications to other types of data as EEG data (Durieux, 2015).

Despite promising results of some studies, the use of machine learning in PD is still in its early stage. This is likely caused by the limited sample sizes (Arbabshirani et al., 2017). However, a unique international, multicenter clinical, imaging and biologic specimens dataset of PD patients has been collected, managed and made available by the Parkinson's Progression Markers Initiative (PPMI) (Marek et al., 2011). A recent study using PPMI data investigated strategies to handle challenges of large datasets, such as heterogeneity or missing data, and subsequently

produced models for PD classification and prediction (Dinov et al., 2016). Future studies can possibly provide additional insights on how to address availability, integration and analytics of big data to advance the usability of MRI of PD in clinical practice.

Individual classification

Advanced neuroimaging approaches are of special interest for their potential to characterize unique morphological characteristics and connectivity patterns of neurodegenerative diseases (Agosta et al., 2017). For example, due to the high availability of 3 Tesla MRI scanners, the analysis of hippocampal subfields has gained increasing attention (Agosta et al., 2017). We showed that regional hippocampal differences between DLB and PD may be important in the distinction between the two disorders in chapter 3. However, except for the model that was built to identify PD patients at an individual level in chapter 6, the results in this thesis cannot be applied to individual patients. Neuroimaging studies in PD have largely provided average estimates at a group level. Although these studies are valuable for the discovery of relevant disease markers, the discriminative ability at the individual level of these neuroimaging measures is typically not evaluated. Neuroimaging-based single-subject prediction of neurodegenerative diseases has gained attention in recent years. In PD, a study using machine learning for the analysis of resting-state fMRI data showed that it was possible to predict motor scores (Movement Disorder Society unified Parkinson's disease rating scale; MDS-UPDRS - part III) on an individual patient level (correlation = 0.35, $p = 0.001$; mean sum of squares = 222.17, $p = 0.002$) (Hou et al., 2016). Another study showed that machine learning in combination with multimodal MRI data for the differentiation of PD patients with a non-postural instability and gait difficulty subtype from patients with a postural instability and gait difficulty subtype resulted an accuracy of 92.3% (specificity = 97.0%, sensitivity = 84.2% and AUC = 0.96) (Gu et al., 2016). These findings provide preliminary evidence that neuroimaging-based inference in the individual heterogeneity in clinical features, disease course, and treatment response of PD might be possible.

8 Nederlandse samenvatting

Van het proefschrift “Nieuwe benaderingswijzen in beeldvorming van de hersenen bij patiënten met de ziekte van Parkinson”

De ziekte van Parkinson

De ziekte van Parkinson wordt gekenmerkt door traagheid van bewegen (bradykinesie), beven (tremor) en stijfheid (rigiditeit). Naast deze zogenaamde motorische kenmerken (i.e. met betrekking tot bewegen), zijn er ook niet-motorische kenmerken van de ziekte, waaronder problemen met nadenken, stemmingsklachten, slaapstoornissen, slaperigheid overdag, reukstoornis en autonome stoornissen, zoals problemen met de spijsvertering of bloedsomloop. De ontstaanswijze van de ziekte van Parkinson is nog niet duidelijk. De motorische kenmerken van de ziekte van Parkinson worden in verband gebracht met het verlies van dopaminerge cellen in de substantia nigra (zwarte kern; zie afbeelding 1). Daarnaast verspreidt de ziekte zich door de rest van de hersenen, wat hoogstwaarschijnlijk bijdraagt aan de niet-motorische kenmerken van de ziekte.

De mate, expressie en snelheid van verergering van klachten bij de ziekte van Parkinson kunnen sterk verschillen van persoon tot persoon. Dit ondersteunt dat er mogelijk subgroepen van patiënten met de ziekte van Parkinson zijn, die bepaalde kenmerken van ziekte delen. De identificatie van subgroepen zou kunnen leiden tot meer inzicht in het ziekteproces van de ziekte van Parkinson. Tot op heden is het niet goed gelukt om op basis van ziektekenmerken patiënten te verdelen in subgroepen.

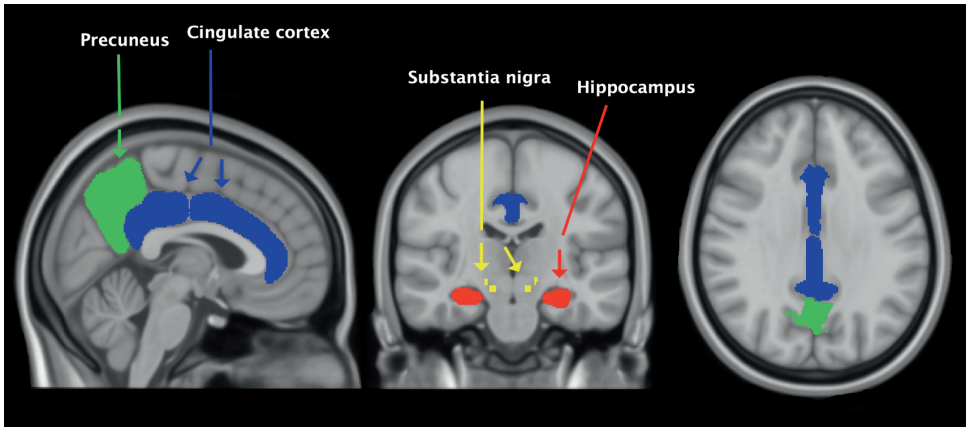
Dementie met Lewylichaampjes

Dementie met Lewylichaampjes vertoont belangrijke gelijkenissen met de ziekte van Parkinson, zoals de hierboven beschreven motorische en niet-motorische kenmerken. Vooral in de beginfase kan dementie met Lewylichaampjes lastig te onderscheiden zijn van de ziekte van Parkinson. Het ziekteverloop van dementie met Lewylichaampjes is echter vaak sneller invaliderend dan bij de ziekte van Parkinson, en ook de tolerantie en werkzaamheid van medicatie kan verminderd zijn, wat maakt dat een goed onderscheid tussen beide aandoeningen belangrijk is.

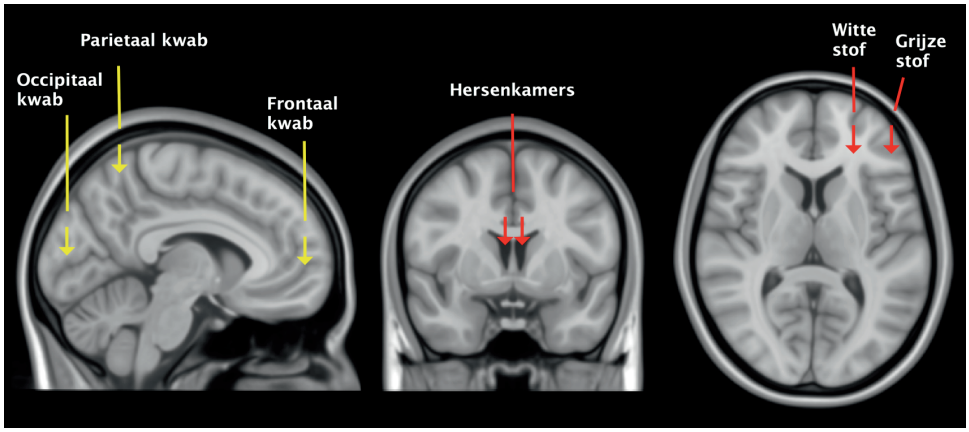
Onderzoeksdoel van dit proefschrift

In dit proefschrift hebben we de hersenen van patiënten met de ziekte van Parkinson en dementie met Lewylichaampjes bestudeerd door middel van beeldvorming met magnetische resonantie (“magnetische resonantie imaging”; MRI). We hebben hierbij geavanceerde benaderingswijzen gebruikt, die mogelijk behulpzaam kunnen zijn bij het identificeren van om karakteristieke veranderingen in de hersenen van patiënten met de ziekte van Parkinson te identificeren, kunnen

helpen in de differentiatie van mogelijke subgroepen en bij kunnen dragen aan het onderscheid tussen de ziekte van Parkinson en dementie met Lewylichaampjes.



Afbeelding 1



Afbeelding 2

Samenvatting van de bevindingen

In **hoofdstuk 2** hebben we zogenaamde structurele hersennetwerken onderzocht bij de ziekte van Parkinson. Dit zijn groepen hersengebieden die overeenkomsten in structuur van de grijze stof (zie afbeelding 2) vertonen. De resultaten in dit hoofdstuk laten zien dat specifieke netwerken achteruitgaan bij de ziekte van Parkinson ten opzichte van gezonde controlepersonen. Dit zijn de zogenaamde

cingulate cortex (cingulate hersenschors; zie afbeelding 1) netwerken. Achteruitgang van deze netwerken bleek geassocieerd met de ernst van met name niet-motorische klachten, namelijk problemen met het denkvermogen en slaperigheid overdag.

In **hoofdstuk 3** hebben we onderzocht of er structurele verschillen te vinden zijn tussen de grijze stof van de hersenen van patiënten met de ziekte van Parkinson en patiënten met dementie met Lewylichaampjes. De resultaten van deze studie laten een kleinere hippocampus (zeepaardje; zie afbeelding 1) zien bij patiënten met dementie met Lewylichaampjes ten opzichte van patiënten met de ziekte van Parkinson, waarbij met name de kop en het middendeel van de hippocampus is aangetast.

In **hoofdstuk 4** hebben we de gesteldheid van de gehele witte stof (zie afbeelding 2) in de hersenen van patiënten met de ziekte van Parkinson onderzocht. Zowel leeftijd als de ziekte van Parkinson tasten de witte stof aan. Daarom hebben we gekeken of leeftijd mogelijk een sterker effect heeft op achteruitgang van de witte stof in patiënten met de ziekte van Parkinson dan in gezonde controlepersonen. We hebben gevonden dat patiënten met de ziekte van Parkinson meer wittestofafwijkingen hebben dan gezonde controlepersonen, met name vóór in de hersenen gelokaliseerd en diep in de witte stof, dichtbij de hersenkamers (met hersenvocht gevulde holten in de hersenen; zie afbeelding 2). De achteruitgang van de witte stof met toename van de leeftijd is gelijk voor beide groepen. De hoeveelheid wittestofafwijkingen is geassocieerd met leeftijd, maar daarnaast ook met klachten van het denkvermogen en met balansproblemen. Deze wittestofafwijkingen zijn doorgaans met het blote oog zichtbaar. We hebben ook gekeken naar afwijkingen die niet met het blote oog zichtbaar zijn. Dit hebben we gedaan in de witte stof waarin geen wittestofafwijkingen gevonden zijn, dus in de witte stof die "gezond" lijkt te zijn. Hierbij hebben we geen verschillen tussen patiënten met de ziekte van Parkinson en gezonde controlepersonen kunnen vaststellen.

In **hoofdstuk 5** hebben we opnieuw netwerken in de hersenen bij patiënten met de ziekte van Parkinson onderzocht. Dit keer middels zogenaamde functionele netwerken. Deze bestaan uit hersengebieden in de grijze stof die samenhang vertonen in activiteitspatronen op functionele MRI, wat connectiviteit wordt genoemd. Het functioneren van deze netwerken wordt geassocieerd met

bepaalde hersenfuncties, zoals het denkvermogen. Allereerst hebben we de hersenen als één groot netwerk beschouwd. We hebben gevonden dat frontale (dit is het voorste deel van de hersenschors; zie afbeelding 2) en pariëtale (dit deel van de hersenschors is aan de achter/bovenzijde gelegen, van opzij gezien; zie afbeelding 2) een hogere connectiviteit vertonen met het totale hersennetwerk vergeleken met gezonde controlepersonen. In frontale en occipitale (dit is het achterste deel van de hersenschors; zie afbeelding 2) gebieden hebben we juist een lagere connectiviteit met de rest van het netwerk gevonden. Vervolgens hebben de we hersenen opgedeeld in acht bekende afzonderlijke functionele netwerken, en zagen we met name toegenomen connectiviteit bij patiënten met de ziekte van Parkinson, waaronder in het sensorimotore netwerk (geassocieerd met motorische taken) en in de visuele netwerken. Beide methoden tezamen wezen op het belang van een aantal gebieden die veranderde functionele connectiviteit vertonen, waaronder de posterieure cingulate cortex en de precuneus (zie afbeelding 1). Uit eerder onderzoek is gebleken dat dit sterk geconnecteerde hersengebieden zijn. De regionaal veranderde connectiviteit bij patiënten met de ziekte van Parkinson is niet geassocieerd met klachten van de ziekte, wat er mogelijk op duidt dat enkelvoudige veranderingen op het niveau van functionele connectiviteit niet per se gerelateerd zijn aan kenmerken van ziekte, maar een complexer effect hebben.

In **hoofdstuk 6** hebben we het gebruik van zogenaamd "machinaal leren" toegepast op functionele MRI-data voor individuele classificatie van patiënten met de ziekte van Parkinson. Bij machinaal leren worden computer-algoritmes gebruikt die zonder interventie van buitenaf leren van data. We hebben gevonden dat het mogelijk is om met deze benaderingswijze patiënten met de ziekte van Parkinson in redelijke mate te kunnen onderscheiden van gezonde controlepersonen op een individueel niveau.

Afsluitende opmerkingen

Structurele en functionele connectiviteit

In dit proefschrift hebben we laten zien dat netwerkbenaderingen waardevolle inzichten kunnen opleveren in de structurele en functionele hersenarchitectuur van patiënten met de ziekte van Parkinson. Mogelijke laten neurodegeneratieve ziekten netwerk-gestuurd verval zien van specifieke hersengebieden. In hoofdstuk 2 en 3 hebben we laten zien dat de hersenen van patiënten met dementie met Lewylichaampjes en patiënten met de ziekte van Parkinson, verval tonen van het

zogenoemde anterieure (voorste) en posterieure (achterste) cingulate cortexnetwerk. Het anterieure cingulate cortexnetwerk vertoont overlap met een netwerk dat gevonden is in eerdere studies met patiënten met de ziekte van Parkinson. Dit eerder gevonden netwerk vertoont eveneens verval bij patiënten met de ziekte van Parkinson, wat geassocieerd is met een ernstigere vorm van de ziekte van Parkinson. Gezamenlijk laten deze bevindingen zien dat de cingulate cortex aangetast is bij de ziekte van Parkinson, en dat veranderingen in netwerken waarbij de cingulate cortex betrokken is, gerelateerd zijn aan ziekteprogressie.

Daarnaast hebben we veranderde functionele connectiviteit gevonden in hersengebieden van het structurele posterieure cingulate cortex-netwerk, namelijk in de precuneus en posterieure cingulate cortex (hoofdstuk 5). Deze structuren worden gezien als prominente gebieden in de hersenarchitectuur die een belangrijke rol spelen bij het integreren van informatie van diverse hersengebieden. Veranderingen in deze structuren hebben mogelijk dan ook grote gevolgen voor de werking van het totale hersennetwerk. In patiënten met de ziekte van Parkinson hangen veranderingen in de (functionele en/of structurele) connectiviteit van deze structuren wellicht samen met specifieke kenmerken van de ziekte. Wij hebben bijvoorbeeld in hoofdstuk 2 gevonden dat verval van het posterieure cingulate cortex netwerk gerelateerd is aan met name niet-motorische klachten.

Leeftijd

Diverse studies suggereren dat leeftijd een belangrijke rol speelt in de ziekte van Parkinson. Toename van de leeftijd is bijvoorbeeld geassocieerd met een snellere achteruitgang in motorische klachten en ernstiger klachten van het denkvermogen. Onze resultaten laten achteruitgang zien van de grijze stof in zowel patiënten met dementie met Lewylichaampjes als in patiënten met de ziekte van Parkinson, vergeleken met gezonde controlepersonen. De gebieden die achteruitgang laten zien, zijn gebieden die vaak ook achteruitgaan met toenemende leeftijd, zoals de hippocampus en cingulate cortex. Verder hebben we regiospecifieke achteruitgang van functionele connectiviteit van met name de precuneus en posterieure cingulate cortex gevonden. Dit zijn gebieden zijn waarvan bekend is dat de functionele connectiviteit vaak aangetast wordt met toename van de leeftijd. Deze resultaten suggereren dat de ziekte van Parkinson gebieden aantast die al aangedaan zijn door het verouderingsproces, of dat het leeftijdseffect op de hersenen beïnvloed wordt door ziekte. Onze resultaten in hoofdstuk vier laten zien dat wittestofafwijkingen mogelijk al aanwezig zijn in een vroeg stadium van de

ziekte van Parkinson, wat andere wittestofstudies naar de ziekte van Parkinson ondersteunen.

Dopaminerge medicatie

De patiënten in dit onderzoek gebruikten tijdens deelname hun normale medicatie voor de ziekte van Parkinson (dopaminerge medicatie), met uitzondering van een groep patiënten die (nog) nooit medicatie had gebruikt. Het gebruik van dopaminerge medicatie tijdens een MRI-scan kan problematisch zijn, omdat dit de interpretatie van met name functionele data kan bemoeilijken. Er zijn aanwijzingen dat dopaminerge medicatie functionele connectiviteitsveranderingen die geassocieerd zijn met symptomen van de ziekte van Parkinson, normaliseert. Dit zou betekenen dat de veranderingen die we gevonden hebben, nog uitgesprokener zouden zijn als de patiënten geen medicatie zouden hebben genomen. Daarnaast zijn er mogelijk kleine functionele connectiviteits-veranderingen die niets te maken hebben met symptomen van de ziekte van Parkinson. Het gebruik van dopaminerge medicatie door patiënten tijdens een MRI-scan heeft echter ook voordelen, zo is er minder kans op verstoringen van de scan door beweging. Ook veroorzaakt chronisch gebruik van dopaminerge medicatie waarschijnlijk langdurige functionele connectiviteitsveranderingen die niet verdwijnen als iemand kortdurend stopt met medicatie, wat eveneens de interpretatie van data kan bemoeilijken. Beide methoden hebben dus voor- en nadelen en het is belangrijk de dopaminerge status van patiënten te overwegen bij de interpretatie van MRI-data.

Studiepopulatie

Voor sommige studies beschreven in dit proefschrift was het gebruik van een controlegroep vereist. Gezonde controlepersonen zijn geselecteerd uit de Leiden Lang Leven studie. Er zijn een aantal kleine verschillen in enkele verzamelde variabelen en de methode van dataverzameling. Zo zijn patiënten met de ziekte van Parkinson gescand met een andere hoofdspoel dan de gezonde controlepersonen. Hier is rekening mee gehouden met de keuze van data-analyse, maar het kan van invloed geweest zijn op de bevindingen. Patiënten en controlepersonen kwamen overeen in leeftijd en geslachtsverdeling op groepsniveau, omdat het bekend is dat leeftijd en geslacht een belangrijke invloed hebben op MRI-kenmerken van de hersenen. In hoofdstuk vier hadden we graag patiënten en controlepersonen verzameld die daarnaast overeenkwamen in

cardiovasculair risicoprofiel, al bleken beide groepen uiteindelijk niet te verschillen in de verzamelde cardiovasculaire risicofactoren.

Toekomstperspectieven

Opkomende methodes van data-analyse

In dit proefschrift hebben we vijf verschillende MRI-sequenties (verschillende soorten MRI opnamen) gebruikt. Hierdoor waren we in staat hersengebieden te vinden die zowel veranderde structurele als functionele connectiviteit hadden, zoals de cingulate cortex. Het combineren van structurele en functionele MRI wordt steeds vaker gebruikt om meer inzicht te verkrijgen in hersenveranderingen bij neurodegeneratieve ziekten. Daarnaast is het combineren van verschillende beeldvormende technieken (modaliteiten) in opkomst, zoals een combinatie van MRI met "positron-emissie tomografie" (PET; nucleair beeldvormend onderzoek, hierbij wordt een kleine hoeveelheid radioactieve stof gebruikt), "magneto-encefalografie" (MEG; een techniek die magnetische velden gebruikt om de hersenactiviteit in kaart te brengen) en/of "elektro-encefalografie" (EEG; elektrische meting van hersenactiviteit). Het is aangetoond dat een combinatie van modaliteiten patiënten met dementie met Lewylichaampjes beter onderscheidt van patiënten met de ziekte van Alzheimer dan data van één modaliteit dat doet.

In hoofdstuk 6 gebruikten we machinaal leren, een vorm van kunstmatige intelligentie die toenemend wordt gebruikt wordt in MRI-studies om neurodegeneratieve aandoeningen te bestuderen. Een nieuwe toepassing van machinaal leren is de exploratie van nog onontdekte subtypes van ziekte op basis van functionele MRI-data. Componenten van op deze wijze geïdentificeerde subtypes kunnen mogelijk dienen als marker voor de differentiatie van subgroepen met verschillende patronen van abnormaal functionerende connectiviteit en potentieel verschillende klinische profielen. In de toekomst kan deze techniek mogelijk toegepast worden op andere datasoorten, zoals PET, MEG of EEG-data.

Het gebruik van machinaal leren bij de ziekte van Parkinson staat nog in de kinderschoenen. Dit wordt waarschijnlijk mede veroorzaakt door gelimiteerde aantallen personen die meedoen aan MRI-studies. Een recent initiatief heeft echter een grote groep patiënten met de ziekte van Parkinson verzameld (Parkinson's Progression Markers Initiative; PPMI) en onderzoekt daarnaast strategieën om met grote datasets om te gaan. Toekomstige studies kunnen inzicht bieden in zaken als beschikbaarheid, integratie en analyse van grote datasets om de bruikbaarheid van MRI in de klinische praktijk van de ziekte van Parkinson te verbeteren.

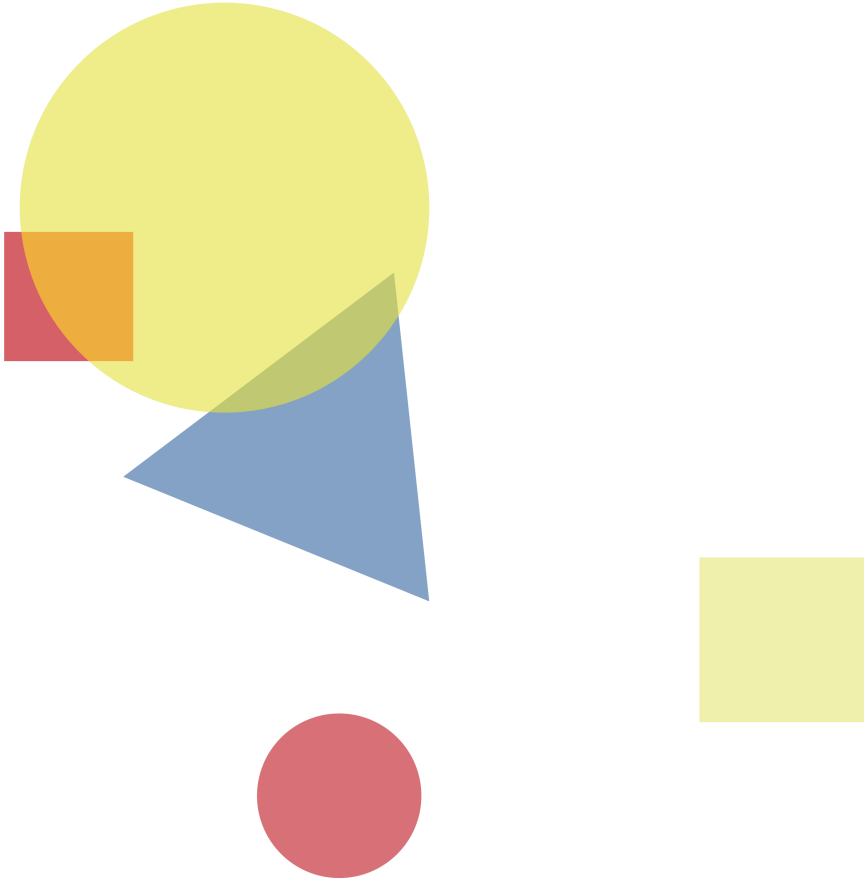
Individuele classificatie

Geavanceerde beeldvorming van de hersenen biedt potentie om unieke hersenkenmerken van neurodegeneratieve aandoeningen in kaart te brengen. Zo is er bijvoorbeeld meer aandacht voor de analyse van deelgebieden (zoals ook in hoofdstuk 3 beschreven is) van de hippocampus door de toenemende beschikbaarheid van 3 Tesla MRI-scanners. MRI-studies zijn echter vaak uitgevoerd op groepsniveau, waardoor ze niet direct bruikbaar zijn voor de individuele patiënt. Ook in dit proefschrift zijn de resultaten die we rapporteren op groepsniveau, met uitzondering van de resultaten in hoofdstuk 6. De laatste jaren is er meer aandacht voor de toepassing van studieresultaten op individueel niveau. Enkele studies bij patiënten met de ziekte van Parkinson tonen interessante resultaten op individueel niveau. Een studie gebruikte machinaal leren voor de analyse van functionele MRI en liet zien dat het mogelijk was om het niveau van functioneren van het bewegen te voorspellen van individuele patiënten met de ziekte van Parkinson. Een andere studie gebruikte machinaal leren in combinatie met multimodale MRI-data en was zo in staat om op individueel niveau patiënten met de ziekte van Parkinson bij wie balansproblemen op de voorgrond stonden, te onderscheiden van patiënten bij wie dit niet zo was. Deze bevindingen geven hoop dat beeldvorming van de hersenen tot hulp kan zijn bij de individuele verschillen in symptomen, ziekte-verloop en respons op behandelingen bij patiënten met de ziekte van Parkinson.

9

Appendices

Abbreviations
References
List of publications
Dankwoord
Curriculum vitae



ABBREVIATIONS

AD	Alzheimer's disease
Alpha-SynA	Alpha-synuclein aggregates
AUC	Area under the curve
BOLD	Blood oxygen level dependent
C-ICA	Cluster-wise independent component analysis
DA	Dopamine agonists
DLB	Dementia with Lewy bodies
DMN	Default mode network
DTI	Diffusion tensor imaging
DWI	Diffusion-weighted imaging
ECM	Eigenvector centrality mapping
EEG	Electroencephalography
FA	Fractional anisotropy
FFC	Full correlation functional connectivity
FFD	Full correlation functional connectivity dynamics
FLAIR	Fluid attenuated inversion recovery
fMRI	Functional magnetic resonance imaging
FOV	Field of view
FSL	FMRIB's software library
FWE	Familywise error
ICA-AROMA	Independent component analysis based automatic removal of motion artifacts
LDE-Dopa	Levodopa dose equivalent of daily levodopa
LLS	Leiden Longevity study
LUMC	Leiden University Medical Center
MC-FLIRT	Motion correction FMRIB's linear image registration tool
MD	Mean diffusivity
MDS-UPDRS	Movement Disorder Society unified Parkinson's disease rating scale
MEG	Magnetoencephalography
MMSE	Mini-mental state examination
MNI	Montreal Neurological Institute
MTI	Magnetization transfer imaging
MTR	Magnetization transfer ratio
NAWM	Normal appearing white matter

PD	Parkinson's disease
PET	Positron-emission tomography
PFC	Partial correlation functional connectivity
PFD	Partial correlation functional connectivity dynamics
PPMI	Parkinson's progression markers initiative
PROPARK	Profiling Parkinson's disease
ROC	Receiver operator characteristic
SCN	Structural covariance network
SCOPA-COG	Scales for outcomes in Parkinson's disease - cognition
SCOPA-PC	Scales for outcomes in Parkinson's disease – psychiatric complications
SENS-PD	Severity of non-dopaminergic symptoms in Parkinson's disease
SIENAX	Structural image evaluation using normalization of atrophy cross-sectional
SMA	Supplementary motor area
TBSS	Tract-based spatial statistics
TE	Echo time
TFCE	Threshold-free cluster enhancement
TR	Repetition time
VBM	Voxel-based morphometry
WMH	White matter hyperintensity

REFERENCES

Acharya, H.J., Bouchard, T.P., Emery, D.J., Camicioli, R.M., 2006. Axial signs and magnetic resonance imaging correlates in Parkinson's disease. Can J Neurol Sci. 34, 56–61. doi:10.1017/s0317167100005795

Adeli, E., Shi, F., An, L., Wee, C.Y., Wu, G., Wang, T., Shen, D., 2016. Joint feature-sample selection and robust diagnosis of Parkinson's disease from MRI data. Neuroimage 141, 206–219. doi:10.1016/j.neuroimage.2016.05.054

Adler, C.H., Beach, T.G., 2016. Neuropathological basis of nonmotor manifestations of Parkinson's disease. Mov. Disord. 31, 1114–1119. doi:10.1002/mds.26605

Agosta, F., Galantucci, S., Filippi, M., 2017. Advanced magnetic resonance imaging of neurodegenerative diseases. Neurol. Sci. 38, 41–51. doi:10.1007/s10072-016-2764-x

Alexander-Bloch, A., Raznahan, A., Bullmore, E., Giedd, J., 2013. The convergence of maturational change and structural covariance in human cortical networks. J. Neurosci. 33, 2889–99. doi:10.1523/JNEUROSCI.3554-12.2013

Altmann-Schneider, I., Van Der Grond, J., Slagboom, P.E., Westendorp, R.G.J., Maier, A.B., Van Buchem, M.A., De Craen, A.J.M., 2013. Lower susceptibility to cerebral small vessel disease in human familial longevity: The Leiden longevity study. Stroke 44, 9–14. doi:10.1161/STROKEAHA.112.671438

Alves, G., Wentzel-Larsen, T., Aarsland, D., Larsen, J.P., 2005. Progression of motor impairment and disability in Parkinson disease: A population-based study. Neurology 65, 1436–1441. doi:10.1212/01.wnl.0000183359.50822.f2

Amoroso, N., La Rocca, M., Monaco, A., Bellotti, R., Tangaro, S., 2018. Complex networks reveal early MRI markers of Parkinson's disease. Med. Image Anal. 48, 12–24. doi:10.1016/j.media.2018.05.004

Anderson, E., Nutt, J., 2011. The long-duration response to levodopa: Phenomenology, potential mechanisms and clinical implications. Park. Relat. Disord. 17, 587–592. doi:10.1016/j.parkreldis.2011.03.014

Andersson, J.L.R., Jenkinson, M., Smith, S., 2007. Non-linear registration aka spatial normalisation FMRIB Technial Report TR07JA2.

Andersson, J.L.R., Sotiropoulos, S.N., 2016. An integrated approach to correction for off-resonance effects and subject movement in diffusion MR imaging. Neuroimage 125, 1063–1078. doi:10.1016/j.neuroimage.2015.10.019

Andrews, T.J., Halpern, S.D., Purves, D., 1997. Correlated size variations in human visual cortex, lateral geniculate nucleus, and optic tract. J. Neurosci. 17, 2859–2868.

Arbabshirani, M.R., Plis, S., Sui, J., Calhoun, V.D., 2017. Single subject prediction of brain disorders in neuroimaging: Promises and pitfalls. Neuroimage 145, 137–165. doi:10.1016/j.neuroimage.2016.02.079

Arena, J.E., Cerquetti, D., Rossi, M., Chaves, H., Rollan, C., Dossi, D.E., Merello, M., 2016. Parkinsonism and Related Disorders Influence of white matter MRI hyper-intensities on acute L-dopa response in patients with Parkinson's disease. Park. Relat. Disord. 24, 126–128. doi:10.1016/j.parkreldis.2016.01.017

Atkinson-Clement, C., Pinto, S., Eusebio, A., Coulon, O., 2017. Diffusion tensor imaging in Parkinson's disease: Review and meta-analysis. doi:10.1016/j.nicl.2017.07.011

Baggio, H.-C., Sala-Llonch, R., Segura, B., Marti, M.-J., Valldeoriola, F., Compta, Y., Tolosa, E., Junqué, C., 2014. Functional brain networks and cognitive deficits in Parkinson's disease. Hum. Brain Mapp. 35, 4620–4634. doi:10.1002/hbm.22499

Baggio, H.C., Segura, B., Junque, C., 2015. Resting-state functional brain networks in Parkinson's disease. CNS Neurosci. Ther. 21, 793–801. doi:10.1111/cns.12417

Baik, K., Cha, J., Ham, J.H., Baek, G., Sunwoo, M.K., Hong, J.Y., Shin, N., Kim, J.S., Lee, J.-M., Lee, S.-K., Sohn, Y.H., Lee, P.H., 2014. Dopaminergic modulation of resting-state functional

connectivity in de novo patients with Parkinson's disease. Hum. Brain Mapp. 35, 5431–5441. doi:10.1002/hbm.22561

Barnes, J., Ourselin, S., Fox, N.C., 2009. Clinical application of measurement of hippocampal atrophy in degenerative dementias. Hippocampus 19, 510–516. doi:10.1002/hipo.20617

Beach, T.G., Adler, C.H., Lue, L., Sue, L.I., Bachalakuri, J., Henry-Watson, J., Sasse, J., Boyer, S., Shirohi, S., Brooks, R., Eschbacher, J., White, C.L., Akiyama, H., Caviness, J., Shill, H.A., Connor, D.J., Sabbagh, M.N., Walker, D.G., Consortium, the A.P.D., 2009. Unified staging system for Lewy body disorders: correlation with nigrostriatal degeneration, cognitive impairment and motor dysfunction. Acta Neuropathol. 117, 613–634. doi:10.1007/s00401-009-0538-8

Beckmann, C.F., DeLuca, M., Devlin, J.T., Smith, S.M., 2005. Investigations into resting-state connectivity using independent component analysis. Philos. Trans. R. Soc. Lond. B. Biol. Sci. 360, 1001–13. doi:10.1098/rstb.2005.1634

Beckmann, Mackay, Filippini, Smith, 2009. Group comparison of resting-state FMRI data using multi-subject ICA and dual regression. Neuroimage 47, S148. doi:10.1073/pnas.0811879106

Berg, D., Postuma, R.B., Adler, C.H., Bloem, B.R., Chan, P., Dubois, B., Gasser, T., Goetz, C.G., Halliday, G., Joseph, L., Lang, A.E., Liepelt-Scarfone, I., Litvan, I., Marek, K., Obeso, J., Oertel, W., Olanow, C.W., Poewe, W., Stern, M., Deuschl, G., 2015. MDS research criteria for prodromal Parkinson's disease. Mov. Disord. 30, 1600–1601. doi:10.1002/mds.26431

Beyer, M.K., Aarsland, D., Greve, O.J., Larsen, J.P., 2006. Visual rating of white matter hyperintensities in Parkinson's disease. Mov. Disord. 21, 223–229. doi:10.1002/mds.20704

Binnewijzend, M.A.A., Adriaanse, S.M., Van der Flier, W.M., Teunissen, C.E., de Munck, J.C., Stam, C.J., Scheltens, P., van Berckel, B.N.M., Barkhof, F., Wink, A.M., 2014. Brain network alterations in Alzheimer's disease measured by Eigenvector centrality in fMRI are related to cognition and CSF biomarkers. Hum. Brain Mapp. 35, 2383–2393. doi:10.1002/hbm.22335

Blahak, C., Baezner, H., Pantoni, L., Poggesi, A., Chabriat, H., Erkinjuntti, T., Fazekas, F., Ferro, J.M., Langhorne, P., O'Brien, J., Visser, M.C., Wahlund, L.O., Waldemar, G., Wallin, A., Inzitari, D., Hennerici, M.G., 2009. Deep frontal and periventricular age related white matter changes but not basal ganglia and infratentorial hyperintensities are associated with falls: Cross sectional results from the LADIS study. J. Neurol. Neurosurg. Psychiatry 80, 608–613. doi:10.1136/jnnp.2008.154633

Bohnen, N.I., Albin, R.L., 2011. White matter lesions in Parkinson disease. Nat. Rev. Neurol. 7, 229–36. doi:10.1038/nrneurol.2011.21

Borroni, B., Premi, E., Formenti, A., Turrone, R., Alberici, A., Cottini, E., Rizzetti, C., Gasparotti, R., Padovani, A., 2015. Structural and functional imaging study in dementia with Lewy bodies and Parkinson's disease dementia. Parkinsonism Relat. Disord. 21, 1049–1055. doi:10.1016/J.PARKRELDIS.2015.06.013

Brown, R.E., Basheer, R., McKenna, J.T., Strecker, R.E., McCarley, R.W., 2012. Control of Sleep and Wakefulness. Physiol. Rev. 92, 1087–1187. doi:10.1152/physrev.00032.2011

Buckner, R.L., Sepulcre, J., Talukdar, T., Krienen, F.M., Liu, H., Hedden, T., Andrews-Hanna, J.R., Sperling, R.A., Johnson, K.A., 2009. Cortical hubs revealed by intrinsic functional connectivity: Mapping, assessment of stability, and relation to Alzheimer's disease. J. Neurosci. 29, 1860–1873. doi:10.1523/JNEUROSCI.5062-08.2009

Buckner, R.L., Snyder, A.Z., Shannon, B.J., LaRossa, G., Sachs, R., Fotenos, A.F., Sheline, Y.I., Klunk, W.E., Mathis, C.A., Morris, J.C., Mintun, M.A., 2005. Molecular, structural, and functional characterization of Alzheimer's disease: Evidence for a relationship between default activity, amyloid, and memory. J. Neurosci. 25, 7709–7717. doi:10.1523/jneurosci.2177-05.2005

Burciu, R.G., Ofori, E., Archer, D.B., Wu, S.S., Pasternak, O., McFarland, N.R., Okun, M.S., Vaillancourt, D.E., 2017. Progression marker of Parkinson's disease: A 4-year multi-site imaging study. Brain 140, 2183–2192. doi:10.1093/brain/awx146

Calhoun, V.D., Sui, J., 2016. Multimodal fusion of brain imaging data: A key to finding the missing link(s) in complex mental Illness. Biol. Psychiatry Cogn. Neurosci. Neuroimaging 1, 230–244.

doi:10.1016/j.bpsc.2015.12.005

Chahine, L.M., Weintraub, D., Hawkins, K.A., Siderowf, A., Eberly, S., Oakes, D., Seibyl, J., Stern, M.B., Marek, K., Jennings, D., Russell, D., Fiocco, A., Sethi, K., Jackson, P., Frank, S., Thomas, C.A., James, R.C., Simuni, T., Borushko, E., Stern, M., Rick, J., Hauser, R., Khavarian, L., Richard, I., Deeley, C., Liang, G.S., Infeld, L., Adler, C.H., Duffy, A.K., Saunders-Pullman, R., Evatt, M.L., McMurray, B., Lai, E., Johnson, S., DeBakey, M.E., Subramanian, I., Gratiano, A., Chung, K., Lobb, B., O'Conner, S., 2016. Cognition in individuals at risk for Parkinson's: Parkinson associated risk syndrome (PARS) study findings. Mov. Disord. 31, 86–94. doi:10.1002/mds.26373

Chang, C., Glover, G.H., 2010. Time-frequency dynamics of resting-state brain connectivity measured with fMRI. Neuroimage 50, 81–98. doi:10.1016/j.neuroimage.2009.12.011

Chaudhuri, K.R., Healy, D.G., Schapira, A.H. V, 2006. Non-motor symptoms of Parkinson's disease: diagnosis and management. Lancet. Neurol. 5, 235–45. doi:10.1016/S1474-4422(06)70373-8

Chaudhuri, K.R., Schapira, A.H. V, 2009. Non-motor symptoms of Parkinson's disease: dopaminergic pathophysiology and treatment. Lancet. Neurol. 8, 464–74. doi:10.1016/S1474-4422(09)70068-7

Chiang, P., Chen, H., Lu, C., Chen, P., Chen, M., -hsiao Yang, I., Tsai, N., Lin, W., 2017. White matter damage and systemic inflammation in Parkinson's disease. BMC Neurosci. 18, 48. doi:10.1186/s12868-017-0367-y

Chondrogiorgi, M., Tzarouchi, L.C., Zikou, A.K., Astrakas, L.G., Kosta, P., Argyropoulou, M.I., Konitsiotis, S., 2016. Multimodal imaging evaluation of excessive daytime sleepiness in Parkinson's disease. Int. J. Neurosci. 126, 422–8. doi:10.3109/00207454.2015.1023437

Christopher, L., Duff-Canning, S., Koshimori, Y., Segura, B., Boileau, I., Chen, R., Lang, A.E., Houle, S., Rusjan, P., Strafella, A.P., 2015. Salience network and parahippocampal dopamine dysfunction in memory-impaired parkinson disease. Ann. Neurol. 77, 269–280. doi:10.1002/ana.24323

Chung, J.W., Burciu, R.G., Ofori, E., Shukla, P., Okun, M.S., Hess, C.W., Vaillancourt, D.E., 2017. Parkinson's disease diffusion MRI is not affected by acute antiparkinsonian medication. NeuroImage Clin. 14, 417–421. doi:10.1016/j.nicl.2017.02.012

Claassen, D.O., Dobolyi, D.G., Isaacs, D.A., Roman, O.C., Herb, J., Wylie, S.A., Neimat, J.S., Donahue, M.J., Hedera, P., Zald, D.H., Landman, B.A., Bowman, A.B., Dawant, B.M., Rane, S., 2016. Linear and curvilinear trajectories of cortical loss with advancing age and disease duration in Parkinson's disease. Aging Dis. 7, 220-229. doi:10.14336/AD.2015.1110

Cochrane, C.J., Ebmeier, K.P., 2013. Diffusion tensor imaging in parkinsonian syndromes: a systematic review and meta-analysis. Neurology 80, 857–64. doi:10.1212/WNL.0b013e318284070c

Compta, Y., Buongiorno, M., Bargalló, N., Valldeoriola, F., Muñoz, E., Tolosa, E., Ríos, J., Cámara, A., Fernández, M., Martí, M.J., 2016. White matter hyperintensities, cerebrospinal amyloid-β and dementia in Parkinson's disease. J. Neurol. Sci. 367, 284–290. doi:10.1016/J.JNS.2016.06.009

Dadar, M., Zeighami, Y., Yau, Y., Fereshtehnejad, S.M., Maranzano, J., Postuma, R.B., Dagher, A., Collins, D.L., 2018. White matter hyperintensities are linked to future cognitive decline in de novo Parkinson's disease patients. NeuroImage Clin. 20, 892–900. doi:10.1016/j.nicl.2018.09.025

Dalaker, T.O., Larsen, J.P., Bergsland, N., Beyer, M.K., Alves, G., Dwyer, M.G., Tysnes, O.B., Benedict, R.H.B., Kelemen, A., Bronnick, K., Zivadinov, R., 2009. Brain atrophy and white matter hyperintensities in early Parkinson's disease. Mov. Disord. 24, 2233–2241. doi:10.1002/mds.22754

Damier, P., Hirsch, E.C., Agid, Y., Graybiel, A.M., 1999. The substantia nigra of the human brain: II. Patterns of loss of dopamine-containing neurons in Parkinson's disease. Brain 122, 1437–1448. doi:10.1093/brain/122.8.1437

Damoiseaux, J.S., Rombouts, S.A.R.B., Barkhof, F., Scheltens, P., Stam, C.J., Smith, S.M., Beckmann, C.F., 2006. Consistent resting-state networks across healthy subjects. Proc. Natl. Acad. Sci. U. S. A. 103, 13848–13853. doi:10.1073/pnas.0601417103

de Haan, W., Mott, K., van Straaten, E.C.W., Scheltens, P., Stam, C.J., 2012. Activity dependent degeneration explains hub vulnerability in Alzheimer's disease. PLoS Comput. Biol. 8, e1002582. doi:10.1371/journal.pcbi.1002582

De Rijk, M.C., Launer, L.J., Berger, K., Breteler, M.M.B., Dartigues, J.F., Baldereschi, M., Fratiglioni, L., Lobo, A., Martinez-Lage, J., Trenkwalder, C., Hofman, A., 2000. Prevalence of Parkinson's disease in Europe: A collaborative study of population-based cohorts. Neurologic Diseases in the Elderly Research Group. Neurology 54, 21–23. doi:10.1212/WNL.54.11.21A

de Schipper, L.J., Hafkemeijer, A., van der Grond, J., Marinus, J., Henselmans, J.M.L., van Hilten, J.J., 2018. Altered whole-brain and network-based functional connectivity in Parkinson's disease. Front. Neurol. 15, 587–593. doi:10.3389/fneur.2018.00419

de Schipper, L.J., van der Grond, J., Marinus, J., Henselmans, J.M.L., van Hilten, J.J., 2017. Loss of integrity and atrophy in cingulate structural covariance networks in Parkinson's disease. NeuroImage Clin. 15, 587–593. doi:10.1016/j.nicl.2017.05.012

de Vos, F., Koini, M., Schouten, T.M., Seiler, S., van der Grond, J., Lechner, A., Schmidt, R., de Rooij, M., Rombouts, S.A.R.B., 2018. A comprehensive analysis of resting state fMRI measures to classify individual patients with Alzheimer's disease. Neuroimage 167, 62–72. doi:10.1016/j.neuroimage.2017.11.025

Debette, S., Markus, H.S., 2010. The clinical importance of white matter hyperintensities on brain magnetic resonance imaging: Systematic review and meta-analysis. BMJ 341, c3666. doi:10.1136/bmj.c3666

Deco, G., Jirsa, V.K., McIntosh, A.R., 2011. Emerging concepts for the dynamical organization of resting-state activity in the brain. Nat. Rev. Neurosci. 12, 43–56. doi:10.1038/nrn2961

Delli Pizzi, S., Franciotti, R., Bubbico, G., Thomas, A., Onofrj, M., Bonanni, L., 2016. Atrophy of hippocampal subfields and adjacent extrahippocampal structures in dementia with Lewy bodies and Alzheimer's disease. Neurobiol. Aging 40, 103–109. doi:10.1016/j.neurobiolaging.2016.01.010

Dinov, I.D., Heavner, B., Tang, M., Glusman, G., Chard, K., Darcy, M., Madduri, R., Pa, J., Spino, C., Kesselman, C., Foster, I., Deutsch, E.W., Price, N.D., Van Horn, J.D., Ames, J., Clark, K., Hood, L., Hampstead, B.M., Dauer, W., Toga, A.W., 2016. Predictive big data analytics: A study of Parkinson's disease using large, complex, heterogeneous, incongruent, multi-source and incomplete observations. PLoS One 11, e0157077. doi:10.1371/journal.pone.0157077

Dorsey, E.R., Sherer, T., Okun, M.S., Bloem, B.R., 2018. The Emerging Evidence of the Parkinson Pandemic. J. Parkinsons. Dis. 8, 3–8. doi:10.3233/JPD-181474

Douaud, G., Smith, S., Jenkinson, M., Behrens, T., Johansen-Berg, H., Vickers, J., James, S., Voets, N., Watkins, K., Matthews, P.M., James, A., 2007. Anatomically related grey and white matter abnormalities in adolescent-onset schizophrenia. Brain 130, 2375–2386. doi:10.1093/brain/awm184

Drysdale, A.T., Grosenick, L., Downar, J., Dunlop, K., Mansouri, F., Meng, Y., Fetcho, R.N., Zebley, B., Oathes, D.J., Etkin, A., Schatzberg, A.F., Sudheimer, K., Keller, J., Mayberg, H.S., Gunning, F.M., Alexopoulos, G.S., Fox, M.D., Pascual-Leone, A., Voss, H.U., Casey, B.J., Dubin, M.J., Liston, C., 2017. Resting-state connectivity biomarkers define neurophysiological subtypes of depression. Nat. Med. 23, 264. doi:10.1038/nm.4246

Duncan, G.W., Firbank, M.J., Yarnall, A.J., Khoo, T.K., Brooks, D.J., Barker, R.A., Burn, D.J., O'Brien, J.T., 2016. Gray and white matter imaging: A biomarker for cognitive impairment in early Parkinson's disease? Mov. Disord. 31, 103–110. doi:10.1002/mds.26312

Dunet, V., Fartaria, M.J., Deverdun, J., Le Bars, E., Maury, F., Castelnovo, G., Kober, T., Cuadra, M.B., Geny, C., Marechal, B., de Champfleur, N.M., 2019. Episodic memory decline in Parkinson' s disease: relation with white matter hyperintense lesions and influence of quantification method. Brain Imaging Behav. 13, 810–818. doi:10.1007/s11682-018-9909-x

Durieux, J., 2015. Clusterwise independent component analysis (C-ICA) for multi-subject fMRI data: A novel unsupervised method for assessing differences across subjects (groups) in functional

connectivity patterns (Master's thesis).
Eckert, T., Peschel, T., Heinze, H.J., Rotte, M., 2006. Increased pre-SMA activation in early PD patients during simple self-initiated hand movements. J. Neurol. 253, 199–207. doi:10.1007/s00415-005-0956-z
Erten-Lyons, D., Woltjer, R., Kaye, J., Mattek, N., Dodge, H.H., Green, S., Tran, H., Howieson, D.B., Wild, K., Silbert, L.C., 2013. Neuropathologic basis of white matter hyperintensity accumulation with advanced age. Neurology 81, 977–983. doi:10.1212/WNL.0b013e3182a43e45
Eversfield, C.L., Orton, L.D., 2018. Auditory and visual hallucination prevalence in Parkinson's disease and dementia with Lewy bodies: a systematic review and meta-analysis. Psychol Med. 26, 1–12. doi:10.1017/S0033291718003161
Fazekas, F., Chawluk, J.B., Alavi, A., 1987. MR signal abnormalities at 1.5 T in Alzheimer's dementia and normal aging. Am. J. Neuroradiol. 149, 351–356. doi:10.2214/ajr.149.2.351
Fereshtehnejad, S.-M., Montplaisir, J.Y., Pelletier, A., Gagnon, J.-F., Berg, D., Postuma, R.B., 2017. Validation of the MDS research criteria for prodromal Parkinson's disease: Longitudinal assessment in a REM sleep behavior disorder (RBD) cohort. Mov. Disord. 32, 865–873. doi:10.1002/mds.26989
Ferreira, L.K., Busatto, G.F., 2013. Resting-state functional connectivity in normal brain aging. Neurosci. Biobehav. Rev. 37, 384–400. doi:10.1016/j.neubiorev.2013.01.017
Filippini, N., MacIntosh, B.J., Hough, M.G., Goodwin, G.M., Frisoni, G.B., Smith, S.M., Matthews, P.M., Beckmann, C.F., Mackay, C.E., 2009. Distinct patterns of brain activity in young carriers of the APOE-epsilon4 allele. Proc Natl Acad Sci U S A 106, 7209–7214. doi:10.1073/pnas.0811879106
Flodin, P., Gospic, K., Petrovic, P., Fransson, P., 2012. Effects of L-Dopa and Oxazepam on Resting-State Functional Magnetic Resonance Imaging Connectivity: A Randomized, Cross-Sectional Placebo Study. Brain Connect. 2, 246–253. doi:10.1089/brain.2012.0081
Fluss, R., Faraggi, D., Reiser, B., 2005. Estimation of the Youden Index and its associated cutoff point. Biometrical J. 47, 458–472. doi:10.1002/bimj.200410135
Folstein, M.F., Folstein, S.E., McHugh, P.R., 1975. "Mini-mental state". A practical method for grading the cognitive state of patients for the clinician. J. Psychiatr. Res. 12, 189–198. doi:10.1016/0022-3956(75)90026-6
Foltynie, T., Brayne, C., Barker, R.A., 2002. The heterogeneity of idiopathic Parkinson's disease. J. Neurol. 249, 138–145.
Fox, M.D., Raichle, M.E., 2007. Spontaneous fluctuations in brain activity observed with functional magnetic resonance imaging. Nat. Rev. Neurosci. 8, 700–711. doi:10.1038/nrn2201
Friedman, J., Hastie, T., Tibshirani, R., 2010. Regularization paths for generalized linear models via coordinate descent. J. Stat. Softw. 33, 1–22. doi:10.18637/jss.v033.i01
Galluzzi, S., Lanni, C., Pantoni, L., Filippi, M., Frisoni, G.B., 2008. White matter lesions in the elderly: Pathophysiological hypothesis on the effect on brain plasticity and reserve. J. Neurol. Sci. 273, 3–9. doi:10.1016/j.jns.2008.06.023
Gama, R.L., Távora, D.G., Bomfim, R.C., Silva, C.E., de Bruin, V.M., de Bruin, P.F.C., 2010. Sleep disturbances and brain MRI morphometry in Parkinson's disease, multiple system atrophy and progressive supranuclear palsy - a comparative study. Parkinsonism Relat. Disord. 16, 275–9. doi:10.1016/j.parkreldis.2010.01.002
Gazzina, S., Premi, E., Turrone, R., Acosta-Cabronero, J., Rizzetti, M.C., Cotelli, M.S., Gasparotti, R., Padovani, A., Borroni, B., 2016. Subcortical matter in the α-synucleinopathies spectrum: an MRI pilot study. J. Neurol. 263, 1575–1582. doi:10.1007/s00415-016-8173-5
Geng, G., Henry, R., Rae, C., 2012. Effects of 8 and 32-Channel Phase Array Coils on DTI Metrics, in: Proc Intl Soc Mag Reson Med.
Gibb, W.R., Lees, A.J., 1988. The relevance of the Lewy body to the pathogenesis of idiopathic Parkinson's disease. J. Neurol. Neurosurg. Psychiatry 51, 745–52. doi:10.1136/jnnp-2012-302969

Goetz, C.G., Luo, S., Wang, L., Tilley, B.C., LaPelle, N.R., Stebbins, G.T., 2015. Handling missing values in the MDS-UPDRS. Mov. Disord. 30, 1632–1638. doi:10.1002/mds.26153

Goetz, C.G., Tilley, B.C., Shaftman, S.R., Stebbins, G.T., Fahn, S., Martinez-Martin, P., Poewe, W., Sampaio, C., Stern, M.B., Dodel, R., Dubois, B., Holloway, R., Jankovic, J., Kulisevsky, J., Lang, A.E., Lees, A., Leurgans, S., LeWitt, P.A., Nyenhuis, D., Olanow, C.W., Rascol, O., Schrag, A., Teresi, J.A., van Hilten, J.J., LaPelle, N., 2008. Movement Disorder Society-sponsored revision of the Unified Parkinson's Disease Rating Scale (MDS-UPDRS): scale presentation and clinimetric testing results. Mov. Disord. 23, 2129–21270. doi:10.1002/mds.22340

Gomperts, S.N., 2014. Imaging the role of amyloid in PD dementia and dementia with Lewy bodies. Curr. Neurol. Neurosci. Rep. 14, 472–481. doi:10.1007/s11910-014-0472-6

Good, C., Johnsrude, I., Ashburner, J., Henson, R., Friston, K., Frackowiak, R., 2001. A Voxel-Based Morphometric Study of Ageing in 465 Normal Adult Human Brains. Neuroimage 14, 21–36. doi:10.1006/nimg.2001.0786

Göttlich, M., Münte, T.F., Heldmann, M., Kasten, M., Hagenah, J., Krämer, U.M., 2013. Altered resting state brain networks in Parkinson's disease. PLoS One 8, e77336. doi:10.1371/journal.pone.0077336

Grady, C.L., 2008. Cognitive neuroscience of aging. Ann. N. Y. Acad. Sci. 1124, 127–144. doi:10.1196/annals.1440.009

Gratwicke, J., Jahanshahi, M., Foltynie, T., 2015. Parkinson's disease dementia: a neural networks perspective. Brain 138, 1454–1476. doi:10.1093/brain/awv104

Gregory, S., Long, J.D., Tabrizi, S.J., Rees, G., 2017. Measuring compensation in neurodegeneration using MRI. Curr. Opin. Neurol. 30, 380–387. doi:10.1097/WCO.0000000000000469

Greve, D.N., Fischl, B., 2009. Accurate and robust brain image alignment using boundary-based registration. Neuroimage 48, 63–72. doi:10.1016/j.neuroimage.2009.06.060

Grueter, B.E., Schulz, U.G., 2012. Age-related cerebral white matter disease (Leukoaraiosis): A review. Postgrad. Med. J. 88, 79–87. doi:10.1136/postgradmedj-2011-130307

Gu, Q., Zhang, H., Xuan, M., Luo, W., Huang, P., Xia, S., Zhang, M., 2016. Automatic classification on multi-modal MRI data for diagnosis of the postural instability and gait difficulty subtype of Parkinson's disease. J. Parkinsons. Dis. 6, 545–556. doi:10.3233/JPD-150729

Hafkemeijer, A., Altmann-Schneider, I., de Craen, A.J., Slagboom, P.E., van der Grond, J., Rombouts, S.A., 2014. Associations between age and gray matter volume in anatomical brain networks in middle-aged to older adults. Aging Cell 13, 1068–1074. doi:10.1111/acel.12271

Hafkemeijer, A., Möller, C., Dopper, E.G.P., Jiskoot, L.C., Schouten, T.M., van Swieten, J.C., van der Flier, W.M., Vrenken, H., Pijnenburg, Y.A.L., Barkhof, F., Scheltens, P., van der Grond, J., Rombouts, S.A.R.B., 2015. Resting state functional connectivity differences between behavioral variant frontotemporal dementia and Alzheimer's disease. Front. Hum. Neurosci. 9, 474. doi:10.3389/fnhum.2015.00474

Hafkemeijer, A., Möller, C., Dopper, E.G.P., Jiskoot, L.C., van den Berg-Huysmans, A.A., van Swieten, J.C., van der Flier, W.M., Vrenken, H., Pijnenburg, Y.A.L., Barkhof, F., Scheltens, P., van der Grond, J., Rombouts, S.A.R.B., 2016. Differences in structural covariance brain networks between behavioral variant frontotemporal dementia and Alzheimer's disease. Hum. Brain Mapp. 37, 978–988. doi:10.1002/hbm.23081

Hafkemeijer, A., van der Grond, J., Rombouts, S.A.R.B., 2012. Imaging the default mode network in aging and dementia. Biochim. Biophys. Acta - Mol. Basis Dis. 1822, 431–441. doi:10.1016/j.bbadis.2011.07.008

Hagmann, P., Cammoun, L., Gigandet, X., Meuli, R., Honey, C.J., Van Wedeen, J., Sporns, O., 2008. Mapping the structural core of human cerebral cortex. PLoS Biol. 6, e159. doi:10.1371/journal.pbio.0060159

Hall, J.M., Ehgoetz Martens, K.A., Walton, C.C., O'Callaghan, C., Keller, P.E., Lewis, S.J.G., Moustafa, A.A., 2016. Diffusion alterations associated with Parkinson's disease symptomatology: A review of the literature. Parkinsonism Relat. Disord. 33, 12–26. doi:10.1016/j.parkreldis.2016.09.026

Ham, J.H., Lee, J.J., Sunwoo, M.K., Hong, J.Y., Sohn, Y.H., Lee, P.H., 2016. Effect of olfactory impairment and white matter hyperintensities on cognition in Parkinson's disease. Park. Relat. Disord. 24, 95–99. doi:10.1016/j.parkreldis.2015.12.017

Harding, A. J., Broe, G.A., Halliday, G.M., 2002. Visual hallucinations in Lewy body disease relate to Lewy bodies in the temporal lobe. Brain 125, 391–403. doi:10.1093/brain/awf033

Harding, Antony J., Lakay, B., Halliday, G.M., 2002. Selective hippocampal neuron loss in dementia with lewy bodies. Ann. Neurol. 51, 125–128. doi:10.1002/ana.10071

Heitz, C., Noblet, V., Cretin, B., Philippi, N., Kremer, L., Stackfleth, M., Hubele, F., Armspach, J., Namer, I., Blanc, F., 2015. Neural correlates of visual hallucinations in dementia with Lewy bodies. Alzheimers. Res. Ther. 7, 6–14. doi:10.1186/s13195-014-0091-0

Hindriks, R., Adhikari, M.H., Murayama, Y., Ganzetti, M., Mantini, D., Logothetis, N.K., Deco, G., 2016. Can sliding-window correlations reveal dynamic functional connectivity in resting-state fMRI? Neuroimage 127, 242–256. doi:10.1016/j.neuroimage.2015.11.055

Hoerl, A.E., Kennard, R.W., 1970. Ridge regression: Biased estimation for nonorthogonal problems. Technometrics 12, 55–67. doi:10.1080/00401706.1970.10488634

Holiga, Š., Mueller, K., Möller, H.E., Urgošík, D., Růžička, E., Schroeter, M.L., Jech, R., 2015. Resting-state functional magnetic resonance imaging of the subthalamic microlesion and stimulation effects in Parkinson's disease: Indications of a principal role of the brainstem. NeuroImage. Clin. 9, 264–274. doi:10.1016/j.nicl.2015.08.008

Hou, Y., Luo, C., Yang, J., Ou, R., Song, W., Wei, Q., Cao, B., Zhao, B., Wu, Y., Shang, H.F., Gong, Q., 2016. Prediction of individual clinical scores in patients with Parkinson's disease using resting-state functional magnetic resonance imaging. J. Neurol. Sci. 366, 27–32. doi:10.1016/j.jns.2016.04.030

Hutchison, R.M., Womelsdorf, T., Allen, E.A., Bandettini, P.A., Calhoun, V.D., Corbetta, M., Della Penna, S., Duyn, J.H., Glover, G.H., Gonzalez-Castillo, J., Handwerker, D.A., Keilholz, S., Kiviniemi, V., Leopold, D.A., de Pasquale, F., Sporns, O., Walter, M., Chang, C., 2013. Dynamic functional connectivity: Promise, issues, and interpretations. Neuroimage 80, 360–378. doi:10.1016/j.neuroimage.2013.05.079

Jellinger, K.A., 2012. Neuropathology of sporadic Parkinson's disease: Evaluation and changes of concepts. Mov. Disord. 27, 8–30. doi:10.1002/mds.23795

Jellinger, K.A., 2009. Formation and development of Lewy pathology: A critical update. J. Neurol. 256, 270–279. doi:10.1007/s00415-009-5243-y

Jenkinson, M., Bannister, P., Brady, M., Smith, S., 2002a. Improved Methods for the Registration and Motion Correction of Brain Images. Neuroimage 17, 825–841. doi:10.1016/S1053-8119(02)91132-8

Jenkinson, M., Bannister, P., Brady, M., Smith, S., 2002b. Improved optimisation for the robust and accurate linear registration and motion correction of brain images. Neuroimage 17, 825–841. doi:10.1016/S1053-8119(02)91132-8

Jernigan, T.L., Archibald, S.L., Fennema-Notestine, C., Gamst, A.C., Stout, J.C., Bonner, J., Hesselink, J.R., 2001. Effects of age on tissues and regions of the cerebrum and cerebellum. Neurobiol. Aging 22, 581–594. doi:10.1016/S0197-4580(01)00217-2

Jonas, J., Frismand, S., Vignal, J.P., Colnat-Coulbois, S., Koessler, L., Vespignani, H., Rossion, B., Maillard, L., 2014. Right hemispheric dominance of visual phenomena evoked by intracerebral stimulation of the human visual cortex. Hum. Brain Mapp. 35, 3360–3371. doi:10.1002/hbm.22407

Jones, D.T., Vemuri, P., Murphy, M.C., Gunter, J.L., Senjem, M.L., Machulda, M.M., Przybelski, S.A., Gregg, B.E., Kantarci, K., Knopman, D.S., Boeve, B.F., Petersen, R.C., Jack, C.R., 2012. Non-stationarity in the "resting brain's" modular architecture. PLoS One 7, e39731. doi:10.1371/journal.pone.0039731

Kaasinen, V., Aalto, S., Någren, K., Hietala, J., Sonninen, P., Rinne, J.O., 2003. Extrastriatal dopamine D2 receptors in Parkinson's disease: A longitudinal study. J. Neural Transm. 110, 591–601.

doi:10.1007/s00702-003-0816-x
Kalaitzakis, M.E., Graeber, M.B., Gentleman, S.M., Pearce, R.K.B., 2008. Striatal β-amyloid deposition in Parkinson disease with Dementia. J. Neuropathol. Exp. Neurol. 67, 155–161. doi:10.1097/NEN.0b013e31816362aa
Kantarci, K., Lowe, V.J., Boeve, B.F., Weigand, S.D., Senjem, M.L., Przybelski, S.A., Dickson, D.W., Parisi, J.E., Knopman, D.S., Smith, G.E., Ferman, T.J., Petersen, R.C., Jack, C.R., 2012. Multimodality imaging characteristics of dementia with Lewy bodies. Neurobiol. Aging 33, 2091–2105. doi:10.1016/j.neurobiolaging.2011.09.024
Kato, S., Watanabe, H., Senda, J., Hirayama, M., Ito, M., Atsuta, N., Kaga, T., Katsuno, M., Naganawa, S., Sobue, G., 2012. Widespread cortical and subcortical brain atrophy in Parkinson's disease with excessive daytime sleepiness. J. Neurol. 259, 318–326. doi:10.1007/s00415-011-6187-6
Kenny, E.R., Burton, E.J., O'Brien, J.T., 2008. A volumetric magnetic resonance imaging study of entorhinal cortex volume in dementia with lewy bodies. A comparison with Alzheimer's disease and Parkinson's disease with and without dementia. Dement. Geriatr. Cogn. Disord. 26, 218–225. doi:10.1159/000153432
Kim, J., Criaud, M., Cho, S.S., Díez-Cirarda, M., Mihaescu, A., Coakeley, S., Ghadery, C., Valli, M., Jacobs, M.F., Houle, S., Strafella, A.P., 2017. Abnormal intrinsic brain functional network dynamics in Parkinson's disease. Brain 140, 2955–2967. doi:10.1093/brain/awx233
Kim, K.W., MacFall, J.R., Payne, M.E., 2008. Classification of white matter lesions on magnetic resonance imaging in elderly persons. Biol. Psychiatry 64, 273–280. doi:10.1016/j.biopsych.2008.03.024
Kramer, M.L., Schulz-Schaeffer, W.J., 2007. Presynaptic alpha-synuclein aggregates, not Lewy bodies, cause neurodegeneration in Dementia with Lewy bodies. J. Neurosci. 27, 1405–1410. doi:10.1523/JNEUROSCI.4564-06.2007
Kucyi, A., Hove, M.J., Esterman, M., Hutchison, R.M., Valera, E.M., 2017. Dynamic brain network correlates of spontaneous fluctuations in attention. Cereb. Cortex 27, 1831–1840. doi:10.1093/cercor/bhw029
Kurani, A.S., Seidler, R.D., Burciu, R.G., Comella, C.L., Corcos, D.M., Okun, M.S., MacKinnon, C.D., Vaillancourt, D.E., 2015. Subthalamic nucleus-sensorimotor cortex functional connectivity in de novo and moderate Parkinson's disease. Neurobiol. Aging 36, 462–469. doi:10.1016/j.neurobiolaging.2014.07.004
Lebedev, A. V., Westman, E., Simmons, A., Lebedeva, A., Siepel, F.J., Pereira, J.B., Aarsland, D., 2014. Large-scale resting state network correlates of cognitive impairment in Parkinson's disease and related dopaminergic deficits. Front. Syst. Neurosci. 8, 45. doi:10.3389/fnsys.2014.00045
Lee, S.J., Kim, J.S., Lee, K.S., An, J.Y., Kim, W., Kim, Y.I., Kim, B.S., Jung, S.L., 2009. The severity of leukoaraiosis correlates with the clinical phenotype of Parkinson's disease. Arch. Gerontol. Geriatr. 49, 255–259. doi:10.1016/j.archger.2008.09.005
Lee, S.J., Lee, D.G., 2016. The cross-sectional and longitudinal relationships between white matter hyperintensities and dementia in patients with Parkinson's disease: A retrospective analysis of 132 patients in a single center. Arch. Gerontol. Geriatr. 62, 133–137. doi:10.1016/j.archger.2015.10.006
Leech, R., Sharp, D.J., 2014. The role of the posterior cingulate cortex in cognition and disease. Brain 137, 12–32. doi:10.1093/brain/awt162
Levy, G., 2007. The relationship of Parkinson disease with aging. Arch. Neurol. 64, 1242–1246. doi:10.1001/archneur.64.9.1242
Lewis, S.J.G., Dove, A., Robbins, T.W., Barker, R.A., Owen, A.M., 2003. Cognitive impairments in early Parkinson's disease are accompanied by reductions in activity in frontostriatal neural circuitry. J. Neurosci. 23, 6351–6356. doi:23/15/6351 [pii]
Leys, D., Pruvo, J.P., Parent, M., Vermersch, P., Soetaert, G., Steinling, M., Delacourte, A., Defossez, A., Rapoport, A., Clarisse, J., Petit, H., 1991. Could Wallerian degeneration contribute to

"leuko-araiosis" in subjects free of any vascular disorder? J. Neurol. Neurosurg. Psychiatry 54, 46–50. doi:10.1136/jnnp.54.1.46

Lim, S.Y., Fox, S.H., Lang, A.E., 2009. Overview of the extranigral aspects of parkinson disease. Arch. Neurol. 66, 167–172. doi:10.1001/archneurol.2008.561

Linazasoro, G., 2007. Classical Parkinson disease versus Parkinson complex - Reflections against staging and in favour of heterogeneity. Eur. J. Neurol. 14, 721–728. doi:10.1111/j.1468-1331.2007.01853.x

Lippa, C.F., Smith, T.W., Swearer, J.M., 1994. Alzheimer's disease and Lewy body disease: A comparative clinicopathological study. Ann. Neurol. 35, 81–88. doi:10.1002/ana.410350113

Liu, L., Wang, Q., Adeli, E., Zhang, L., Zhang, H., Shen, D., 2016. Feature selection based on iterative canonical correlation analysis for automatic diagnosis of Parkinson's disease, in: Lecture Notes in Computer Science (Including Subseries Lecture Notes in Artificial Intelligence and Lecture Notes in Bioinformatics). doi:10.1007/978-3-319-46723-8_1

Lockhart, S.N., DeCarli, C., 2014. Structural Imaging Measures of Brain Aging. Neuropsychol. Rev. 24, 271–289. doi:10.1007/s11065-014-9268-3

Lohmann, G., Margulies, D.S., Horstmann, A., Pleger, B., Lepsien, J., Goldhahn, D., Schloegl, H., Stumvoll, M., Villringer, A., Turner, R., 2010. Eigenvector Centrality Mapping for Analyzing Connectivity Patterns in fMRI Data of the Human Brain. PLoS One 5, e10232. doi:10.1371/journal.pone.0010232

Lou, Y., Huang, P., Li, D., Cen, Z., Wang, B., Gao, J., Xuan, M., Yu, H., Zhang, M., Luo, W., 2015. Altered brain network centrality in depressed Parkinson's disease patients. Mov. Disord. 30, 1777–1784. doi:10.1002/mds.26321

Luo, X., Qiu, T., Jia, Y., Huang, P., Xu, X., Yu, X., Shen, Z., Jiaerken, Y., Guan, X., Zhou, J., Zhang, M., 2017. Intrinsic functional connectivity alterations in cognitively intact elderly APOE **ε**4 carriers measured by eigenvector centrality mapping are related to cognition and CSF biomarkers: a preliminary study. Brain Imaging Behav. 11, 1290–1301. doi:10.1007/s11682-016-9600-z

Mak, E., Su, L., Williams, G.B., O'Brien, J.T., 2014. Neuroimaging characteristics of dementia with Lewy bodies. Alzheimer's Res. Ther. 6, 18. doi:10.1186/alzrt248

Mak, E., Su, L., Williams, G.B., Watson, R., Firbank, M., Blamire, A., O'Brien, J., 2016. Differential atrophy of hippocampal subfields: A comparative study of dementia with lewy bodies and Alzheimer disease. Am. J. Geriatr. Psychiatry 24, 136–143. doi:10.1016/j.jagp.2015.06.006

Marek, K., Jennings, D., Lasch, S., Siderowf, A., Tanner, C., Simuni, T., Coffey, C., Kieburtz, K., Flagg, E., Chowdhury, S., Poewe, W., Mollenhauer, B., Sherer, T., Frasier, M., Meunier, C., Rudolph, A., Casaceli, C., Seibyl, J., Mendick, S., Schuff, N., Zhang, Y., Toga, A., Crawford, K., Ansbach, A., de Blasio, P., Piovella, M., Trojanowski, J., Shaw, L., Singleton, A., Hawkins, K., Eberling, J., Russell, D., Leary, L., Factor, S., Sommerfeld, B., Hogarth, P., Pighetti, E., Williams, K., Standaert, D., Guthrie, S., Hauser, R., Delgado, H., Jankovic, J., Hunter, C., Stern, M., Tran, B., Leverenz, J., Baca, M., Frank, S., Thomas, C.A., Richard, I., Deeley, C., Rees, L., Sprenger, F., Lang, E., Shill, H., Obradov, S., Fernandez, H., Winters, A., Berg, D., Gauss, K., Galasko, D., Fontaine, D., Mari, Z., Gerstenhaber, M., Brooks, D., Malloy, S., Barone, P., Longo, K., Comery, T., Ravina, B., Grachev, I., Gallagher, K., Collins, M., Widnell, K.L., Ostrowizki, S., Fontoura, P., La-Roche, F.H., Ho, T., Luthman, J., van der Brug, M., Reith, A.D., Taylor, P., 2011. The Parkinson Progression Marker Initiative (PPMI). Prog. Neurobiol. 95, 629–635. doi:10.1016/j.pneurobio.2011.09.005

Marinus, J., Visser, M., Verwey, N.A., Verhey, F.R.J., Middelkoop, H. a. M., Stiggelbout, A.M., Hilten, J.J. van, 2003. Assessment of cognition in Parkinson's disease. Neurology 61, 1222–1228. doi:10.1212/01.WNL.0000091864.39702.1C

McCann, H., Cartwright, H., Halliday, G.M., 2016. Neuropathology of **α**-synuclein propagation and braak hypothesis. Mov. Disord. 31, 152–160. doi:10.1002/mds.26421

McKeith, I.G., Boeve, B.F., Dickson, D.W., Halliday, G., Taylor, J.-P., Weintraub, D., Aarsland, D., Galvin, J., Attems, J., Ballard, C.G., Bayston, A., Beach, T.G., Blanc, F., Bohnen, N., Bonanni, L.,

Bras, J., Brundin, P., Burn, D., Chen-Plotkin, A., Duda, J.E., El-Agnaf, O., Feldman, H., Ferman, T.J., Ffytche, D., Fujishiro, H., Galasko, D., Goldman, J.G., Gomperts, S.N., Graff-Radford, N.R., Honig, L.S., Iranzo, A., Kantarci, K., Kaufer, D., Kukull, W., Lee, V.M.Y., Leverenz, J.B., Lewis, S., Lippa, C., Lunde, A., Masellis, M., Masliah, E., McLean, P., Mollenhauer, B., Montine, T.J., Moreno, E., Mori, E., Murray, M., O'Brien, J.T., Orimo, S., Postuma, R.B., Ramaswamy, S., Ross, O.A., Salmon, D.P., Singleton, A., Taylor, A., Thomas, A., Tiraboschi, P., Toledo, J.B., Trojanowski, J.Q., Tsuang, D., Walker, Z., Yamada, M., Kosaka, K., 2017. Diagnosis and management of dementia with Lewy bodies: Fourth consensus report of the DLB Consortium. Neurology 89, 88–100. doi:10.1212/WNL.0000000000004058

McKeith, I.G., Dickson, D.W., Lowe, J., Emre, M., O'Brien, J.T., Feldman, H., Cummings, J., Duda, J.E., Lippa, C., Perry, E.K., Aarsland, D., Arai, H., Ballard, C.G., Boeve, B., Burn, D.J., Costa, D., Del Ser, T., Dubois, B., Galasko, D., Gauthier, S., Goetz, C.G., Gomez-Tortosa, E., Halliday, G., Hansen, L.A., Hardy, J., Iwatsubo, T., Kalaria, R.N., Kaufer, D., Kenny, R.A., Korczyn, A., Kosaka, K., Lee, V.M.Y., Lees, A., Litvan, I., Londos, E., Lopez, O.L., Minoshima, S., Mizuno, Y., Molina, J.A., Mukaetova-Ladinska, E.B., Pasquier, F., Perry, R.H., Schulz, J.B., Trojanowski, J.Q., Yamada, M., 2005. Diagnosis and management of dementia with Lewy bodies: Third report of the DLB consortium. Neurology 65, 1863–1872. doi:10.1212/01.wnl.0000187889.17253.b1

Melzer, T.R., Myall, D.J., MacAskill, M.R., Pitcher, T.L., Livingston, L., Watts, R., Keenan, R.J., Dalrymple-Alford, J.C., Anderson, T.J., 2015. Tracking Parkinson's disease over one year with multimodal magnetic resonance imaging in a group of older patients with moderate disease. PLoS One 10, e0143923. doi:10.1371/journal.pone.0143923

Menon, V., Uddin, L.Q., 2010. Saliency, switching, attention and control: a network model of insula function. Brain Struct. Funct. 214, 655–667. doi:10.1007/s00429-010-0262-0

Mestre, T.A., Eberly, S., Tanner, C., Grimes, D., Lang, A.E., Oakes, D., Marras, C., 2018. Reproducibility of data-driven Parkinson's disease subtypes for clinical research. Park. Relat. Disord. 156, 102–106. doi:10.1016/j.parkreldis.2018.07.009

Moccia, M., Tedeschi, E., Ugga, L., Erro, R., Picillo, M., Caranci, F., Barone, P., Brunetti, A., 2016. White matter changes and the development of motor phenotypes in de novo Parkinson's Disease. J. Neurol. Sci. 367, 215–219. doi:10.1016/j.jns.2016.06.015

Möller, C., Hafkemeijer, A., Pijnenburg, Y.A.L., Rombouts, S.A.R.B., van der Grond, J., Dopper, E., van Swieten, J., Versteeg, A., Steenwijk, M.D., Barkhof, F., Scheltens, P., Vrenken, H., van der Flier, W.M., 2015. Different patterns of cortical gray matter loss over time in behavioral variant FTD and AD. Neurobiol. Aging 38, 21–31. doi:10.1016/j.neurobiolaging.2015.10.020

Montembeault, M., Joubert, S., Doyon, J., Carrier, J., Gagnon, J.F., Monchi, O., Lungu, O., Belleville, S., Brambati, S.M., 2012. The impact of aging on gray matter structural covariance networks. Neuroimage 63, 754–759. doi:10.1016/j.neuroimage.2012.06.052

Montembeault, M., Rouleau, I., Provost, J.-S., Brambati, S.M., 2016. Altered Gray Matter Structural Covariance Networks in Early Stages of Alzheimer's Disease. Cereb. Cortex 26, 2650–2662. doi:10.1093/cercor/bhv105

Ng, B., Varoquaux, G., Poline, J.B., Thirion, B., Greicius, M.D., Poston, K.L., 2017. Distinct alterations in Parkinson's medication-state and disease-state connectivity. NeuroImage Clin. 16, 575–585. doi:10.1016/j.nicl.2017.09.004

O'Malley, K.L., 2010. The role of axonopathy in Parkinson's disease. Exp. Neurobiol. 19, 115–159. doi:10.5607/en.2010.19.3.115

Oakes, T.R., Fox, A.S., Johnstone, T., Chung, M.K., Kalin, N., Davidson, R.J., 2007. Integrating VBM into the General Linear Model with voxelwise anatomical covariates. Neuroimage 34, 500–508. doi:10.1016/j.neuroimage.2006.10.007

Ofori, E., Krismer, F., Burciu, R.G., Pasternak, O., McCracken, J.L., Lewis, M.M., Du, G., McFarland, N.R., Okun, M.S., Poewe, W., Mueller, C., Gizewski, E.R., Schocke, M., Kremser, C., Li, H., Huang, X., Seppi, K., Vaillancourt, D.E., 2017. Free water improves detection of changes in the substantia nigra in parkinsonism: A multisite study. Mov. Disord. 32, 1457–1464.

doi:10.1002/mds.27100
Onu, M., Badea, L., Roceanu, A., Tivarus, M., Bajenaru, O., 2015. Increased connectivity between sensorimotor and attentional areas in Parkinson's disease. Neuroradiology 57, 957–968. doi:10.1007/s00234-015-1556-y
Pan, P.L., Song, W., Shang, H.F., 2012. Voxel-wise meta-analysis of gray matter abnormalities in idiopathic Parkinson's disease. Eur. J. Neurol. 19, 199–206. doi:10.1111/j.1468-1331.2011.03474.x
Panman, J.L., To, Y.Y., van der Ende, E.L., Poos, J.M., Jiskoot, L.C., Meeter, L.H.H., Dopper, E.G.P., Bouts, M.J.R.J., van Osch, M.J.P., Rombouts, S.A.R.B., van Swieten, J.C., van der Grond, J., Papma, J.M., Hafkemeijer, A., 2019. Bias introduced by multiple head coils in MRI research: An 8 channel and 32 channel coil comparison. Front. Neurosci. 13, 1–9. doi:10.3389/fnins.2019.00729
Pantoni, L., 2010. Cerebral small vessel disease: from pathogenesis and clinical characteristics to therapeutic challenges. Lancet Neurol. 9, 689–701. doi:10.1016/S1474-4422(10)70104-6
Paolini, M., Keeser, D., Ingrisch, M., Werner, N., Kindermann, N., Reiser, M., Blautzik, J., 2015. Resting-state networks in healthy adult subjects: a comparison between a 32-element and an 8-element phased array head coil at 3.0 Tesla. Acta radiol. 56, 605–613. doi:10.1177/0284185114567703
Patenaude, B., Smith, S.M., Kennedy, D.N., Jenkinson, M., 2011. A Bayesian model of shape and appearance for subcortical brain segmentation. Neuroimage 56, 907–922. doi:10.1016/j.neuroimage.2011.02.046
Peng, B., Wang, S., Zhou, Z., Liu, Y., Tong, B., Zhang, T., Dai, Y., 2017. A multilevel-ROI-features-based machine learning method for detection of morphometric biomarkers in Parkinson's disease. Neurosci. Lett. 651, 88–94. doi:10.1016/j.neulet.2017.04.034
Peng, J., Wang, P., Zhou, N., Zhu, J., 2009. Partial correlation estimation by joint sparse regression models. J. Am. Stat. Assoc. 104, 735–746. doi:10.1198/jasa.2009.0126
Piccini, P., Pavese, N., Canapicchi, R., Paoli, C., Del Dotto, P., Puglioli, M., Rossi, G., Bonuccelli, U., 1995. White Matter Hyperintensities in Parkinson's Disease: Clinical Correlations. Arch. Neurol. 52, 191–194. doi:10.1001/archneur.1995.00540260097023
Pievani, M., de Haan, W., Wu, T., Seeley, W.W., Frisoni, G.B., 2011. Functional network disruption in the degenerative dementias. Lancet Neurol. 10, 829–843. doi:10.1016/S1474-4422(11)70158-2
Pievani, M., Filippini, N., van den Heuvel, M.P., Cappa, S.F., Frisoni, G.B., 2014. Brain connectivity in neurodegenerative diseases - from phenotype to proteinopathy. Nat. Rev. Neurol. 10, 620–633. doi:10.1038/nrneurol.2014.178
Postuma, R.B., Berg, D., Stern, M., Poewe, W., Olanow, C.W., Oertel, W., Marek, K., Litvan, I., Lang, A.E., Halliday, G., Goetz, C.G., Gasser, T., Dubois, B., Chan, P., Bloem, B.R., Adler, C.H., Deuschl, G., 2016. Abolishing the 1-year rule: How much evidence will be enough? Mov. Disord. 31, 1623–1627. doi:10.1002/mds.26796
Postuma, R.B., Berg, D., Stern, M., Poewe, W., Olanow, C.W., Oertel, W., Obeso, J., Marek, K., Litvan, I., Lang, A.E., Halliday, G., Goetz, C.G., Gasser, T., Dubois, B., Chan, P., Bloem, B.R., Adler, C.H., Deuschl, G., 2015. MDS clinical diagnostic criteria for Parkinson's disease. Mov. Disord. 30, 1591–1601. doi:10.1002/mds.26424
Pozorski, V., Oh, J.M., Adluru, N., Merluzzi, A.P., Theisen, F., Okonkwo, O., Barzgari, A., Krislov, S., Sojkova, J., Bendlin, B.B., Johnson, S.C., Alexander, A.L., Gallagher, C.L., 2018. Longitudinal white matter microstructural change in Parkinson's disease. Hum. Brain Mapp. 39, 4150–4161. doi:10.1002/hbm.24239
Prodoehl, J., Burciu, R.G., Vaillancourt, D.E., 2014. Resting State Functional Magnetic Resonance Imaging in Parkinson's Disease. Curr. Neurol. Neurosci. Rep. 14, 448. doi:10.1007/s11910-014-0448-6
Pruim, R.H.R., Mennes, M., Buitelaar, J.K., Beckmann, C.F., 2015a. Evaluation of ICA-AROMA and alternative strategies for motion artifact removal in resting state fMRI. Neuroimage 112, 278–

287. doi:10.1016/j.neuroimage.2015.02.063
Pruim, R.H.R., Mennes, M., van Rooij, D., Llera, A., Buitelaar, J.K., Beckmann, C.F., 2015b. ICA-AROMA: A robust ICA-based strategy for removing motion artifacts from fMRI data. Neuroimage 112, 267–277. doi:10.1016/j.neuroimage.2015.02.064
Raz, N., Lindenberger, U., Rodrigue, K.M., Kennedy, K.M., Head, D., Williamson, A., Dahle, C., Gerstorf, D., Acker, J.D., 2005. Regional brain changes in aging healthy adults: General trends, individual differences and modifiers. Cereb. Cortex 5, 1676–1689. doi:10.1093/cercor/bhi044
Resnick, S.M., Pham, D.L., Kraut, M.A., Zonderman, A.B., Davatzikos, C., 2003. Longitudinal magnetic resonance imaging studies of older adults: a shrinking brain. J. Neurosci. 23, 3295–3301.
Ritz, M.F., Grond-Ginsbach, C., Fluri, F., Kloss, M., Tolnay, M., Peters, N., Engelter, S., Lyrer, P., 2017. Cerebral small vessel disease is associated with dysregulation in the ubiquitin proteasome system and other major cellular pathways in specific brain regions. Neurodegener. Dis. 17, 261–275. doi:10.1159/000478529
Rossi, M.E., Ruottinen, H., Saunamäki, T., Elovaara, I., Dastidar, P., 2014. Imaging brain iron and diffusion patterns: a follow-up study of Parkinson's disease in the initial stages. Acad. Radiol. 21, 64–71. doi:10.1016/j.acra.2013.09.018
Sabatini, U., Boulanouar, K., Fabre, N., Martin, F., Carel, C., Colonnese, C., Bozzao, L., Berry, I., Montastruc, J.L., Chollet, F., Rascol, O., 2000. Cortical motor reorganization in akinetic patients with Parkinson's disease: a functional MRI study. Brain 123, 394–403. doi:10.1093/brain/123.2.394
Sabattoli, F., Boccardi, M., Galluzzi, S., Treves, A., Thompson, P.M., Frisoni, G.B., 2008. Hippocampal shape differences in dementia with Lewy bodies. Neuroimage 41, 699–705. doi:10.1016/j.neuroimage.2008.02.060
Saeed, U., Compagnone, J., Aviv, R.I., Strafella, A.P., Black, S.E., Lang, A.E., Masellis, M., 2017. Imaging biomarkers in Parkinson's disease and Parkinsonian syndromes: Current and emerging concepts. Transl. Neurodegener. 6, 8. doi:10.1186/s40035-017-0076-6
Sakai, K., Yamada, K., 2018. Machine learning studies on major brain diseases: 5-year trends of 2014-2018. Jpn. J. Radiol. 37, 34–72. doi:10.1007/s11604-018-0794-4
Sanchez-Castaneda, C., Rene, R., Ramirez-Ruiz, B., Campdelacreu, J., Gascon, J., Falcon, C., Calopa, M., Jauma, S., Juncadella, M., Junque, C., 2009. Correlations between gray matter reductions and cognitive deficits in dementia with Lewy Bodies and Parkinson's disease with dementia. Mov. Disord. 24, 1740–1746. doi:10.1002/mds.22488
Sartor, J., Bettecken, K., Bernhard, F.P., Hofmann, M., Gladow, T., Lindig, T., Ciliz, M., ten Kate, M., Geritz, J., Heinzel, S., Benedictus, M., Scheltens, P., Hobert, M.A., Maetzler, W., 2017. White matter changes-related gait and executive function deficits: Associations with age and Parkinson's disease. Front. Aging Neurosci. 9, 213. doi:10.3389/fnagi.2017.00213
Schoonheim, M.M., Geurts, J.J.G., Wiebenga, O.T., De Munck, J.C., Polman, C.H., Stam, C.J., Barkhof, F., Wink, A.M., 2014. Changes in functional network centrality underlie cognitive dysfunction and physical disability in multiple sclerosis. Mult. Scler. J. 20, 1058–1065. doi:10.1177/1352458513516892
Schouten, T.M., Koini, M., De Vos, F., Seiler, S., Van Der Grond, J., Lechner, A., Hafkemeijer, A., Möller, C., Schmidt, R., De Rooij, M., Rombouts, S.A.R.B., 2016. Combining anatomical, diffusion, and resting state functional magnetic resonance imaging for individual classification of mild and moderate Alzheimer's disease. NeuroImage Clin. 11, 46–51. doi:10.1016/j.nicl.2016.01.002
Schulz-Schaeffer, W.J., 2015. Is cell death primary or secondary in the pathophysiology of idiopathic Parkinson's disease? Biomolecules 5, 1467–1479. doi:10.3390/biom5031467
Schulz-Schaeffer, W.J., 2010. The synaptic pathology of **α**-synuclein aggregation in dementia with Lewy bodies, Parkinson's disease and Parkinson's disease dementia. Acta Neuropathol. 120, 131–143. doi:10.1007/s00401-010-0711-0
Seeley, W.W., Crawford, R.K., Zhou, J., Miller, B.L., Greicius, M.D., 2009. Neurodegenerative diseases

target large-scale human brain networks. Neuron 62, 42–52. doi:10.1016/j.neuron.2009.03.024
Seeley, W.W., Menon, V., Schatzberg, A.F., Keller, J., Glover, G.H., Kenna, H., Reiss, A.L., Greicius, M.D., 2007. Dissociable intrinsic connectivity networks for salience processing and executive control. J. Neurosci. 27, 2349–56. doi:10.1523/JNEUROSCI.5587-06.2007
Segall, J.M., Allen, E.A., Jung, R.E., Erhardt, E.B., Arja, S.K., Kiehl, K.A., Calhoun, V.D., 2012. Correspondence between structure and function in the human brain at rest. Front Neuroinformatics 6, 10. doi:10.3389/fninf.2012.00010
Shirer, W.R., Ryali, S., Rykhlevskaia, E., Menon, V., Greicius, M.D., 2012. Decoding subject-driven cognitive states with whole-brain connectivity patterns. Cereb. Cortex 22, 158–165. doi:10.1093/cercor/bhr099
Simioni, A.C., Dagher, A., Fellows, L.K., 2016. Compensatory striatal-cerebellar connectivity in mild-moderate Parkinson's disease. NeuroImage Clin. 10, 54–62. doi:10.1016/j.nicl.2015.11.005
Simuni, T., Caspell-Garcia, C., Coffey, C., Lasch, S., Tanner, C., Marek, K., 2016. How stable are Parkinson's disease subtypes in de novo patients: Analysis of the PPMI cohort? Park. Relat. Disord. 28, 62–67. doi:10.1016/j.parkreldis.2016.04.027
Smith, S.M., 2002. Fast robust automated brain extraction. Hum. Brain Mapp. 17, 143–155. doi:10.1002/hbm.10062
Smith, S.M., Jenkinson, M., Johansen-Berg, H., Rueckert, D., Nichols, T.E., Mackay, C.E., Watkins, K.E., Ciccarelli, O., Cader, M.Z., Matthews, P.M., Behrens, T.E.J., 2006. Tract-based spatial statistics: voxelwise analysis of multi-subject diffusion data. Neuroimage 31, 1487–1505. doi:10.1016/j.neuroimage.2006.02.024
Smith, S.M., Jenkinson, M., Woolrich, M.W., Beckmann, C.F., Behrens, T.E.J., Johansen-Berg, H., Bannister, P.R., De Luca, M., Drobnjak, I., Flitney, D.E., Niazy, R.K., Saunders, J., Vickers, J., Zhang, Y., De Stefano, N., Brady, J.M., Matthews, P.M., 2004. Advances in functional and structural MR image analysis and implementation as FSL. Neuroimage 23, 208–219. doi:10.1016/j.neuroimage.2004.07.051
Smith, S.M., Miller, K.L., Salimi-Khorshidi, G., Webster, M., Beckmann, C.F., Nichols, T.E., Ramsey, J.D., Woolrich, M.W., 2011. Network modelling methods for FMRI. Neuroimage 54, 875–891. doi:10.1016/j.neuroimage.2010.08.063
Smith, S.M., Nichols, T.E., 2009. Threshold-free cluster enhancement: Addressing problems of smoothing, threshold dependence and localisation in cluster inference. Neuroimage 44, 83–98. doi:10.1016/j.neuroimage.2008.03.061
Smith, S.M., Zhang, Y., Jenkinson, M., Chen, J., Matthews, P.M., Federico, A., De Stefano, N., 2002. Accurate, robust, and automated longitudinal and cross-sectional brain change analysis. Neuroimage 17, 479–89. doi:10.1006/nimg.2002.1040
Spreng, R.N., Turner, G.R., 2013. Structural covariance of the default network in healthy and pathological aging. J. Neurosci. 33, 15226–15234. doi:10.1523/JNEUROSCI.2261-13.2013
Stephen, J.M., Coffman, B.A., Jung, R.E., Bustillo, J.R., Aine, C.J., Calhoun, V.D., 2013. Using joint ICA to link function and structure using MEG and DTI in schizophrenia. Neuroimage 83, 418–430. doi:10.1016/j.neuroimage.2013.06.038
Sterling, N.W., Du, G., Lewis, M.M., Swavely, S., Kong, L., Styner, M., Huang, X., 2017. Cortical gray and subcortical white matter associations in Parkinson's disease. Neurobiol. Aging 49, 100–108. doi:10.1016/j.neurobiolaging.2016.09.015
Sterling, N.W., Lewis, M.M., Du, G., Huang, X., 2016. Structural imaging and Parkinson's disease: Moving toward quantitative markers of disease progression. J. Parkinsons. Dis. 27, 557–567. doi:10.3233/JPD-160824
Surmeier, D.J., Obeso, J.A., Halliday, G.M., 2017. Selective neuronal vulnerability in Parkinson disease. Nat. Rev. Neurosci. 18, 101–113. doi:10.1038/nrn.2016.178
Tagawa, R., Hashimoto, H., Nakanishi, A., Kawarada, Y., Muramatsu, T., Matsuda, Y., Kataoka, K., Shimada, A., Uchida, K., Yoshida, A., Higashiyama, S., Kawabe, J., Kai, T., Shiomi, S., Mori, H., Inoue, K., 2015. The Relationship Between Medial Temporal Lobe Atrophy and Cognitive

Impairment in Patients With Dementia With Lewy Bodies. J. Geriatr. Psychiatry Neurol. 28, 249–254. doi:10.1177/0891988715590210

Tagliaferro, P., Kareva, T., Oo, T.F., Yarygina, O., Kholodilov, N., Burke, R.E., 2015. An early axonopathy in a hLRRK2(R1441G) transgenic model of Parkinson disease. Neurobiol. Dis. 82, 359–371. doi:10.1016/j.nbd.2015.07.009

Tahmasian, M., Bettray, L.M., van Eimeren, T., Drzezga, A., Timmermann, L., Eickhoff, C.R., Eickhoff, S.B., Eggers, C., 2015. A systematic review on the applications of resting-state fMRI in Parkinson's disease: Does dopamine replacement therapy play a role? Cortex 73, 80–105. doi:10.1016/j.cortex.2015.08.005

Tahmasian, M., Eickhoff, S.B., Giehl, K., Schwartz, F., Herz, D.M., Drzezga, A., van Eimeren, T., Laird, A.R., Fox, P.T., Khazaie, H., Zarei, M., Eggers, C., Eickhoff, C.R., 2017. Resting-state functional reorganization in Parkinson's disease: An activation likelihood estimation meta-analysis. Cortex 92, 119–138. doi:10.1016/j.cortex.2017.03.016

Tam, C.W.C., Burton, E.J., McKeith, I.G., Burn, D.J., O'Brien, J.T., 2005. Temporal lobe atrophy on MRI in Parkinson disease with dementia: a comparison with Alzheimer disease and dementia with Lewy bodies. Neurology 64, 861–865. doi:10.1212/01.WNL.0000153070.82309.D4

Tambasco, N., Nigro, P., Romoli, M., Simoni, S., Parnetti, L., Calabresi, P., 2015. Magnetization transfer MRI in dementia disorders, Huntington's disease and parkinsonism. J. Neurol. Sci. 353, 1–8. doi:10.1016/j.jns.2015.03.025

Teipel, S.J., Grothe, M.J., Metzger, C.D., Grimmer, T., Sorg, C., Ewers, M., Franzmeier, N., Meisenzahl, E., Klöppel, S., Borchardt, V., Walter, M., Dyrba, M., 2017. Robust detection of impaired resting state functional connectivity networks in Alzheimer's disease using elastic net regularized regression. Front. Aging Neurosci. 8, 1–9. doi:10.3389/fnagi.2016.00318

Teipel, S.J., Kurth, J., Krause, B., Grothe, M.J., 2015. The relative importance of imaging markers for the prediction of Alzheimer's disease dementia in mild cognitive impairment - Beyond classical regression. NeuroImage Clin. 8, 583–593. doi:10.1016/j.nicl.2015.05.006

Tessitore, A., Amboni, M., Esposito, F., Russo, A., Picillo, M., Marcuccio, L., Pellecchia, M.T., Vitale, C., Cirillo, M., Tedeschi, G., Barone, P., 2012. Resting-state brain connectivity in patients with Parkinson's disease and freezing of gait. Parkinsonism Relat. Disord. 18, 781–787. doi:10.1016/j.parkreldis.2012.03.018

Tessitore, A., Giordano, A., Russo, A., Tedeschi, G., 2016. Structural connectivity in Parkinson's disease. Park. Relat. Disord. 22, S56–S59. doi:10.1016/j.parkreldis.2015.09.018

Tholfsen, L.K., Larsen, J.P., Schulz, J., Tysnes, O.-B., Gjerstad, M.D., 2015. Development of excessive daytime sleepiness in early Parkinson disease. Neurology 85, 162–168. doi:10.1212/WNL.0000000000001737

Tibshirani, R., 1996. Regression shrinkage and selection via the Lasso. J. R. Stat. Soc. Ser. B 58, 267–288. doi:10.2307/2346101

Tiehuis, A.M., Vincken, K.L., Mali, W.P.T.M., Kappelle, L.J., Anbeek, P., Algra, A., Biessels, G.J., 2008. Automated and visual scoring methods of cerebral white matter hyperintensities: Relation with age and cognitive function. Cerebrovasc. Dis. 25, 59–66. doi:10.1159/000111500

Tomlinson, C.L., Stowe, R., Patel, S., Rick, C., Gray, R., Clarke, C.E., 2010. Systematic review of levodopa dose equivalency reporting in Parkinson's disease. Mov. Disord. 25, 2649–2653. doi:10.1002/mds.23429

Utevsky, A. V., Smith, D. V., Huettel, S.A., 2014. Precuneus Is a Functional Core of the Default-Mode Network. J. Neurosci. 34, 932–940. doi:10.1523/JNEUROSCI.4227-13.2014

Vaillancourt, D.E., Spraker, M.B., Prodoehl, J., Abraham, I., Corcos, D.M., Zhou, X.J., Comella, C.L., Little, D.M., 2009. High-resolution diffusion tensor imaging in the substantia nigra of de novo Parkinson disease. Neurology 72, 1378–1384. doi:10.1212/01.wnl.0000340982.01727.6e

van den Heuvel, M.P., Hulshoff Pol, H.E., 2010. Exploring the brain network: A review on resting-state fMRI functional connectivity. Eur. Neuropsychopharmacol. 20, 519–534. doi:10.1016/j.euroneuro.2010.03.008

van den Heuvel, M.P., Sporns, O., 2011. Rich-Club Organization of the Human Connectome. J. Neurosci. 31, 15775–15786. doi:10.1523/JNEUROSCI.3539-11.2011

van den Heuvel, M.P., Sporns, O., Collin, G., Scheewe, T., Mandl, R.C.W., Cahn, W., Goñi, J., Hulshoff Pol, H.E., Kahn, R.S., 2013. Abnormal rich club organization and functional brain dynamics in schizophrenia. JAMA psychiatry 70, 783–792. doi:10.1001/jamapsychiatry.2013.1328

van der Heeden, J.F., Marinus, J., Martinez-Martin, P., van Hilten, J.J., 2016. Evaluation of severity of predominantly non-dopaminergic symptoms in Parkinson's disease: The SENS-PD scale. Park. Relat. Disord. 35, 29–44. doi:10.1016/j.parkreldis.2016.02.016

van der Heeden, J.F., Marinus, J., Martinez-Martin, P., van Hilten, J.J., 2014. Importance of nondopaminergic features in evaluating disease severity of Parkinson disease. Neurology 82, 412–418. doi:10.1212/WNL.0000000000000087

van Dijk, K.R.A., Sabuncu, M.R., Buckner, R.L., 2012. The influence of head motion on intrinsic functional connectivity MRI. Neuroimage 59, 431–438. doi:10.1016/j.neuroimage.2011.07.044

van Duinkerken, E., Schoonheim, M.M., Ijzerman, R.G., Moll, A.C., Landeira-Fernandez, J., Klein, M., Diamant, M., Snoek, F.J., Barkhof, F., Wink, A.M., 2017. Altered eigenvector centrality is related to local resting-state network functional connectivity in patients with longstanding type 1 diabetes mellitus. Hum. Brain Mapp. 38, 3623–3636. doi:10.1002/hbm.23617

Vernooij, M.W., de Groot, M., van der Lugt, A., Ikram, M.A., Krestin, G.P., Hofman, A., Niessen, W.J., Breteler, M.M.B., 2008. White matter atrophy and lesion formation explain the loss of structural integrity of white matter in aging. Neuroimage 43, 470–477. doi:10.1016/j.neuroimage.2008.07.052

Veselý, B., Rektor, I., 2016. The contribution of white matter lesions (WML) to Parkinson's disease cognitive impairment symptoms: A critical review of the literature. Park. Relat. Disord. 22, 166–170. doi:10.1016/j.parkreldis.2015.09.019

Visser, M., Verbaan, D., Van Rooden, S.M., Stiggelbout, A.M., Marinus, J., Van Hilten, J.J., 2007. Assessment of psychiatric complications in Parkinson's disease: The SCOPA-PC. Mov. Disord. 22, 2221–2228. doi:10.1002/mds.21696

Vo, A., Sako, W., Fujita, K., Peng, S., Mattis, P.J., Skidmore, F.M., Ma, Y., Uluğ, A.M., Eidelberg, D., 2017. Parkinson's disease-related network topographies characterized with resting state functional MRI. Hum. Brain Mapp. 38, 617–630. doi:10.1002/hbm.23260

Vossel, S., Geng, J.J., Fink, G.R., 2014. Dorsal and ventral attention systems: distinct neural circuits but collaborative roles. Neuroscientist 20, 150–159. doi:10.1177/1073858413494269

Wardlaw, J.M., Ferguson, K.J., Graham, C., 2004. White matter hyperintensities and rating scales - Observer reliability varies with lesion load. J. Neurol. 251, 584–590. doi:10.1007/s00415-004-0371-x

Wardlaw, J.M., Smith, C., Dichgans, M., 2013. Mechanisms of sporadic cerebral small vessel disease: Insights from neuroimaging. Lancet Neurol. 12, 483–497. doi:10.1016/S1474-4422(13)70060-7

Watson, R., Colloby, S.J., 2016. Imaging in dementia with Lewy bodies. J. Geriatr. Psychiatry Neurol. 29, 254–260. doi:10.1177/0891988716654984

Weingarten, C.P., Sundman, M.H., Hickey, P., Chen, N., 2015. Neuroimaging of Parkinson's disease: Expanding views. Neurosci. Biobehav. Rev. 59, 16–52. doi:10.1016/j.neubiorev.2015.09.007

Wersching, H., Duning, T., Lohmann, H., Mohammadi, S., Stehling, C., Fobker, M., Conty, M., Minnerup, J., Ringelstein, E.B., Berger, K., Deppe, M., Knecht, S., 2010. Serum C-reactive protein is linked to cerebral microstructural integrity and cognitive function. Neurology 74, 1022–1029. doi:10.1212/WNL.0b013e3181d7b45b

Wink, A.M., de Munck, J.C., van der Werf, Y.D., van den Heuvel, O.A., Barkhof, F., 2012. Fast eigenvector centrality mapping of voxel-wise connectivity in functional magnetic resonance imaging: implementation, validation, and interpretation. Brain Connect. 2, 265–274. doi:10.1089/brain.2012.0087

Winkler, A.M., Ridgway, G.R., Webster, M.A., Smith, S.M., Nichols, T.E., 2014. Permutation inference for the general linear model. Neuroimage 92, 381–397. doi:10.1016/j.neuroimage.2014.01.060

Wolters, E.C., 2008. Variability in the clinical expression of Parkinson's disease. J. Neurol. Sci. 266, 197–203. doi:10.1016/j.jns.2007.08.016

Wu, T., Wang, L., Chen, Y., Zhao, C., Li, K., Chan, P., 2009. Changes of functional connectivity of the motor network in the resting state in Parkinson's disease. Neurosci. Lett. 460, 6–10. doi:10.1016/j.neulet.2009.05.046

Yao, N., Pang, S., Cheung, C., Chang, R.S. kwan, Lau, K.K., Suckling, J., Yu, K., Mak, H.K.F., McAlonan, G., Ho, S.L., Chua, S. eng, 2015. Resting activity in visual and corticostriatal pathways in Parkinson's disease with hallucinations. Park. Relat. Disord. 21, 131–137. doi:10.1016/j.parkreldis.2014.11.020

Yavuz, B.B., Ariogul, S., Cankurtaran, M., Oguz, K.K., Halil, M., Dagli, N., Cankurtaran, E.S., 2007. Hippocampal atrophy correlates with the severity of cognitive decline. Int. Psychogeriatrics 19, 67–77. doi:10.1017/S1041610206004303

Zeighami, Y., Ulla, M., Iturria-Medina, Y., Dadar, M., Zhang, Y., Larcher, K.M.H., Fonov, V., Evans, A.C., Collins, D.L., Dagher, A., 2015. Network structure of brain atrophy in de novo parkinson's disease. Elife 4, e08440. doi:10.7554/eLife.08440

Zhang, D., Liu, X., Chen, J., Liu, B., Wang, J., 2015. Widespread increase of functional connectivity in Parkinson's disease with tremor: A resting-state fMRI study. Front. Aging Neurosci. 7, 6. doi:10.3389/fnagi.2015.00006

Zhang, Y., Brady, M., Smith, S., 2001. Segmentation of brain MR images through a hidden Markov random field model and the expectation-maximization algorithm. IEEE Trans Med Imaging 20, 45–57. doi:10.1109/42.906424

Zhang, Y., Wu, I.W., Tosun, D., Foster, E., Schuff, N., 2016. Progression of regional microstructural degeneration in Parkinson's disease: A multicenter diffusion tensor imaging study. PLoS One 11, e0165540. doi:10.1371/journal.pone.0165540

Zhu, K., van Hilten, J.J., Marinus, J., 2016. Course and risk factors for excessive daytime sleepiness in Parkinson's disease. Parkinsonism Relat. Disord. 24, 34–40. doi:10.1016/j.parkreldis.2016.01.020

Zielinski, B.A., Gennatas, E.D., Zhou, J., Seeley, W.W., 2010. Network-level structural covariance in the developing brain. Proc. Natl. Acad. Sci. U. S. A. 107, 18191–18196. doi:10.1073/pnas.1003109107

Zigmond, a S., Snaith, R.P., 1983. The hospital anxiety and depression scale. Acta Psychiatr. Scand. 67, 361–370. doi:10.1111/j.1600-0447.1983.tb09716.x

Zou, H., Hastie, T., 2005. Regularization and variable selection via the elastic net. J. R. Stat. Soc. Ser. B Stat. Methodol. 67, 301–320. doi:10.1111/j.1467-9868.2005.00503.x

Zwanenburg, J.J.M., Hendrikse, J., Visser, F., Takahara, T., Luijten, P.R., 2010. Fluid attenuated inversion recovery (FLAIR) MRI at 7.0 Tesla: Comparison with 1.5 and 3.0 Tesla. Eur. Radiol. 20, 915–922. doi:10.1007/s00330-009-1620-2

LIST OF PUBLICATIONS

de Schipper, L.J., Hafkemeijer, A., van der Grond, J., Marinus, J., Henselmans, J.M.L., van Hilten, J.J., 2019. Regional structural hippocampal differences between dementia with lewy bodies and Parkinson's disease. J. Parkinsons. Dis. doi:10.3233/jpd-191600

de Schipper, L.J., Hafkemeijer, A., Bouts, M.J.R.J., Grond, J. van der, Marinus, J., Henselmans, J.M.L., van Hilten, J.J., 2019. Age- and disease-related cerebral white matter changes in Parkinson's disease. Neurobiol. Aging. doi:10.1016/j.neurobiolaging.2019.05.004

de Schipper, L.J., Hafkemeijer, A., van der Grond, J., Marinus, J., Henselmans, J.M.L., van Hilten, J.J., 2018. Altered whole-brain and network-based functional connectivity in Parkinson's disease. Front. Neurol. doi:10.3389/fneur.2018.00419

de Schipper, L.J., van der Grond, J., Marinus, J., Henselmans, J.M.L., van Hilten, J.J., 2017. Loss of integrity and atrophy in cingulate structural covariance networks in Parkinson's disease. NeuroImage Clin. doi:10.1016/j.nicl.2017.05.012

de Schipper, L.J., Baharoglu, M.I., Roos, Y.B.W.E.M., de Beer, F., 2017. Medical treatment for spontaneous anticoagulation-related intracerebral hemorrhage in the Netherlands. J. Stroke Cerebrovasc. Dis. doi:10.1016/j.jstrokecerebrovasdis.2017.03.019

de Schipper, L.J., Boon, A.J.W., Munts, A.G., 2015. Foot drop dystonia resulting from parkin (PARK2) mutation. Mov. Disord. Clin. Pract. doi:10.1002/mdc3.12169

de Schipper, L.J., Vermeulen, M., Eeckhout, A.M., Foncke, E.M.J., 2014. Diagnosis and management of functional neurological symptoms: The Dutch experience. Clin. Neurol. doi:10.1016/j.clineuro.2014.04.020

DANKWOORD

Graag wil ik iedereen bedanken die heeft bijgedragen aan de totstandkoming van dit proefschrift. Het was een periode waarin ik veel heb geleerd. Mijn dank gaat uit naar alle deelnemers van dit onderzoek. Heel erg bedankt dat jullie bereid waren deel te nemen. Zonder jullie data was dit onderzoek er niet geweest, en daarnaast heb ik mogen zien hoe divers de ziekte van Parkinson kan verlopen. Natuurlijk wil ik ook graag alle de neurologen bedanken die me met deze mensen in contact hebben gebracht.

Bob, bedankt dat me hebt aangenomen. Daarnaast heel erg bedankt voor je enthousiasme en je capaciteit om altijd te denken in (veel) mogelijkheden, ook toen ik twijfelde over de opleiding neurologie. Han, naast je epidemiologische kennis en snelle werk, zorgde je op de juiste momenten voor nuancering. Jeroen, dank, voor onze wekelijkse gesprekken, over onderzoek doen en alles daarbuiten. Hanneke, dank je voor je inzet, je interesse en het aandragen van patiënten voor ons onderzoek.

Gerty en Gerda, ik heb ontzettend veel aan jullie hulp gehad en ik ben vaak even binnen gelopen voor een praatje of een vraag. Anne, Frank, Mark en Annette: hartelijk dank voor jullie hulp met MRI-data-analyse. Daarnaast wil ik graag alle andere mensen van de afdelingen neurologie en radiologie bedanken die hebben geholpen met dit project.

Lieve kamergenoten van C2-192, ik heb echt een hele leuke tijd gehad in de "bunker". Alle mensen van het Gortercentrum wil ik graag bedanken voor de warme opname in de groep. Lieve mede-onderzoekers van de afdeling neurologie, bedankt voor de gezelligheid en natuurlijk de koffiecartoons. Linda, dankjewel voor je enthousiasme en je hulp bij wetenschappelijke vraagstukken, ook al voor mijn tijd in Leiden. Dankjewel ook aan alle andere mensen die me geënthousiasmeerd hebben voor het doen van wetenschappelijk onderzoek.

Dankjewel lieve vrienden voor alle support door de jaren heen (pieken en dalen!).

Lieve papa en mama, lieve zusjes, heel veel dank voor alle keren dat jullie me raad gaven, mijn horizon verbreedden of simpelweg luisterden en steeds vertrouwen in me hadden. Elbert, jij hebt in elk geval nooit ergens over getwijfeld, wat ik als erg geruststellend heb ervaren. Tot slot lieve kleine Julius, jij plaatst alles weer in perspectief.

CURRICULUM VITAE

Laura Jansje de Schipper was born on the 28th of February 1988 in Knokke-Heist, Belgium. She was raised in West-Zeeuws Vlaanderen. After graduating cum laude at the Zeldenrust-Steelantcollege in Terneuzen in 2006, she moved to Amsterdam to study Medicine at the VU University in Amsterdam. During her studies she enjoyed doing research at the Department of Neurology and the Department of Psychiatry concerning functional neurological movement disorders. This resulted in her first publication and she developed a special interest in neurological movement disorders. She obtained her medical degree in 2012, after which she worked as a physician at the Department of Neurology of the Kennemer Gasthuis hospital in Haarlem. In 2014 she started her PhD research at the Leiden University Medical Center at the Department of Neurology and the Department of Radiology under the supervision of professor J.J. van Hilten, Dr. J. Marinus and Dr. J. van der Grond. This project was focused on advanced neuroimaging approaches in Parkinson's disease and resulted in the publication of this thesis, as a part of the Profiling Parkinson's disease (PROPARK) study. Laura is currently working at "Stichting Eerstelijns Zorggroep". The main focus of her work is to enhance primary care programs for patients with chronic disease.

